

DONALD E. LEE

☎ 714-723-1515

✉ delee1000@gmail.com



linkedin.com/in/donald-e-lee/



Baltimore, MD

EDUCATION

2019 – 2024
Baltimore, MD

PhD, Pharmaceutical Sciences
University of Maryland, Baltimore
Advisor: Joga Gobburu, PhD

2012 – 2016
Irvine, CA

Post-Baccalaureate, Biological Sciences & Biomedical Engineering
University of California, Irvine

2010 – 2011
Washington, D.C.

Post-Baccalaureate, Pre-Health
American University

2004 – 2008
La Jolla, CA

B.A., Political Science – International Relations
University of California, San Diego

SKILLS

Clinical Pharmacology

Study design, DDI, QT, bioequivalence, dose optimization

Pharmacometrics

PK/PD, modeling and simulation, clinical trial simulation, MIDD, biostatistics

Software

Pumas, Julia, R, MATLAB, Phoenix NLME, WinNonlin

EXPERIENCE

2019 – Present
Baltimore, MD

Graduate Research Assistant
Pharmaceutical Sciences, School of Pharmacy,
University of Maryland, Baltimore

- Trained in drug development, regulatory strategy, clinical pharmacology, and pharmacometrics
- Applied PK modeling and simulation to projects that included preclinical and clinical data to inform dosing and drug development decisions
- Contributed to writing FDA grant that was awarded for “Best Practices for Establishing the Suitability of a Model Integrated Approach to Demonstrate the Bioequivalence of Long-Acting Injectable Products”
- Served as lead for CRO work involving model-integrated evidence to establish bioequivalence for a long-acting product that led to two regulatory meetings
- Developed questions and responses for meetings with regulatory agency for CRO work
- Helped plan and served as instructor for “Intermediate PHMX: Mastering Clinical Trial Simulations & IVIVC Workshop”

Aug – Dec 2022
Silver Spring, MD

ORISE Fellow

Division of Pharmacometrics, Office of Clinical Pharmacology
U.S. Food and Drug Administration

- Identified predictors of placebo response in major depression trials to address the high failure rate of pediatric trials
- Investigated utility of applying machine learning vs traditional statistical approaches to identify predictors of placebo response

May – Aug 2022
Princeton, NJ

Clinical Pharmacology and Pharmacometrics Intern

Bristol Myers Squibb

- Conducted QT risk assessment for MYK-224 based on *in vitro*, *in vivo*, and first-in-human data
- Developed preliminary concentration-QTc model to characterize the relationship between MYK-224 concentration and QTc interval in healthy subjects

2016 – 2019
Irvine, CA

Lab Manager

Division of Endocrinology, Department of Medicine
University of California, Irvine

- Led research on the role of neuronal synaptic proteins in pancreatic β cells in regulating insulin secretion and β -cell maturation
- Investigated drug delivery platforms for synaptic proteins as potential therapeutics for Type 2 diabetes
- Performed cell culture, molecular biology techniques, and immunofluorescence microscopy
- Mentored 6 students and staff scientists

2013 – 2019
Irvine, CA

Research Assistant (EEG Signal Processing Team Lead)

Department of Neurology
University of California, Irvine

- Performed EEG signal processing for consciousness, cardiac arrest, and resuscitation biomedical research
- Led 4+ EEG signal processing projects resulting in publications and conference abstracts
- Mentored 4 students

KEY PHD PROJECTS

Model-integrated
BE (MIBE) assessment for
long-acting injectables

Purpose: To establish MIBE approaches to support BE for long-acting injectables

Contribution: Formulated and tested MIBE approaches by performing large-scale BE trial simulations

Impact: Proposed a conceptual framework to implement MIBE to accelerate generic drug development

Model-informed evidence
to establish BE for a long-
acting leuprolide product

Purpose: To facilitate establishing BE for a long-acting leuprolide product with model-informed evidence

Contribution: Served as CRO lead, which included communication with sponsor, writing of reports and modeling analyses plans, involvement in regulatory strategy, and performance of pop-PK modeling and simulation analyses to investigate:

1) partial and full replicate crossover designs without washout and model-based removal of carryover effects

2) parallel design with MIBE (i.e., abbreviated BE trial and virtual BE assessment)

Impact: Two meetings with regulatory agency to establish agreement on model-integrated approach

Dose optimization of
rifampin in prosthetic
joint-associated infection

Purpose: To optimize rifampin dosing for prosthetic joint-associated infection

Contribution: Developed rifampin PK models in mice and humans with PET imaging plasma and bone data and literature data, and simulated rifampin bone

		exposures in mice and humans with standard- and high-dose regimens
	<i>Impact:</i>	Determined standard-dose rifampin achieves suboptimal exposure in bone, which suggests high-dose rifampin may improve cure rate
Investigation of drug candidates for the treatment of birth asphyxia	<i>Purpose:</i>	To investigate several drug candidates to prevent (prophylaxis) or treat birth asphyxia
	<i>Contribution:</i>	Worked on systems biology model to characterize neuronal metabolism during ischemia and reperfusion
		Characterized maternal-fetal transfer of azithromycin in sheep
		Performed allometric scaling analysis of azithromycin across species to suggest the dose to study in newborn lamb
	<i>Impact:</i>	Performed PK modeling of azithromycin in newborn lamb after undergoing birth asphyxia Determined that azithromycin, while promising in animal models at treating focal ischemia, is unlikely to be a safe and effective treatment for birth asphyxia in humans

AWARDS

2021

Clin PMx SIG Trainee Award

- In recognition of abstract titled “A Pharmacokinetics Model for Rifampin Exposures in Human Bone Using PET Imaging”

PUBLICATIONS

Lee DE, Gobburu JVS. Assessment of model-integrated bioequivalence with abbreviated trials. (*In preparation*)

Lee DE, Goyal RK, Gopalakrishnan M, Gobburu JVS. Accelerating generic drug development with a model-integrated bioequivalence approach. (*In preparation*)

Mike JK, White Y, Hutchings RS, Vento C, Ha J, Manzoor H, **Lee D**, et al. Perinatal Azithromycin Provides Limited Neuroprotection in an Ovine Model of Neonatal Hypoxic-Ischemic Encephalopathy [published online ahead of print, 2023 Oct 17]. *Stroke*. 2023;54(11):2864-2874. doi:10.1161/STROKEAHA.123.043040

Gordon O, **Lee DE**, Liu B, et al. Dynamic PET-facilitated modeling and high-dose rifampin regimens for *Staphylococcus aureus* orthopedic implant-associated infections. *Sci Transl Med*. 2021;13(622). doi:10.1126/scitranslmed.abl6851

Crouzet C, Wilson RH, **Lee D**, et al. Dissociation of Cerebral Blood Flow and Femoral Artery Blood Pressure Pulsatility After Cardiac Arrest and Resuscitation in a Rodent Model: Implications for Neurological Recovery. *J Am Heart Assoc*. 2020;9(1). doi:10.1161/JAHA.119.012691

Lee DE, Wilson RH, Crouzet C, et al. Spreading depolarization and repolarization during cardiac arrest as an ultra-early marker of neurological recovery in a preclinical model. *bioRxiv*. Published online 2019. doi:10.1101/786210 (*In preparation*)

Chessler S, **Lee D**. An alarming increase in HbA1c and near misdiagnosis of diabetes mellitus resulting from a clinical laboratory instrument upgrade and haemoglobin variant. *BMJ Case Reports*. 2018; doi:10.1136/bcr-20180225358.

Vallejo D, Lee SH, **Lee D**, et al. Cell-sized lipid vesicles for cell-cell synaptic therapies. *TECHNOLOGY*. 2017;05(04):201-213. doi:10.1142/S233954781750011X

Lee DE, Lee LG, Siu D, Bazrafkan A, Farahabadi MH, Dinh TJ, Orellana J, Xiong W, Lopour BA, Akbari Y. Neural correlates of consciousness at near-electrocerebral silence in an asphyxial cardiac arrest model. *Brain Connectivity*. 2017;7(3):172-181. doi:10.1089/brain.2016.0471.

Crouzet C, Wilson RH, Bazrafkan A, Farahabadi MH, **Lee D**, Alcocer J, Tromberg BJ, Choi B, Akbari Y. Cerebral blood flow is decoupled from blood pressure and linked to EEG bursting after resuscitation from cardiac arrest. *Biomedical Optics Express*. 2016;7(11):4660-4673. doi:10.1364/BOE.7.004660.

CONFERENCE PRESENTATIONS

Lee DE, Gobburu J. Accelerating Generic Drug Development with an MIBE Approach. Poster session presented at: American Conference on Pharmacometrics 14; 2023 Nov 5-8.

Liu J, **Lee D**, Bhattaram A. Application of Machine Learning Methods to Identify Predictors of Placebo Response in Pediatric Major Depression Disease Studies. Poster session presented at: American Conference on Pharmacometrics 14; 2023 Nov 5-8.

Lee DE, Langevin BA, Gordon O, Jain SK, Gobburu J. A Pharmacokinetics Model for Rifampin Exposures in Human Bone Using PET Imaging. Oral session presented at: American Conference on Pharmacometrics 12; 2021 Nov 8-12.

Lee DE, Gupta P, Maltepe E, Gobburu J. A Computational Model of Cerebral Metabolism during Cerebral Ischemia and Reperfusion. Poster session presented at: American Conference on Pharmacometrics 11; 2020 Nov 9-13.

Akbari Y, **Lee D**, Wilson R, et al. Multimodal detection of spreading depolarization and repolarization during cardiac arrest and resuscitation in a rodent model: An ultra-early biomarker of neurological outcome. Poster session presented at: Society for Neuroscience 2018; 2018 Nov 3-7; San Diego, CA.

Akbari Y, **Lee D**, Wilson R, Crouzet C, et al. Evidence for a Novel Ultra-Early Electrophysiologic Biomarker of Neurological Outcome After Cardiac Arrest Using a Multimodal Rodent Neuro-ICU Platform. Oral session presented at: 16th Annual Neurocritical Care Society Meeting; 2018 Sept 25-28; Boca Raton, FL.
(Top 12 Abstract)

Lee D, Wilson RH, Crouzet C, et al. Spreading depolarization during cardiac arrest in a rodent model as an ultra-early biomarker of neurological outcome after resuscitation. Oral session presented at: International Conference on Spreading Depolarizations 2018; 2018 Sept 22-24; Boca Raton, FL.

Akbari Y, Siu D, **Lee D**, Lee L, Bazrafkan A, Alcocer J, Maki N, Farahabadi M, Wilson R, Lopour B. Dynamic Changes in EEG Coherence During Cardiac Arrest and Resuscitation in A Rodent Model That Mimics A Neuro-Intensive Care Unit. Oral session presented at: American Academy of Neurology 70th Annual Meeting; 2018 April 21-27; Los Angeles, CA.

Akbari Y, **Lee DE**, Siu D, Lee LG, Bazrafkan AK, Gutierrez BP, Moslehyazdi M, Alcocer J, Kim SH, Lopour BA. Acute and Sustained Changes in EEG Coherence During Recovery after Cardiac Arrest in Rodents. Oral session presented at: 15th Annual Neurocritical Care Society Meeting; 2017 Oct 10-13; Waikoloa, HI.

Lee DE, Munder A, Lee SH, Lellouche JP, Vallejo D, Israel L, Lee A, Chessler SD. Development of novel biologic and nanotechnology-based therapeutic agents to enhance insulin secretion and protect β cell function in diabetes. Oral session presented at: Pathways to Cures: Clinical Translational Research Day at UC Irvine; 2017 June 13; Irvine, CA.

Lee DE, Munder A, Lee SH, Lellouche JP, Vallejo D, Israel L, Lee A, Chessler SD. Development of novel biologic and nanotechnology-based therapeutic agents to enhance insulin secretion and protect β cell function in diabetes. Poster session presented at: American Diabetes Association 77th Scientific Sessions; 2017 June 9-13; San Diego, CA.

(Chosen for moderated discussion)

Lee D, Orellana J, Siu D, Sikharia M, Thakor NT, Geocadin RG, Akbari Y. Persistence of EEG activity in the right visual cortex after cardiac arrest in a rodent model. Poster session presented at: Pathways to Cures: Clinical Translational Research Day at UC Irvine; 2014 Jun 27; Irvine, CA.

Akbari Y, Orellana J, **Lee D**, Thakor NT, Geocadin RG. Neurophysiologic resilience of the right occipital lobe during and after brain death from cardiac arrest. Oral session presented at: Critical Care Congress: 43rd Annual Congress of Society of Critical Care Medicine; 2014 Jan 9-13; San Francisco, CA.

Abstract

Title of Dissertation: Model-Informed Approaches to Tackle Challenges in Therapeutics and Generic Drug Development

Donald Lee, Doctor of Philosophy, 2024

Dissertation Directed by: Jogarao Gobburu, PhD, Professor, Department of Practice, Sciences, and Health Outcomes Research, School of Pharmacy

Interest in model-informed approaches across pharma and medicine have dramatically increased in recent years. For the first project in therapeutics, a modeling approach was utilized here to optimize rifampin dosing for orthopedic implant-associated *S. aureus* infection. With a mortality rate of 10-30%, current rifampin dosing regimens may provide inadequate exposures to infected bone tissue. An integrated approach using *in vitro*, *in vivo*, and human data, along with pharmacokinetic (PK) modeling and simulation, was utilized to suggest high-dose rifampin regimens are needed to optimize bone exposures, as bone penetration was shown to be much lower (10-15%) than previously thought. For the second project in generic drug development, a model-integrated bioequivalence (MIBE) framework was proposed to demonstrate the application of MIBE for generic companies. With our MIBE approach, we demonstrate how to prepare for, plan, and implement MIBE in a robust manner that lends credibility to the virtual assessment of bioequivalence from an abbreviated trial. With an example drug of Depo-SubQ Provera 104, we show that with MIBE we can reduce the trial size by 33-50%. Thus, we demonstrate in our work the ability to tackle complex challenges with model-informed approaches to optimize dose and to accelerate generic drug development.

Model-Informed Approaches to Tackle Challenges in
Therapeutics and Generic Drug Development

by
Donald Lee

Dissertation submitted to the faculty of the Graduate School of the
University of Maryland, Baltimore in partial fulfillment
of the requirements for the degree of
Doctor of Philosophy
2024

©Copyright 2024 by Donald Lee

All rights reserved

Table of Contents

List of Tables.....	v
List of Figures.....	vi
List of Abbreviations.....	viii
Chapter 1: Introduction	1
Chapter 2: There Is a Need to Improve Treatment Outcomes for <i>Staphylococcal aureus</i> Orthopedic Implant-Associated Infection	10
Chapter 3: Mice and Human PK Are Dissimilar With ¹¹C-Rifampin Microdosing. 17	
3.1 Introduction	17
3.2 Methods	19
3.3 Results	24
3.4 Discussion	31
3.5 References	33
Chapter 4: Separate Models Are Needed to Translate Findings from Microdose Modeling to Therapeutic Dosing	37
4.1 Introduction	37
4.2 Methods	38
4.3 Results	39
4.4 Discussion	48
4.5 References	50
Chapter 5: Simulations Suggest High-Dose Rifampin Regimens May Be Necessary for Adequate Bone Exposure	53
5.1 Introduction	53
5.2 Methods	54
5.3 Results	54
5.4 Discussion	56
5.5 References	58
Chapter 6: There Is a Need for a Model-Integrated Bioequivalence Framework to Facilitate Generic Drug Development for Long-Acting Injectables	62
Chapter 7: With Model-Integrated Bioequivalence, Bioequivalence Can Be Assessed through a Simulation-Based Approach	70
Chapter 8: Successful Application of Model-Integrated Bioequivalence Is Predicated on Thorough Planning Using Modeling and Simulation	74

Chapter 9: The Credibility of a Model-Integrated Bioequivalence Plan Should Be Thoroughly Assessed to Enhance Confidence	78
9.1 Introduction	78
9.2 Methods	79
9.3 Results	83
9.4 Discussion	94
9.5 Conclusion	102
9.6 References	102
Chapter 10: Discussion	105
Appendix	110
References	149

List of Tables

Table 1 Selection Criteria for Patient Enrollment in the Clinical Study.....	20
Table 2 Parameter Estimates from ¹¹ C-Rifampin Microdose PK Modeling in Mouse and Human.....	26
Table 3 Publications for Building and Validating Rifampin Therapeutic Dose Mouse Model	40
Table 4 Rifampin Therapeutic Dose Mouse Model Parameter Estimates	41
Table 5 Rifampin Therapeutic Dose Human Model Parameter Estimates	46
Table 6 Publications for Validation of Rifampin Therapeutic Dose Human Model	47
Table 7 Simulated Steady-State Cmax and AUC for Bone Tissue with Standard- and High-Dose Rifampin Regimens.....	56
Table 8 Representative Long-Acting Injectables with Product-Specific Guidances Recommending Partial AUCs	64
Table 9 Half-Lives and Times to Steady State for Representative Immediate Release and Long-Acting Product Counterparts.....	65
Table 10 Assessment of Credibility of Model-Integrated Bioequivalence Approach.....	84

List of Figures

Figure 1 Model-Informed Drug Development (MIDD) Methodologies	2
Figure 2 Model-Integrated Evidence (MIE) Methodologies	4
Figure 3 Experimental Scheme to Study Rifampin Dosing for Orthopedic Implant- Associated Infection.....	18
Figure 4 Volumes of Interest (VOIs) for Quantification of ¹¹ C-Rifampin PET	23
Figure 5 ¹¹ C-Rifampin Microdose PK Profiles for Representative Mice and Humans	25
Figure 6 ¹¹ C-Rifampin Microdose PK Model Structure	25
Figure 7 ¹¹ C-Rifampin Microdose Mouse Model Individual Predictions for Plasma	27
Figure 8 ¹¹ C-Rifampin Microdose Mouse Model Individual Predictions for Bone Tissue	28
Figure 9 ¹¹ C-Rifampin Microdose Human Model Individual Predictions for Plasma	29
Figure 10 ¹¹ C-Rifampin Microdose Human Model Individual Predictions for Bone Tissue	30
Figure 11 Rifampin Therapeutic Dose Mouse Model Structure.....	41
Figure 12 Rifampin Therapeutic Dose Mouse Model Structure with Bone Compartments	42
Figure 13 Validation of Rifampin Therapeutic Dose Mouse Model.....	43
Figure 14 Rifampin Therapeutic Dose Human Model Structure.....	44
Figure 15 Rifampin Therapeutic Dose Human Model Structure with Bone Compartments	45
Figure 16 Validation of Rifampin Therapeutic Dose Human Model.....	48

Figure 17 Simulations of Rifampin Concentrations in Bone Tissue with Standard- and High-Dose Regimens	55
Figure 18 Complex Absorption with Long-Acting Injectables.....	63
Figure 19 Consequences of Variability on Bioequivalence Determination	64
Figure 20 Conventional Study Designs to Establish Bioequivalence with Long-Acting Injectables	66
Figure 21 Simulation-Based Bioequivalence Assessment.....	71
Figure 22 Model-Integrated Bioequivalence Framework.....	74
Figure 23 Model-Integrated Bioequivalence Planning Simulation Framework.....	82
Figure 24 Quantitative Predictive Check of the PK Model for Depo-SubQ Provera 104	85
Figure 25 Bioequivalence Power and Type I Error Rate with Conventional BE Analysis	86
Figure 26 Bias and Precision in Parameter Estimates of Abbreviated BE Trials	87
Figure 27 Bioequivalence Power and Type I Error Rate with MIBE	88
Figure 28 Bioequivalence Power and Type I Error Rate with Large Disparity Between Planned and Observed Pivotal Trial Variability	90
Figure 29 Bias and Precision of Parameter Estimates with Rich and Sparse Sampling...	91
Figure 30 Bioequivalence Power and Type I Error Rate with Rich and Sparse Sampling	92
Figure 31 Bioequivalence Power and Type I Error Rate with and without Simulations with Parameter Uncertainty	93

List of Abbreviations

AI	Artificial intelligence
ANDA	Abbreviated new drug application
AUC	Area under the curve
BE	Bioequivalence
BLQ	Below limit of quantification
BOV	Between-occasion variability
BSV	Between-subject variability
CI	Confidence interval
CL	Clearance
C _{max}	Maximum concentration
CP	Clinical pharmacology
CT	Computed tomography
CV	Coefficient of variation
EBE	Empirical Bayes estimate
FDA	Food and Drug Administration
GDUFA	Generic Drug User Fee Amendments
GMR	Geometric mean ratio
IDSA	Infectious Diseases Society of America
MIBE	Model-integrated bioequivalence
MIC	Minimal inhibitory concentration
MIDD	Model-informed drug development
MIE	Model-integrated evidence

ML	Machine learning
MRSA	Methicillin-resistant <i>S. aureus</i>
MTT	Mean transit time
NCA	Noncompartmental analysis
NLME	Non-linear mixed effects modeling
NN	Number of transit compartments
PBPK	Physiologically-based pharmacokinetics
PC	Partition coefficient
PET	Positron emission tomography
PK	Pharmacokinetics
Pop-PK	Population pharmacokinetics
PSG	Product-specific guidance
Q _b	Intercompartmental clearance with bone compartment
QPC	Quantitative predictive check
R	Reference drug product
RSE	Relative standard error
<i>S. aureus</i>	<i>Staphylococcus aureus</i>
SE	Standard error
T	Test drug product
TOST	Two one-sided t-test
TSA	Tryptic soy agar
TSB	Tryptic soy broth
V _b	Volume of bone compartment

Vc	Volume of central compartment
VOI	Volume of interest
VPC	Visual predictive check

Chapter 1: Introduction

Interest in quantitative approaches within pharma and medicine has experienced a dramatic increase in recent years (U.S. Food and Drug Administration 2022c). Earlier this year to further encourage this interest and guide in the consistent application of quantitative approaches for drug development, regulatory decision making, and patient care, the U.S. Food and Drug Administration's (FDA) Center for Drug Evaluation and Research (CDER) announced the creation of the CDER Quantitative Medicine Center of Excellence (U.S. Food and Drug Administration 2024). Moreover, the rapid advancement of artificial intelligence (AI) and machine learning (ML) throughout society has further elevated the importance of quantitative approaches (Terranova et al. 2024).

- *Model-Informed Drug Development*

In recognition of the growing influence of model-informed approaches within drug development, the term model-informed drug development (MIDD) was coined within the last decade (Bruno et al. 2019; Madabushi et al. 2022). Pharmacokinetics (PK) modeling within the MIDD framework uses quantitative methods to understand how drugs move through the body (Figure 1). Empirical PK modeling approaches can often characterize movement of drug with simply one or two compartments (Mould and Upton 2012). Meanwhile, physiologically-based pharmacokinetics (PBPK), a mechanistic modeling approach, aims to characterize a drug's PK with several compartments that represent the body's organs (Jones and Rowland-Yeo 2013).

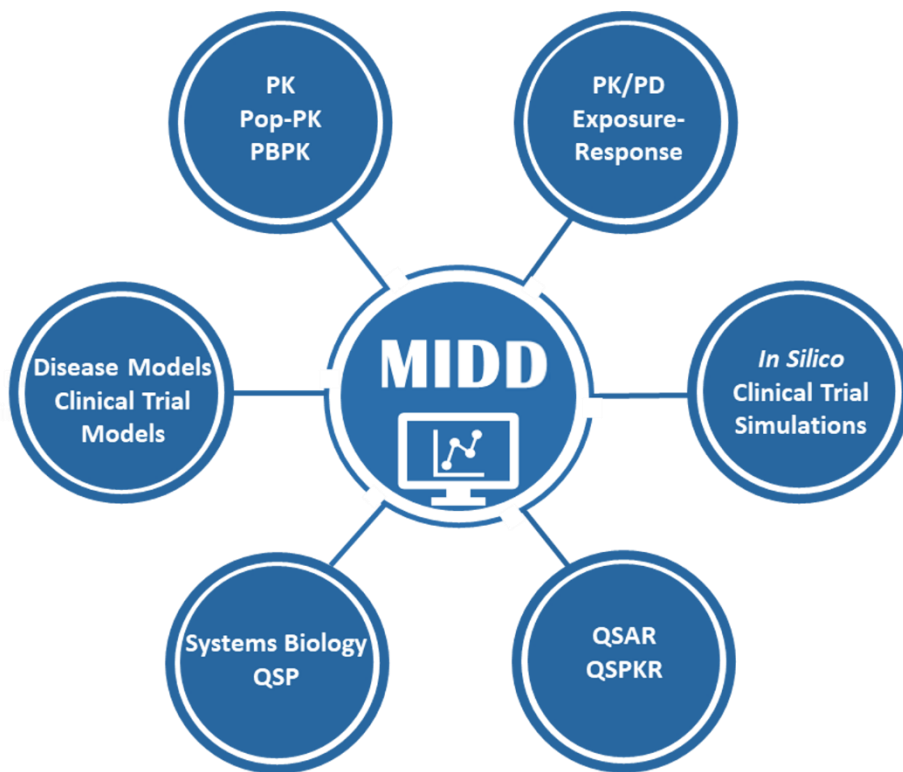


Figure 1 Model-Informed Drug Development (MIDD) Methodologies

Adapted from FDA conference proceedings (Bruno et al. 2019)

Furthermore, with non-linear mixed effects (NLME) modeling approaches, we can characterize variability in PK parameters. This can include variability in drug clearance or volume of distribution between subjects (between-subject variability: BSV) or between different dosing occasions (between-occasion variability: BOV) (Mould and Upton 2013). With such tools, PK modeling and simulation offers the ability to describe not only the average scenario but also variability within a population. Harnessing this capability to capture random effects, clinical trials simulations can be performed to assess a drug’s efficacy or safety and to optimize trial designs (Holford, Ma, and Ploeger 2010; Bonate 2000).

- *Model-Informed Applications in Therapeutics*

Within therapeutics, modeling and simulation is often utilized to fill gaps in knowledge to improve patient care. This includes the use PK modeling with electronic health records to guide clinical dosing decisions (Salem et al. 2022). Bayesian-model informed precision dosing has also been implemented within antimicrobial therapy for drugs requiring therapeutic drug monitoring (Bunn, Gobburu, and Floryance 2023; Oda, Saito, and Jono 2023). Additionally, exposure-response analyses have been utilized to guide off-label use of drugs in understudied populations, such as pregnant women (Ahmadzia et al. 2021). These examples highlight the impact of model-informed approaches not only within drug development by sponsors but also after approval by academic institutions and hospitals when a drug is in common use and incentives may not exist for sponsors to conduct trials.

- *Model-Integrated Evidence*

Under the Generic Drug User Fee Amendments (GDUFA), the FDA has made a commitment to funding research into quantitative methods to drive innovations in generic drug development and regulatory decision making (Yoon et al. 2023). To highlight the growing impact of model-informed approaches within generic drug development, the term model-integrated evidence (MIE) has been coined. Quantitative methods within the MIE framework are summarized in Figure 2. PBPK is utilized to waive trials for locally acting products, such as dermal or ocular products (Tsakalozou et al. 2022). Quantitative clinical pharmacology (CP) and PBPK models have been proposed to assess bioequivalence (BE) virtually through BE trial simulations (Zhao et al. 2019).

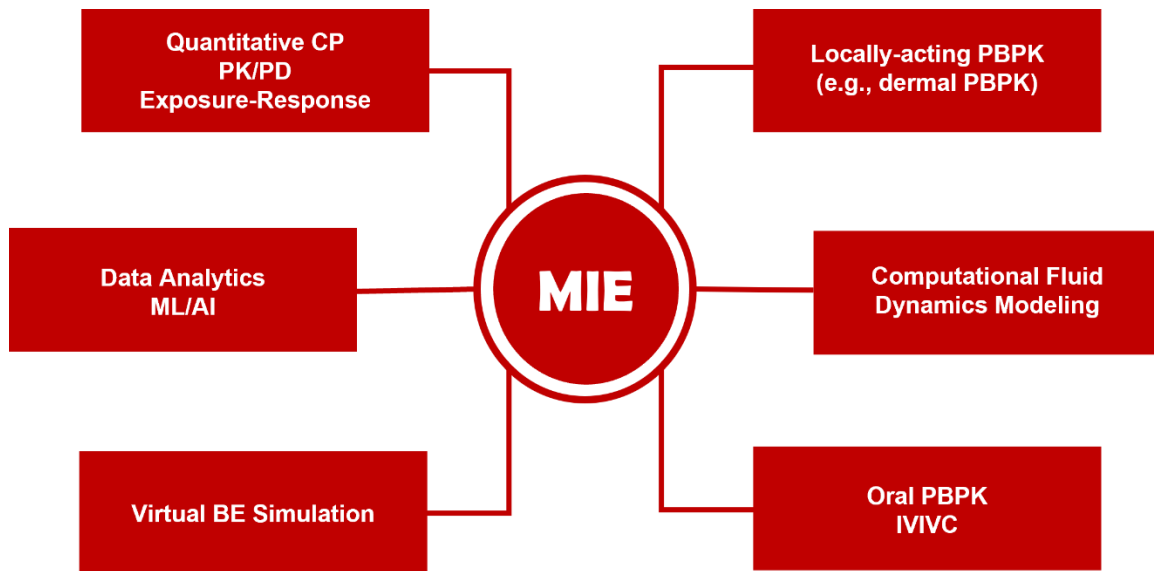


Figure 2 Model-Integrated Evidence (MIE) Methodologies

Adapted from FDA workshop (Tsakalozou et al. 2024)

Broadly, modeling and simulation within the model-informed BE framework can be summarized with three approaches. First, it can be used in the design of BE studies, which has long been utilized by regulatory agencies prior to the GDUFA commitments. For example, simulation studies were utilized by the FDA in the establishment of the reference-scaled average bioequivalence approach for highly variable drug products (Davit et al. 2012). Second, modeling can be used in the analysis of BE studies, such as with the use of modeling to derive individual predictions on which to perform noncompartmental analysis (NCA) (Dubois et al. 2010). Third, modeling and simulation can be used in the assessment of BE. To distinguish this third approach with the first two, when modeling is involved in assessing BE, it is more specifically referred to as model-integrated, or model-integrated bioequivalence (MIBE), as opposed to model-informed (Lee, Gong, et al. 2020).

Model-informed BE approaches provide several potential benefits. These include higher power than the traditional noncompartmental analysis (NCA)-based method on observed concentrations when sampling is sparse and residual error is high (Loingeville et al. 2020; C. Hu et al. 2004; X. Chen et al. 2024). Additional benefits include the ability to perform an abbreviated BE study with reductions in number of subjects, study duration, or PK sampling and assess BE virtually (Gong et al. 2023).

With an MIE approach, however, concerns have been raised regarding how to qualify for MIBE versus how to qualify for population pharmacokinetics (pop-PK) or exposure-response analyses (Sharan et al. 2021). Inflated Type I error rates have also been reported with some MIBE approaches, particularly in the presence of sparse sampling (X. Chen et al. 2024; Loingeville et al. 2020).

- *Application of Model-Informed Approaches to Tackle Challenges in Therapeutics and Generic Drug Development*

In our work here, model-informed approaches were utilized to tackle challenges in therapeutics and generic drug development. The first project in therapeutics was to optimize dosing of rifampin for *Staphylococcal aureus* orthopedic implant-associated infection. This work was an integration of mouse and human experimentation with PK modeling and simulation to determine whether high-dose rifampin regimens can be as effective as standard-dose regimens and potentially shorten treatment regimens. The second project in generic drug development was to develop a framework for model-integrated bioequivalence (MIBE) assessment for long-acting injectables (LAI). With this framework, we aim to assist generic drug companies without extensive experience in

modeling with how to plan and think about implementing an MIBE approach. We also aim to provide confidence in the validity of the MIBE approach by providing an example of the application of a credibility framework borrowed from V&V 40 framework utilized in engineering and computational modeling (ASME 2018).

References

- Ahmadzia, Homa K., Naomi L.C. Luban, Shuhui Li, Dong Guo, Adam Miszta, Jogarao V.S. Gobburu, Jeffrey S. Berger, Andra H. James, Alisa S. Wolberg, and John van den Anker. 2021. “Optimal Use of Intravenous Tranexamic Acid for Hemorrhage Prevention in Pregnant Women.” *American Journal of Obstetrics and Gynecology* 225 (1): 85.e1-85.e11. <https://doi.org/10.1016/j.ajog.2020.11.035>.
- ASME. 2018. “V V - Assessing Credibility of Computational Modeling through Verification and Validation: Application to Medical Devices.” 2018. <https://www.asme.org/codes-standards/find-codes-standards/assessing-credibility-of-computational-modeling-through-verification-and-validation-application-to-medical-devices>.
- Bonate, Peter L. 2000. “Clinical Trial Simulation in Drug Development.” *Pharmaceutical Research*. Vol. 17. <https://doi.org/10.1023/a:1007548719885>.
- Bruno, Rene, Jin Y. Jin, Kimberly Maxfield, Lauren Milligan, Chao Liu, Yaning Wang, Amy E. McKee, and Issam Zineh. 2019. “Proceedings of a Workshop: US Food and Drug Administration-International Society of Pharmacometrics Model-Informed Drug Development in Oncology.” In *Clinical Pharmacology and Therapeutics*, 106:81–83. Nature Publishing Group. <https://doi.org/10.1002/cpt.1421>.
- Bunn, Haden T., Jogarao V.S. Gobburu, and Lindsey M. Floryance. 2023. “Bayesian Model-Guided Antimicrobial Therapy in Pediatrics.” *Frontiers in Pharmacology*. Frontiers Media SA. <https://doi.org/10.3389/fphar.2023.1118771>.
- Chen, Xiaomei, Henrik B. Nyberg, Mark Donnelly, Liang Zhao, Lanyan Fang, Mats O. Karlsson, and Andrew C. Hooker. 2024. “Development and Comparison of Model-integrated Evidence Approaches for Bioequivalence Studies with Pharmacokinetic End Points.” *CPT: Pharmacometrics & Systems Pharmacology*, August. <https://doi.org/10.1002/psp4.13216>.
- Davit, Barbara M., Mei Ling Chen, Dale P. Conner, Sam H. Haidar, Stephanie Kim, Christina H. Lee, Robert A. Lionberger, et al. 2012. “Implementation of a Reference-Scaled Average Bioequivalence Approach for Highly Variable Generic Drug

Products by the Us Food and Drug Administration.” *AAPS Journal* 14 (4): 915–24.
<https://doi.org/10.1208/s12248-012-9406-x>.

- Dubois, Anne, Sandro Gsteiger, Etienne Pigeolet, and France Mentré. 2010. “Bioequivalence Tests Based on Individual Estimates Using Non-Compartmental or Model-Based Analyses: Evaluation of Estimates of Sample Means and Type I Error for Different Designs.” *Pharmaceutical Research* 27 (1): 92–104.
<https://doi.org/10.1007/s11095-009-9980-5>.
- Gong, Yuqing, Peijue Zhang, Miyoung Yoon, Hao Zhu, Ameya Kohojkar, Andrew C. Hooker, Murray P. Ducharme, et al. 2023. “Establishing the Suitability of Model-Integrated Evidence to Demonstrate Bioequivalence for Long-Acting Injectable and Implantable Drug Products: Summary of Workshop.” *CPT: Pharmacometrics and Systems Pharmacology*. American Society for Clinical Pharmacology and Therapeutics. <https://doi.org/10.1002/psp4.12931>.
- Holford, N., S. C. Ma, and B. A. Ploeger. 2010. “Clinical Trial Simulation: A Review.” *Clinical Pharmacology and Therapeutics*. <https://doi.org/10.1038/clpt.2010.114>.
- Hu, Chuanpu, Katy H.P. Moore, Yong H. Kim, and Mark E. Sale. 2004. “Statistical Issues in a Modeling Approach to Assessing Bioequivalence or PK Similarity with Presence of Sparsely Sampled Subjects.” *Journal of Pharmacokinetics and Pharmacodynamics* 31 (4): 321–39.
<https://doi.org/10.1023/B:JOPA.0000042739.44458.e0>.
- Jones, H. M., and K. Rowland-Yeo. 2013. “Basic Concepts in Physiologically Based Pharmacokinetic Modeling in Drug Discovery and Development.” *CPT: Pharmacometrics and Systems Pharmacology* 2 (8): 1–12.
<https://doi.org/10.1038/psp.2013.41>.
- Lee, Jieon, Yuqing Gong, Sid Bhoopathy, Charles E. DiLiberti, Andrew C. Hooker, Amin Rostami-Hodjegan, Stephan Schmidt, et al. 2020. “Public Workshop Summary Report on Fiscal Year 2021 Generic Drug Regulatory Science Initiatives: Data Analysis and Model-Based Bioequivalence.” *Clinical Pharmacology and Therapeutics* 0 (0): 1–6. <https://doi.org/10.1002/cpt.2120>.
- Loingeville, Florence, Julie Bertrand, Thu Thuy Nguyen, Satish Sharan, Kairui Feng, Wanjie Sun, Jing Han, et al. 2020. “New Model-Based Bioequivalence Statistical Approaches for Pharmacokinetic Studies with Sparse Sampling.” *AAPS Journal* 22 (6): 1–8. <https://doi.org/10.1208/s12248-020-00507-3>.
- Madabushi, Rajanikanth, Paul Seo, Liang Zhao, Million Tegenge, and Hao Zhu. 2022. “Review: Role of Model-Informed Drug Development Approaches in the Lifecycle of Drug Development and Regulatory Decision-Making.” *Pharmaceutical Research*. Springer. <https://doi.org/10.1007/s11095-022-03288-w>.

- Mould, D. R., and R. N. Upton. 2012. “Basic Concepts in Population Modeling, Simulation, and Model-Based Drug Development.” *CPT: Pharmacometrics and Systems Pharmacology* 1 (1): 1–14. <https://doi.org/10.1038/psp.2012.4>.
- . 2013. “Basic Concepts in Population Modeling, Simulation, and Model-Based Drug Development - Part 2: Introduction to Pharmacokinetic Modeling Methods.” *CPT: Pharmacometrics and Systems Pharmacology* 2 (4). <https://doi.org/10.1038/psp.2013.14>.
- Oda, Kazutaka, Hideyuki Saito, and Hirofumi Jono. 2023. “Bayesian Prediction-Based Individualized Dosing of Anti-Methicillin-Resistant Staphylococcus Aureus Treatment: Recent Advancements and Prospects in Therapeutic Drug Monitoring.” *Pharmacology and Therapeutics*. Elsevier Inc. <https://doi.org/10.1016/j.pharmthera.2023.108433>.
- Salem, Ahmed M., Tao Niu, Chao Li, Brady S. Moffett, Vijay Ivaturi, and Mathangi Gopalakrishnan. 2022. “Reassessing the Pediatric Dosing Recommendations for Unfractionated Heparin Using Real-World Data: A Pharmacokinetic–Pharmacodynamic Modeling Approach.” *Journal of Clinical Pharmacology* 62 (6): 733–46. <https://doi.org/10.1002/jcph.2007>.
- Terranova, Nadia, Didier Renard, Mohamed H. Shahin, Sujatha Menon, Youfang Cao, Cornelis E.C.A. Hop, Sean Hayes, et al. 2024. “Artificial Intelligence for Quantitative Modeling in Drug Discovery and Development: An Innovation and Quality Consortium Perspective on Use Cases and Best Practices.” *Clinical Pharmacology and Therapeutics* 115 (4): 658–72. <https://doi.org/10.1002/cpt.3053>.
- Tsakalozou, Eleftheria, Khondoker Alam, Andrew Babiskin, and Liang Zhao. 2022. “Physiologically-Based Pharmacokinetic Modeling to Support Determination of Bioequivalence for Dermatological Drug Products: Scientific and Regulatory Considerations.” *Clinical Pharmacology and Therapeutics*. John Wiley and Sons Inc. <https://doi.org/10.1002/cpt.2356>.
- Tsakalozou, Eleftheria, Lanyan Fang, Youwei Bi, Michiel van den Heuvel, Tausif Ahmed, Yu Chung Tsang, Robert Lionberger, Amin Rostami-Hodjegan, and Liang Zhao. 2024. “Experience Learned and Perspectives on Using Model-Integrated Evidence in the Regulatory Context for Generic Drug Products—a Meeting Report.” *The AAPS Journal* 26 (1): 14. <https://doi.org/10.1208/s12248-023-00884-5>.
- U.S. Food and Drug Administration. 2022b. “Successes and Opportunities in Modeling & Simulation for FDA.” <https://www.fda.gov/science-research/about-science-research-fda/modeling-simulation-fda>.
- . 2024. “CDER Establishes New Quantitative Medicine Center of Excellence.” March 25, 2024. <https://www.fda.gov/drugs/drug-safety-and-availability/cder-establishes-new-quantitative-medicine-center-excellence>.

- Yoon, Miyoung, Andrew Babiskin, Meng Hu, Fang Wu, Sam G. Raney, Lanyan Fang, and Liang Zhao. 2023. “Increasing Impact of Quantitative Methods and Modeling in Establishment of Bioequivalence and Characterization of Drug Delivery.” *CPT: Pharmacometrics and Systems Pharmacology*. American Society for Clinical Pharmacology and Therapeutics. <https://doi.org/10.1002/psp4.12930>.
- Zhao, Liang, Myong Jin Kim, Lei Zhang, and Robert Lionberger. 2019. “Generating Model Integrated Evidence for Generic Drug Development and Assessment.” *Clinical Pharmacology and Therapeutics* 105 (2): 338–49. <https://doi.org/10.1002/cpt.1282>.

Chapter 2: There Is a Need to Improve Treatment Outcomes for *Staphylococcal aureus* Orthopedic Implant-Associated Infection

Staphylococcus aureus (*S. aureus*) is a major human pathogen that causes various clinical syndromes, including osteoarticular and device-related infections (Rasigade and Vandenesch 2014; Tong et al. 2015). It is one of the most common pathogens of biofilm-related infection on foreign implanted materials (Richter, Driessche, and Coenye 2017). Bacterial biofilm formation on the implant impedes penetration of immune cells and some antibiotics, creating chronic, persistent infections (Costerton, Stewart, and Greenberg 1999). *S. aureus* orthopedic implant-associated infections are exceedingly difficult to treat and may require surgery and prolonged systemic antibiotics. They are also associated with extended disability and rehabilitation, contributing to worse outcomes (Del Pozo and Patel 2009; Wolf et al. 2012). Although infection rates of orthopedic implant-associated infections have remained at 1 to 2% after primary and 3 to 6% after revision arthroplasty, inpatient costs average \$25,000 to \$107,000 per case, corresponding to an annual healthcare burden of \$3 billion in the United States alone (Kurtz et al. 2012). The emergence of methicillin-resistant *S. aureus* (MRSA) strains poses yet another challenge for the treatment of these complicated infections.

Combination treatment with rifampin is recommended by the Infectious Diseases Society of America (IDSA) for the treatment of staphylococcal implant-associated infections (Baddour et al. 2015; Osmon et al. 2013; Tunkel et al. 2017). Moreover, some experts recommend the combination treatment with rifampin for MRSA infection even without hardware, particularly for osteomyelitis and central nervous system infection (C. Liu et al. 2011). This is because rifampin enhances microbiological clearance (Van Der Auwera, Meunier-Carpentier, and Klastersky 1983; Van der Auwera et al. 1985; Euba et

al. 2009), and high clinical cure rates (>80%) are achieved only with the combinatory use of rifampin (Nguyen et al. 2009; Norden et al. 1986; Norden, Fierer, and Bryant 1983; Li et al. 2019; Zimmerli 1998; Karlsen et al. 2020). The most beneficial effect of combinatory treatment with rifampin was noted in implant-associated, in particular orthopedic implant-associated, infections. The lipophilicity of rifampin, its activity within the acidic environment of biofilms, and its accumulation within neutrophils likely facilitate its activity against implant-associated infections (Bennett 2019).

However, prolonged treatment duration (e.g., 6 to 12 weeks) is required to minimize treatment failure. In a recent randomized controlled study of patients with prosthetic joint infections, treatment failure was 18.1 and 9.4%, respectively, for 6 weeks versus 12 weeks of treatment, even with most patients receiving combinatory treatment with rifampin (70%) (Bernard et al. 2021). Prolonged antibiotic duration is associated with an increased risk of adverse drug events. In one study, every additional 10 days of antibiotic treatment conferred a 3% increased risk of an antibiotic-associated adverse event (Tamma et al. 2017). Prolonged use of antibiotics is also associated with emergence of multiresistant pathogens (Chastre et al. 2003). Thus, development of shorter rifampin-containing antibiotic regimens for the treatment of orthopedic implant-associated infections is an urgent, unmet clinical need. Furthermore, mortality rate of 10-30% for *S. aureus* versus 5-8% for all infecting species suggests treatment regimens could be improved (Zmistowski et al. 2013; Fischbacher and Borens 2019).

Rifampin has potent, dose-dependent sterilizing activity against Gram-positive bacteria including methicillin-susceptible *S. aureus* (MSSA) and MRSA. However, limited data are available regarding rifampin penetration into bone, and published data

report rifampin bone concentrations at single time points using invasive methods (Cluzel et al. 1984; Roth 1984; Sirot et al. 1977; 1983; Iversen et al. 1983; Thabit et al. 2019), precluding the ability to measure area under the concentration-time curve (AUC), which is most predictive of bactericidal activity for rifampin (Swaminathan et al. 2016; J. G. Pasipanodya et al. 2013; Chigutsa et al. 2015; Diacon et al. 2007). Furthermore, recent data showed that pathologically diverse lesions occur simultaneously at different sites within the same patient (Cassat et al. 2018; Hunter 2018). Thus, there is a need for holistic analysis of rifampin concentrations in various anatomic locations, which is generally not feasible with currently available methods that require invasive acquisition of tissue for drug measurement.

References

- Auwers, P Van der, J Klastersky, J P Thys, F Meunier-Carpentier, and J C Legrand. 1985. "Double-Blind, Placebo-Controlled Study of Oxacillin Combined with Rifampin in the Treatment of Staphylococcal Infections." *Antimicrobial Agents and Chemotherapy* 28 (4): 467–72. <https://doi.org/10.1128/AAC.28.4.467>.
- Auwers, P. Van Der, F. Meunier-Carpentier, and J. Klastersky. 1983. "Clinical Study of Combination Therapy with Oxacillin and Rifampin for Staphylococcal Infections." *Clinical Infectious Diseases* 5 (Supplement_3): S515–21. https://doi.org/10.1093/clinids/5.Supplement_3.S515.
- Baddour, Larry M., Walter R. Wilson, Arnold S. Bayer, Vance G. Fowler, Imad M. Tleyjeh, Michael J. Rybak, Bruno Barsic, et al. 2015. "Infective Endocarditis in Adults: Diagnosis, Antimicrobial Therapy, and Management of Complications: A Scientific Statement for Healthcare Professionals from the American Heart Association." *Circulation*. Lippincott Williams and Wilkins. <https://doi.org/10.1161/CIR.0000000000000296>.
- Bennett, John E.; Dolin, Raphael; Blaser, Martin J. 2019. *Mandell, Douglas, and Bennett's Principles and Practice of Infectious Diseases*. 9th ed. Elsevier.
- Bernard, Louis, Cédric Arvieux, Benoit Brunschweiler, Sophie Touchais, Séverine Ansart, Jean-Pierre Bru, Eric Oziol, et al. 2021. "Antibiotic Therapy for 6 or 12 Weeks for

- Prosthetic Joint Infection.” *New England Journal of Medicine* 384 (21): 1991–2001. <https://doi.org/10.1056/NEJMoa2020198>.
- Cassat, James E., Jessica L. Moore, Kevin J. Wilson, Zach Stark, Boone M. Prentice, Raf Van de Plas, William J. Perry, et al. 2018. “Integrated Molecular Imaging Reveals Tissue Heterogeneity Driving Host-Pathogen Interactions.” *Science Translational Medicine* 10 (432). <https://doi.org/10.1126/scitranslmed.aan6361>.
- Chigutsa, Emmanuel, Jotam G. Pasipanodya, Marianne E. Visser, Paul D. van Helden, Peter J. Smith, Frederick A. Sirgel, Tawanda Gumbo, and Helen McIlleron. 2015. “Impact of Nonlinear Interactions of Pharmacokinetics and MICs on Sputum Bacillary Kill Rates as a Marker of Sterilizing Effect in Tuberculosis.” *Antimicrobial Agents and Chemotherapy* 59 (1): 38–45. <https://doi.org/10.1128/AAC.03931-14>.
- Cluzel, R. A., R. Lopitiaux, J. Sirot, and S. Rampon. 1984. “Rifampicin in the Treatment of Osteoarticular Infections Due to Staphylococci.” *Journal of Antimicrobial Chemotherapy* 13 (suppl C): 23–29. https://doi.org/10.1093/jac/13.suppl_C.23.
- Costerton, J. W., Philip S. Stewart, and E. P. Greenberg. 1999. “Bacterial Biofilms: A Common Cause of Persistent Infections.” *Science* 284 (5418): 1318–22. <https://doi.org/10.1126/science.284.5418.1318>.
- Diacon, A. H., R. F. Patientia, A. Venter, P. D. van Helden, P. J. Smith, H. McIlleron, J. S. Maritz, and P. R. Donald. 2007. “Early Bactericidal Activity of High-Dose Rifampin in Patients with Pulmonary Tuberculosis Evidenced by Positive Sputum Smears.” *Antimicrobial Agents and Chemotherapy* 51 (8): 2994–96. <https://doi.org/10.1128/AAC.01474-06>.
- Euba, G., O. Murillo, N. Fernández-Sabé, J. Mascaró, J. Cabo, A. Pérez, F. Tubau, R. Verdaguer, F. Gudiol, and J. Ariza. 2009. “Long-Term Follow-Up Trial of Oral Rifampin-Cotrimoxazole Combination versus Intravenous Cloxacillin in Treatment of Chronic Staphylococcal Osteomyelitis.” *Antimicrobial Agents and Chemotherapy* 53 (6): 2672–76. <https://doi.org/10.1128/AAC.01504-08>.
- Fischbacher, Arnaud, and Olivier Borens. 2019. “Prosthetic-Joint Infections: Mortality Over The Last 10 Years.” *Journal of Bone and Joint Infection* 4 (4): 198–202. <https://doi.org/10.7150/jbji.35428>.
- Hunter, Robert L. 2018. “The Pathogenesis of Tuberculosis: The Early Infiltrate of Post-Primary (Adult Pulmonary) Tuberculosis: A Distinct Disease Entity.” *Frontiers in Immunology* 9 (September). <https://doi.org/10.3389/fimmu.2018.02108>.
- Iversen, P, O S Nielsen, K M Jensen, and P O Madsen. 1983. “Comparison of Concentrations of Rifampin and a New Rifamycin Derivative, DL 473, in Canine Bone.” *Antimicrobial Agents and Chemotherapy* 23 (2): 338–40. <https://doi.org/10.1128/AAC.23.2.338>.

- Karlsen, Øystein Espeland, Pål Borgen, Bjørn Bragnes, Wender Figved, Bjarne Grøgaard, Jonas Rydinge, Lars Sandberg, et al. 2020. “Rifampin Combination Therapy in Staphylococcal Prosthetic Joint Infections: A Randomized Controlled Trial.” *Journal of Orthopaedic Surgery and Research* 15 (1): 365. <https://doi.org/10.1186/s13018-020-01877-2>.
- Kurtz, Steven M., Edmund Lau, Heather Watson, Jordana K. Schmier, and Javad Parvizi. 2012. “Economic Burden of Periprosthetic Joint Infection in the United States.” *Journal of Arthroplasty* 27 (8 SUPPL.). <https://doi.org/10.1016/j.arth.2012.02.022>.
- Li, Ho-Kwong, Ines Rombach, Rhea Zambellas, A. Sarah Walker, Martin A. McNally, Bridget L. Atkins, Benjamin A. Lipsky, et al. 2019. “Oral versus Intravenous Antibiotics for Bone and Joint Infection.” *New England Journal of Medicine* 380 (5): 425–36. <https://doi.org/10.1056/NEJMoa1710926>.
- Liu, Catherine, Arnold Bayer, Sara E Cosgrove, Robert S Daum, Scott K Fridkin, Rachel J Gorwitz, Sheldon L Kaplan, et al. 2011. “Clinical Practice Guidelines by the Infectious Diseases Society of America for the Treatment of Methicillin- Resistant Staphylococcus Aureus Infections in Adults and Children” 52. <https://doi.org/10.1093/cid/ciq146>.
- Norden, Carl W., Richard Bryant, Darwin Palmer, John Z. Montgomerie, and Joseph Wheat. 1986. “Chronic Osteomyelitis Caused by Staphylococcus Aureus: Controlled Clinical Trial of Nafcillin Therapy and Nafcillin-Rifampin Therapy.” *Southern Medical Journal* 79 (8): 947–51. <https://doi.org/10.1097/00007611-198608000-00008>.
- Norden, Carl W., Joshua Fierer, and Richard E. Bryant. 1983. “Chronic Staphylococcal Osteomyelitis: Treatment with Regimens Containing Rifampin.” *Clinical Infectious Diseases* 5 (Supplement_3): S495–501. https://doi.org/10.1093/clinids/5.Supplement_3.S495.
- Nguyen, S., A. Pasquet, L. Legout, E. Beltrand, L. Dubreuil, H. Migaud, Y. Yazdanpanah, and E. Senneville. 2009. “Efficacy and Tolerance of Rifampicin–Linezolid Compared with Rifampicin–Cotrimoxazole Combinations in Prolonged Oral Therapy for Bone and Joint Infections.” *Clinical Microbiology and Infection* 15 (12): 1163–69. <https://doi.org/10.1111/j.1469-0691.2009.02761.x>.
- Osmon, Douglas R, Elie F Berbari, Anthony R Berendt, Daniel Lew, Werner Zimmerli, James M Steckelberg, Nalini Rao, Arlen Hanssen, and Walter R Wilson. 2013. “Diagnosis and Management of Prosthetic Joint Infection: Clinical Practice Guidelines by the Infectious Diseases Society of America.” *Clinical Infectious Diseases* 56 (1): e1–25. <https://doi.org/10.1093/cid/cis803>.
- Pasipanodya, J. G., H. McIlleron, A. Burger, P. A. Wash, P. Smith, and T. Gumbo. 2013. “Serum Drug Concentrations Predictive of Pulmonary Tuberculosis Outcomes.”

- Journal of Infectious Diseases* 208 (9): 1464–73.
<https://doi.org/10.1093/infdis/jit352>.
- Pozo, Jose L. Del, and Robin Patel. 2009. “Infection Associated with Prosthetic Joints.” *New England Journal of Medicine* 361 (8): 787–94.
<https://doi.org/10.1056/NEJMcp0905029>.
- Rasigade, Jean Philippe, and François Vandenesch. 2014. “Staphylococcus Aureus: A Pathogen with Still Unresolved Issues.” *Infection, Genetics and Evolution* 21 (January):510–14. <https://doi.org/10.1016/j.meegid.2013.08.018>.
- Richter, Katharina, Freija Van Den Driessche, and Tom Coenye. 2017. “Innovative Approaches to Treat Staphylococcus Aureus Biofilm-Related Infections,” no. March, 61–70. <https://doi.org/10.1042/EBC20160056>.
- Roth, B. 1984. “Penetration of Parenterally Administered Rifampicin into Bone Tissue.” *Chemotherapy* 30 (6): 358–65. <https://doi.org/10.1159/000238294>.
- Sirof, J, R Lopitiaux, R Cluzel, J J Delisle, and B Sauvezie. 1977. “[Rifampicin Diffusion in Non-Infected Human Bone (Author’s Transl)].” *Annales de Microbiologie* 128 (2): 229–36.
- Sirof, J, L Prive, R Lopitiaux, and Y Glanddier. 1983. “[Diffusion of Rifampicin into Spongy and Compact Bone Tissue during Total Hip Prosthesis Operation].” *Pathologie-Biologie* 31 (5): 438–41.
- Swaminathan, Soumya, Jotam G. Pasipanodya, Geetha Ramachandran, A. K. Hemanth Kumar, Shashikant Srivastava, Devyani Deshpande, Eric Nuermberger, and Tawanda Gumbo. 2016. “Drug Concentration Thresholds Predictive of Therapy Failure and Death in Children With Tuberculosis: Bread Crumb Trails in Random Forests.” *Clinical Infectious Diseases* 63 (suppl 3): S63–74.
<https://doi.org/10.1093/cid/ciw471>.
- Tamma, Pranita D., Edina Avdic, David X. Li, Kathryn Dzintars, and Sara E. Cosgrove. 2017. “Association of Adverse Events With Antibiotic Use in Hospitalized Patients.” *JAMA Internal Medicine* 177 (9): 1308.
<https://doi.org/10.1001/jamainternmed.2017.1938>.
- Thabit, Abrar K., Dania F. Fatani, Maryam S. Bamakhrama, Ola A. Barnawi, Lana O. Basudan, and Shahad F. Alhejaili. 2019. “Antibiotic Penetration into Bone and Joints: An Updated Review.” *International Journal of Infectious Diseases* 81 (April):128–36. <https://doi.org/10.1016/j.ijid.2019.02.005>.
- Tong, Steven Y.C., Joshua S. Davis, Emily Eichenberger, Thomas L. Holland, and Vance G. Fowler. 2015. “Staphylococcus Aureus Infections: Epidemiology, Pathophysiology, Clinical Manifestations, and Management.” *Clinical Microbiology Reviews* 28 (3): 603–61. <https://doi.org/10.1128/CMR.00134-14>.

- Tunkel, Allan R, Rodrigo Hasbun, Adarsh Bhimraj, Karin Byers, Sheldon L Kaplan, W Michael Scheld, Diederik van de Beek, Thomas P Bleck, Hugh J.L. Garton, and Joseph R Zunt. 2017. “2017 Infectious Diseases Society of America’s Clinical Practice Guidelines for Healthcare-Associated Ventriculitis and Meningitis*.” *Clinical Infectious Diseases* 64 (6): e34–65. <https://doi.org/10.1093/cid/ciw861>.
- Wolf, Brian R., Xin Lu, Yue Li, John J. Callaghan, and Peter Cram. 2012. “Adverse Outcomes in Hip Arthroplasty: Long-Term Trends.” *Journal of Bone and Joint Surgery* 94 (14): e103(1). <https://doi.org/10.2106/JBJS.K.00011>.
- Zimmerli, Werner. 1998. “Role of Rifampin for Treatment of Orthopedic Implant–Related Staphylococcal Infections: A Randomized Controlled Trial.” *JAMA* 279 (19): 1537. <https://doi.org/10.1001/jama.279.19.1537>.
- Zmistowski, Benjamin, Joseph A. Karam, Joel B. Durinka, David S. Casper, and Javad Parvizi. 2013. “Periprosthetic Joint Infection Increases the Risk of One-Year Mortality.” *The Journal of Bone & Joint Surgery* 95 (24): 2177–84. <https://doi.org/10.2106/JBJS.L.00789>.

Chapter 3: Mice and Human PK Are Dissimilar With ¹¹C-Rifampin Microdosing

3.1 Introduction

In this study, we used a bidirectional process to integrate findings from animal and human studies (Figure 3). ¹¹C-rifampin, a chemically identical radiolabeled analog of rifampin, was administered, and positron emission tomography (PET) with computed tomography (CT) (DeMarco et al. 2015; Ordonez et al. 2020; Tucker et al. 2018) imaging was performed in prospectively enrolled patients with *S. aureus* bone infections or in patients without *S. aureus* infection to noninvasively measure detailed intralesional rifampin bone concentration-time profiles at several anatomic sites (Ordonez et al. 2020). This provided a translational bridge to facilitate pharmacokinetic (PK) modeling and predict rifampin concentration-time profiles in bone tissues. ¹¹C-rifampin PET studies in a mouse model of *S. aureus* orthopedic implant infection (Thompson et al. 2017) as well as direct rifampin measurements from postmortem bone tissues were performed and applied to an in vitro *S. aureus* biofilm system to assess bacterial killing and biofilm disruption using live, time-lapse imaging (Merritt, Kadouri, and O’Toole 2006). These data were used to design studies to evaluate high-dose rifampin-containing regimens in mice as compared to standard (IDSA-recommended) rifampin regimens, administered at human-equipotent doses achieving similar plasma AUC in mice with *S. aureus* orthopedic implant infection. Mice were assessed for relapse-free cure 6 weeks after completion of antibiotic treatment. High-resolution CT was used to measure bone remodeling (Tucker et al. 2018), and antimicrobial susceptibility testing, as well as whole-genome bacterial sequencing, was performed for all bacterial isolates obtained from mice after treatment completion.

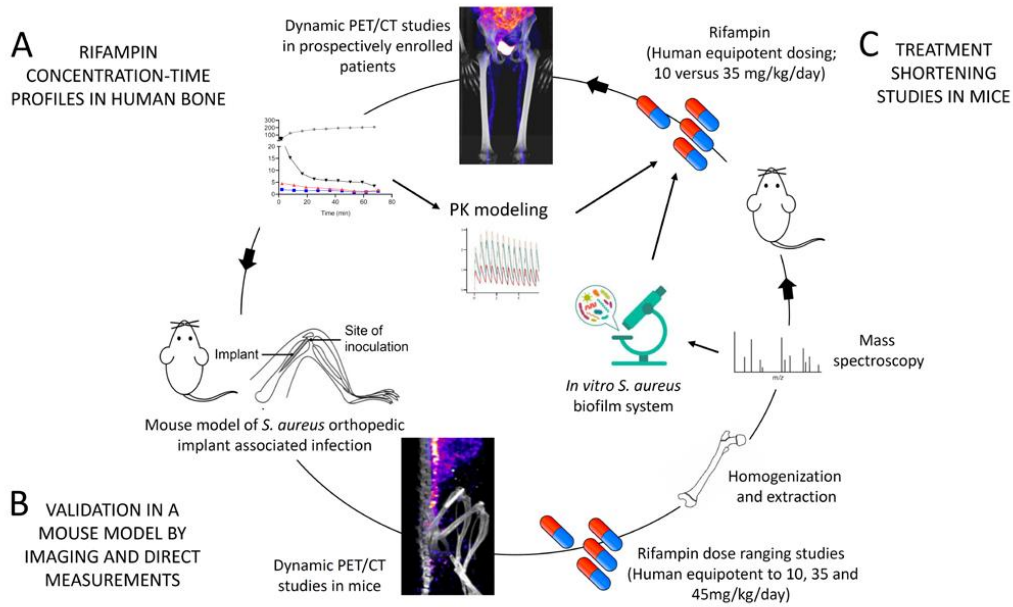


Figure 3 Experimental Scheme to Study Rifampin Dosing for Orthopedic Implant-Associated Infection

We utilized a bidirectional process to integrate findings from animal and human studies. (A) Patients with or without *S. aureus* orthopedic infection were imaged using ^{11}C -rifampin PET/CT. PET signal was quantified in infected and uninfected bone to generate time-activity curves used to calculate area under the concentration-time curve over 45-90 minutes. These data were used to develop a pharmacokinetic (PK) model to predict rifampin exposures in human bone. (B) A validated mouse model of *S. aureus* orthopedic implant infection was used to determine bone concentrations following administration of escalating rifampin oral dosing as well as ^{11}C -rifampin PET/CT. Resulting concentrations were applied to an in vitro *S. aureus* biofilm system to quantify bacterial killing and biofilm disruption using time lapse microscopy. m/z , mass/charge ratio. (C) Efficacy studies in mice compared vancomycin alone to vancomycin with either standard-dose or high-dose rifampin administered at human equipotent doses. Readouts included weekly in vivo bioluminescence, bacterial load, and broth cultures at completion of follow up and high-resolution CT to evaluate adverse bone remodeling. At the end of the study, bacterial isolates recovered from infected tissues were evaluated for phenotypic resistance as well as subjected to whole-genome sequencing.

Here, we describe the ^{11}C -rifampin microdose PK modeling that was performed to describe ^{11}C -rifampin microdose PK in mice and humans, as well as the biodistribution to uninfected and infected bone tissue. Several assumptions were examined, including whether biodistribution to uninfected and infected bone tissue were dissimilar, whether *S. aureus* bone infection patients and tuberculosis (TB) patients

without bone infections had similar ^{11}C -rifamping PK, and whether ^{11}C -rifamping PK could be scaled allometrically between mice and humans.

3.2 Methods

- *Study Design*

All protocols were approved by the Johns Hopkins University Biosafety, Radiation Safety, Animal Care and Use (MO19M382, MO15M421, and SP17M176) and Institutional Review Board Committees (IRB00067243 and IRB00179210). Dynamic ^{11}C -rifampin PET/computed tomography (CT) was used in patients with *S. aureus* bone infections ($n = 3$) as well as patients with pulmonary TB but without orthopedic infection ($n = 12$) (Ordonez et al. 2020) to measure concentration-time profiles in bone and plasma to determine bone-to-plasma AUC ratios ($\text{AUC}_{\text{bone/plasma}}$) at several anatomic sites.

- *Human Studies*

^{11}C -Rifampin was synthesized as a sterile, pyrogen-free solution of high specific activity ($595.87 \pm 158.15 \text{ GBq}/\mu\text{mol}$) and high radio-chemical purity at the Johns Hopkins PET Radiotracer Center using Current Good Manufacturing Practices and used per the U.S. FDA Radioactive Drug Research Committee program guidelines. Three patients with microbiologically confirmed *S. aureus* bone infections were prospectively recruited between February and December 2020. Written informed consent was obtained from all patients, and deidentified images are presented. The eligibility criteria are outlined in Table 1. The subjects received an intravenous bolus of $707.4 \pm 43.7 \text{ MBq}$ of ^{11}C -rifampin followed immediately by a dynamic PET/CT for 60 to 90 min (Biograph

mCT, Siemens) using a multi-bed dynamic protocol. The study team had no role in the diagnosis or clinical management of the patients. There was no external data and safety monitoring board.

Table 1 Selection Criteria for Patient Enrollment in the Clinical Study

Greater than or equal to 18 years of age
Culture confirmation of <i>S. aureus</i> infection from blood or bone
A diagnosis of osteomyelitis confirmed by imaging (e.g., X-ray, CT, MRI)
Patient received appropriate antibiotic treatment for ≤ 6 weeks by the time of ^{11}C -rifampin PET/CT
Not pregnant
Platelet count $>50,000/\text{mm}^3$
Neutrophil count $>1,000/\text{mm}^3$
Serum creatinine <3 times the upper limit of normal
Total bilirubin <3 times the upper limit of normal
Liver transaminases <5 times the upper limit of normal
Did not receive an investigational drug, investigational biologic, or investigational therapeutic device within 30 days prior to ^{11}C -rifampin PET/CT
No prior history of malignancy within 3 years, other than skin basal cell carcinoma
Did not receive a radioisotope within 5 physical half lives prior to ^{11}C -rifampin PET/CT
Adequate venous access
Ability to provide written informed consent

Dynamic PET/CT (Biograph mCT, Siemens) data from 12 patients with confirmed pulmonary TB from a previous study were used to measure bone penetration at various anatomic sites (Ordonez et al. 2020). All patients had a physical exam before imaging by a trained physician, and no findings related to the musculoskeletal system were noted.

- *Bacterial Strains*

The USA300 bioluminescent *S. aureus* strain SAP231 derived from the NRS384 CA-MRSA isolated from an outbreak in the Mississippi prison system was used for all

experiments (Plaut et al. 2013). SAP231 has a stably integrated modified *luxABCDE* operon from the bacterial insect pathogen *Photorhabdus luminescens* and was used previously to study orthopedic implant infections (Bernthal et al. 2010; Thompson et al. 2017; Pribaz et al. 2012). The minimal inhibitory concentrations (MICs) for SAP231 were ≤ 0.5 mg/L for rifampin, 1 mg/L for vancomycin, and \leq mg/L for linezolid, as determined by the microdilution assay ($n = 3$ replicates per antibiotic).

SAP231 was streaked onto tryptic soy agar (TSA) plates [tryptic soy broth (TSB; TSA plus 1.5% Bacto Agar)] (BD Biosciences) and grown overnight at 37°C in a bacterial incubator. Two to three colonies were picked and cultured in TSB at 37°C in a shaking incubator (MaxQ HP 420, Thermo Fisher) (240 rpm) overnight (16 hours), followed by a 1:50 subculture at 37°C for 2 hours to obtain mid-logarithmic phase bacteria. The bacteria were pelleted, washed three times, and resuspended in sterile phosphate-buffered saline. The absorbance (A_{600}) was measured to estimate the number of colony-forming units, which was verified after overnight culture on TSA plates.

- *PET/CT Imaging*

Live mice with *S. aureus* implant infection were imaged after an intravenous dose of 5.03 ± 0.02 MBq of ^{11}C -rifampin via the tail vein, and dynamic PET was performed over 60 min using a nanoScan PET/CT (Mediso) small-animal imager (Pribaz et al. 2012).

- *Image Analysis*

¹¹C-Rifampin PET/CT were visualized using Mirada XD 3.6 (Mirada Medical) or VivoQuant 2020 (Invicro) for human and mice, respectively. 3D spherical Volumes of interest (VOIs) were manually drawn using CT as a guide and applied to the dynamic PET data (Ordonez et al. 2020; Tucker et al. 2018). VOIs are shown in Figure 4. PET signal in blood (left ventricle; corrected to plasma using the individual hematocrit values from each patient or using a 50% hematocrit value in mice), infected bone (visualized on magnetic resonance imaging or CT in human subjects or 25% distal femur in mice), and contralateral uninfected region (e.g., contralateral tibia or foot in humans and contralateral 25% of distal femur in mice) as well as other uninfected bones (humerus head, humerus shaft, and cervical and lumbar spine) was measured. PMOD 4.1 (PMOD Technologies) and VivoQuant 2020, for human and mice, respectively, were used to generate time-activity curves. Tissue density [Hounsfield unit obtained by CT] was used to convert the PET data to per mass of tissue. The implants (identified based on radiodensity >5000 Hounsfield units) were excluded from the image analysis in all studies. Heat map overlays were implemented using R software (R Foundation for Statistical Computing).

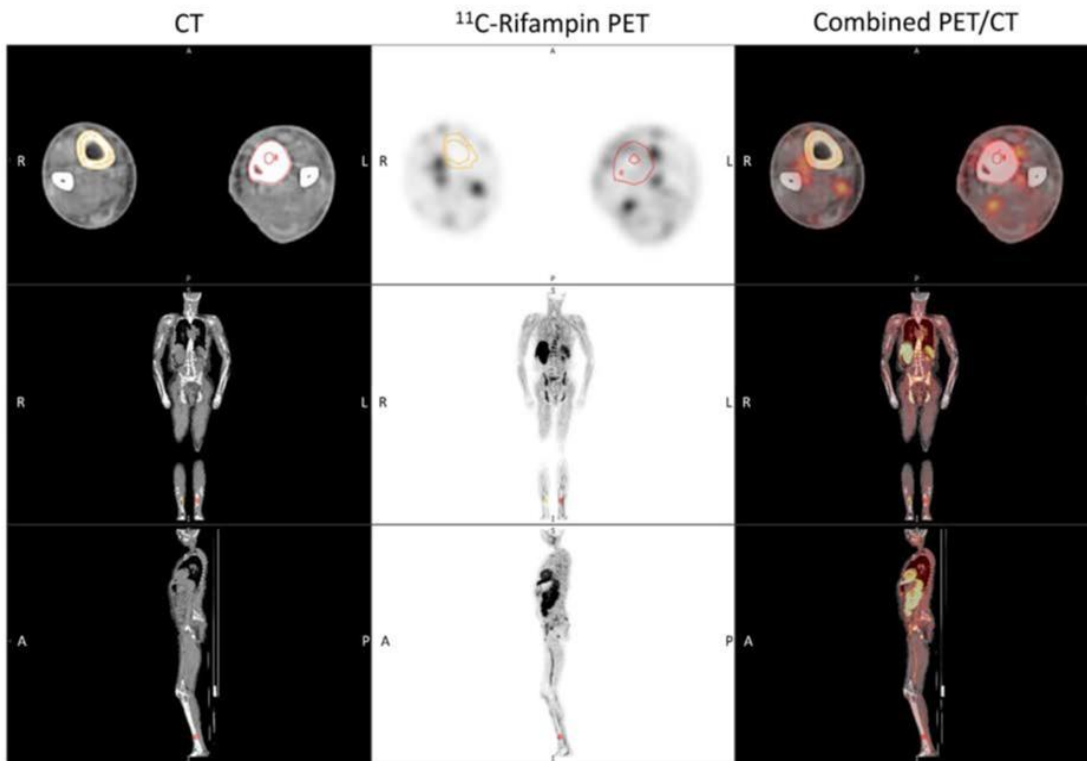


Figure 4 Volumes of Interest (VOIs) for Quantification of ^{11}C -Rifampin PET

VOIs were drawn to quantify ^{11}C -rifampin PET uptake in infected [anatomical left (L), red] and contralateral uninfected tibial bone [anatomical right (R), yellow]. Axial (top), coronal (middle) and sagittal (bottom) views are shown for study participant 1. Areas with high PET activity surrounding the bone represent blood vessels. A- anterior, P - posterior.

- ^{11}C -Rifampin Microdose PK Model Development

Non-linear mixed effects modeling (NLME) was performed with Pumas 2.0 (Pumas-AI) (Rackauckas et al. 2020). For initial model development, modeling was performed on five separate ^{11}C -rifampin PET imaging data sets: combined (mouse + human) ($n = 23$), mouse ($n = 8$), human ($n = 15$), TB human ($n = 12$), and *S. aureus* human ($n = 3$). To describe the intravenous ^{11}C -rifampin PET data, one- and two-compartment models were explored with two additional compartments from the central

compartment for uninfected and infected bone compartments. Averaging uninfected and infected bone concentrations to obtain one bone concentration per sampling timepoint was also explored. With the averaged bone concentrations, model development included exploring two bone compartments to investigate the possibility of surface and deep bone compartments (Rao et al. 1995; Cremers et al. 2003).

Allometric scaling, with normalization to 70kg bodyweight, was applied to the modeling of all five data sets to compare parameter estimates and determine 1) whether the PK was different between TB and *S. aureus* patients and 2) whether the PK was different between mice and humans.

For model refinement, the structural model was selected based on goodness-of-fit plots and parameter identifiability. The final model was evaluated based on goodness-of-fit plots and bootstrapping to evaluate the stability and robustness of the final model.

3.3 Results

Structural models with compartments for uninfected and infected bone compartments were explored. However, a pattern was not observed in terms of uninfected or infected bone tissue having higher ¹¹C-rifampin concentrations (Figure 5) in either mice or humans. Hence, for mice and humans with both uninfected and infected bone samples, the concentrations were averaged to have one bone concentration per timepoint. The final model was a one-compartment model with two additional bone compartments (Figure 6).

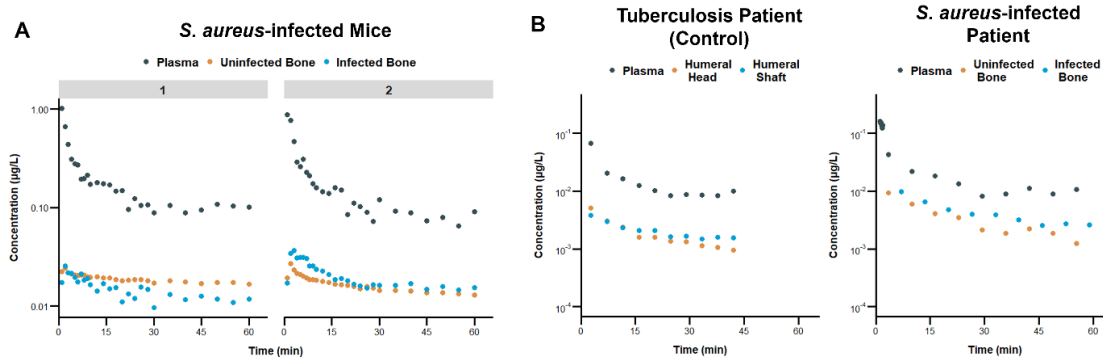


Figure 5 ¹¹C-Rifampin Microdose PK Profiles for Representative Mice and Humans

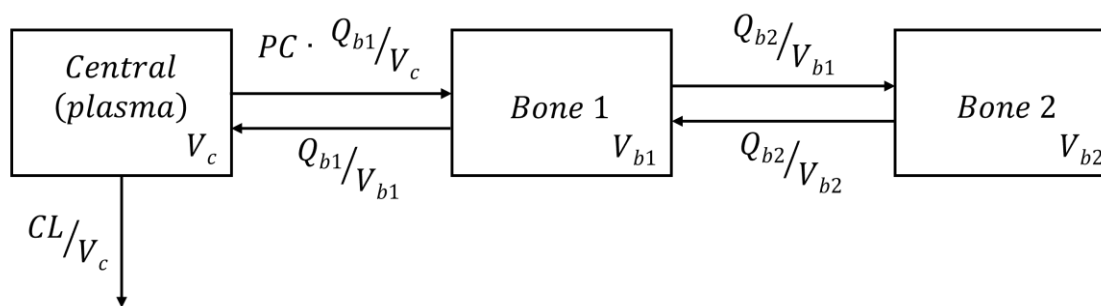


Figure 6 ¹¹C-Rifampin Microdose PK Model Structure

Parameter estimates are shown in Table 2. As parameter estimates were not markedly different between TB and *S. aureus* patients, the PK for both patient populations were not considered to be different. Marked differences, however, were noted in the parameter estimates between mice and humans. Particularly, clearance was about ten times greater in humans than mice. Due to the differences in mice and human PK parameter estimates, the final models and parameter estimates carried forward were those for mice and humans, separately. Rifampin penetration into bone tissue was modeled with a partition coefficient (PC) reflecting the ratio of rifampin concentration in bone over plasma. PC for mice and human were 10 and 15%, respectively. The final models

predicted the plasma and bone concentrations well for both mice and humans (Figures 7-10).

Table 2 Parameter Estimates from ¹¹C-Rifampin Microdose PK Modeling in Mouse and Human

Parameter	Combined (M+H) (n=23)	Mouse (n=8)	Human (n=15)	TB Human (n=12)	S. aureus Human (n=3)
CL (L/min/70kg)	0.18	0.06	0.58	0.60	0.33
Q _{b1} (L/min/70kg)	8.77	4.34	12.8	12.9	15.3
Q _{b2} (L/min/70kg)	21.0	15.3	35.6	34.5	17.9
V _c (L/70kg)	10.9	6.51	10.2	11.5	9.30
V _{b1} (L/70kg)	0.98	0.93	0.00023	0.087	1.22
V _{b2} (L/70kg)	364	556	195	188	284
PC	0.14	0.10	0.15	0.15	0.17

Abbreviations: CL=clearance, Q_b=intercompartmental clearance with bone compartment, V_c=volume of central compartment, V_b=volume of bone compartment, PC=partition coefficient (bone/plasma), M=mouse, H=human

Mouse Plasma (Microdosing)

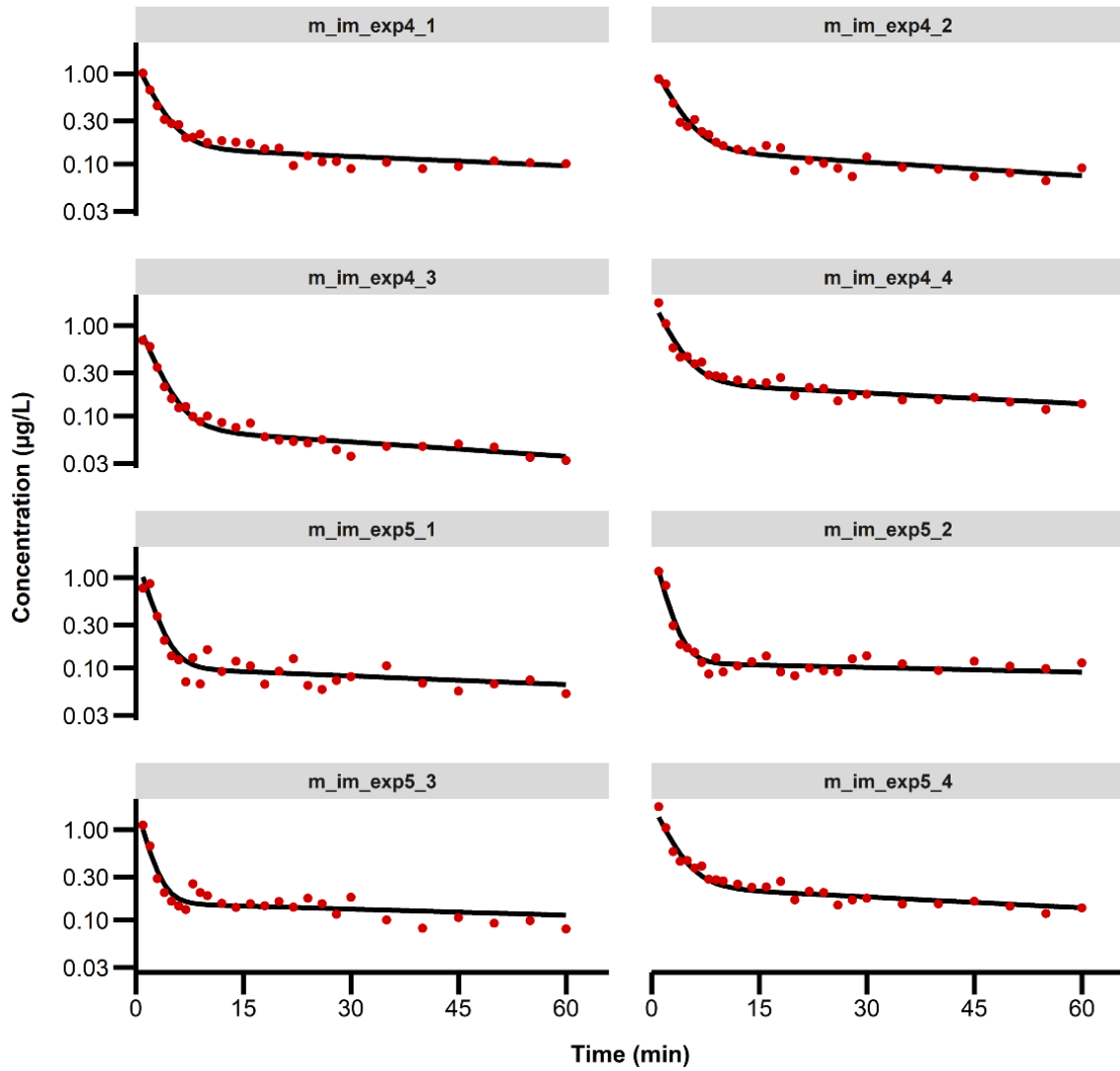


Figure 7 ¹¹C-Rifampin Microdose Mouse Model Individual Predictions for Plasma

Mouse Bone (Microdosing)

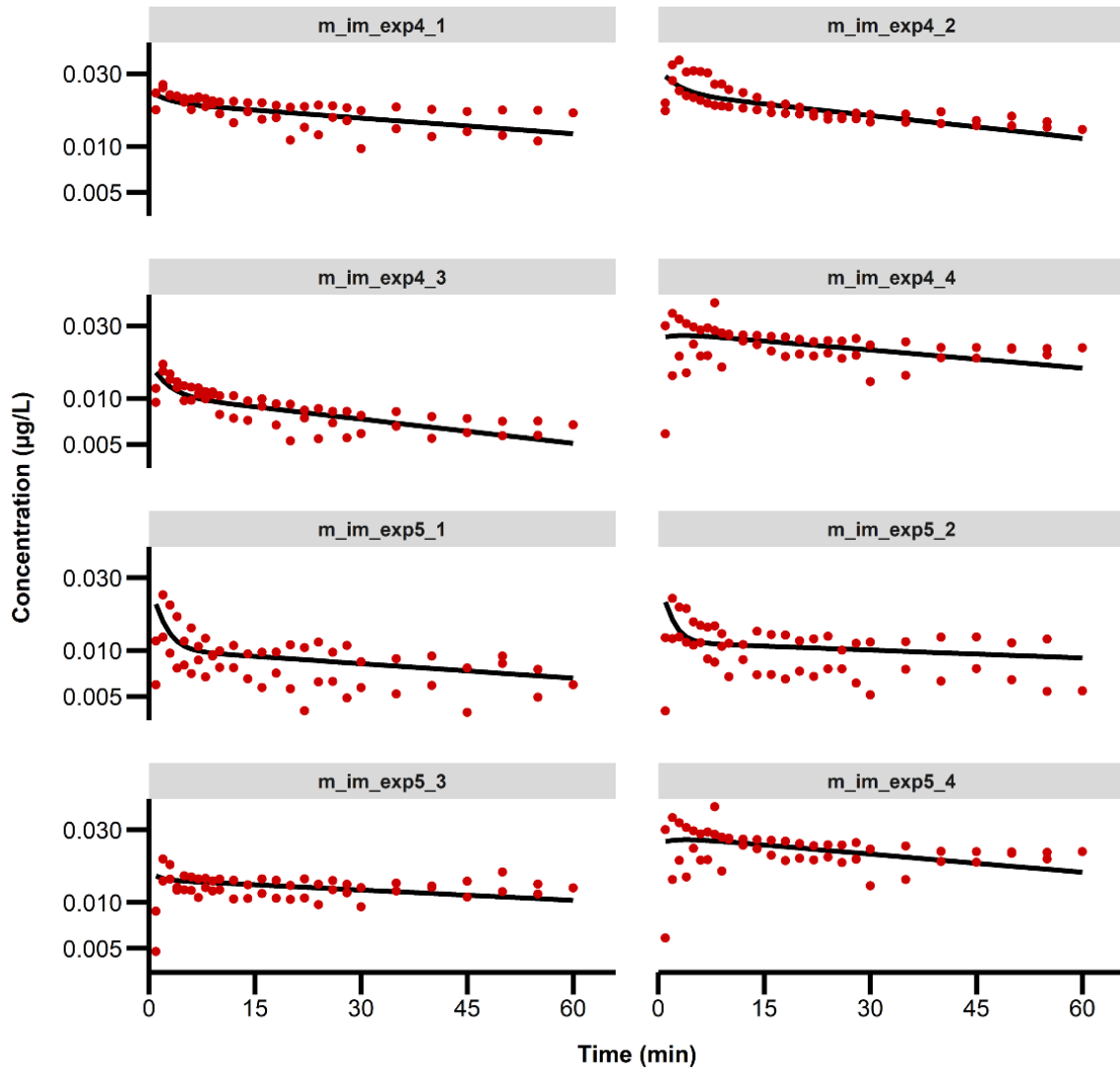


Figure 8 ¹¹C-Rifampin Microdose Mouse Model Individual Predictions for Bone Tissue

Human Plasma (Microdosing)

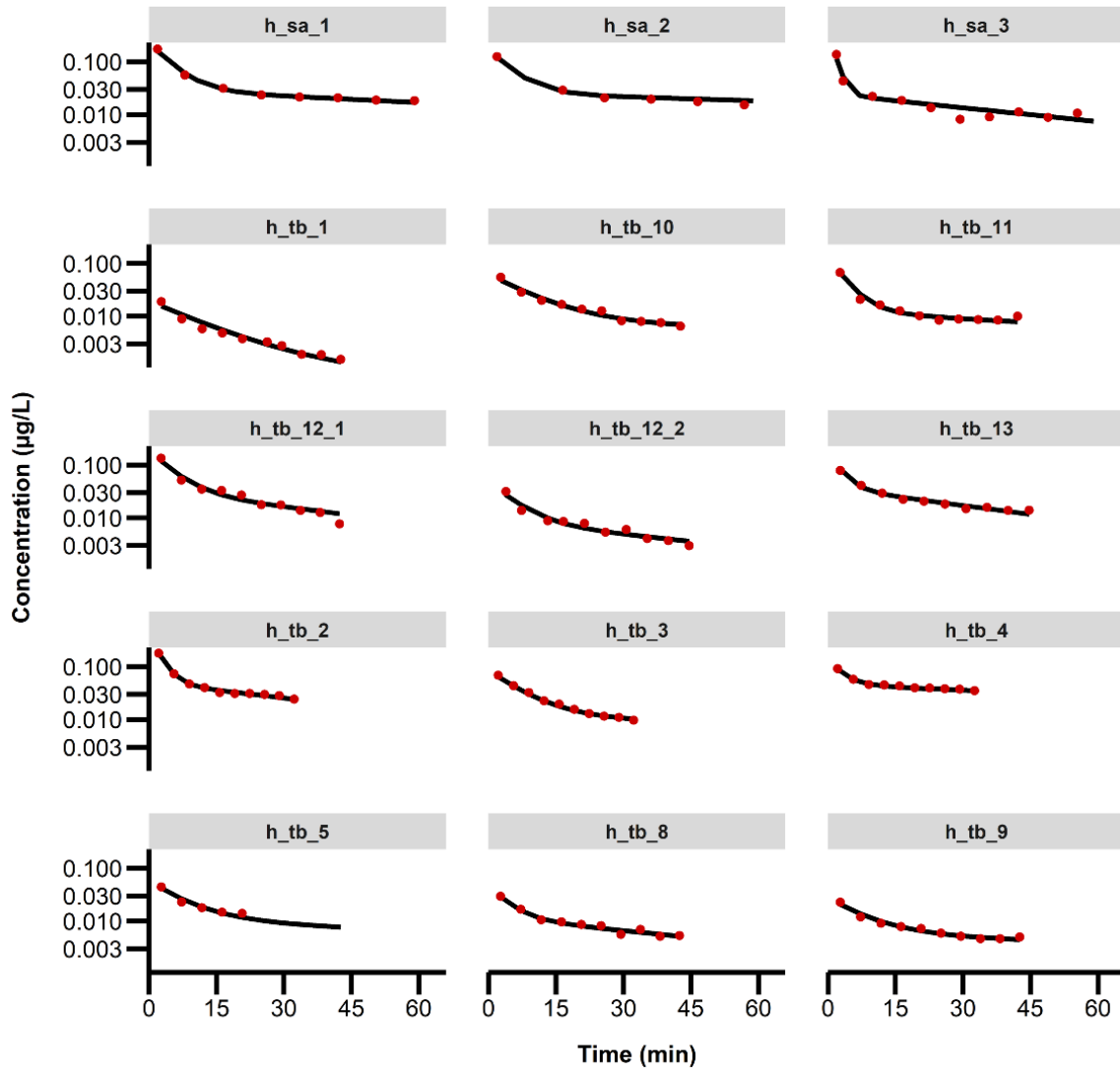


Figure 9 ^{11}C -Rifampin Microdose Human Model Individual Predictions for Plasma

Human Bone (Microdosing)

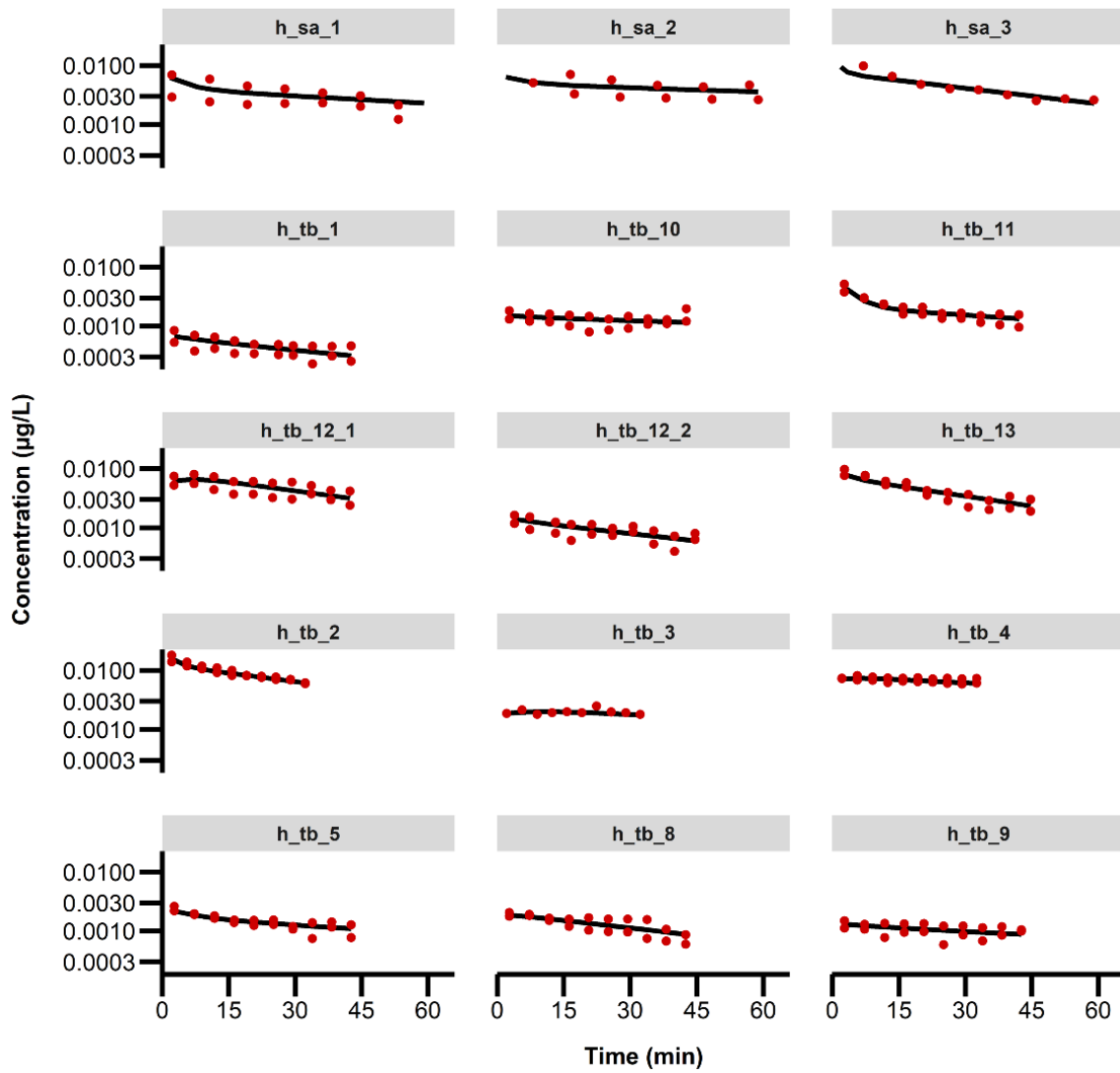


Figure 10 ¹¹C-Rifampin Microdose Human Model Individual Predictions for Bone Tissue

3.4 Discussion

We used a bidirectional process to integrate findings from animal and human studies. Dynamic ^{11}C -rifampin PET/CT, a clinically translatable, noninvasive imaging technology, was performed in patients with and without *S. aureus* orthopedic infection, demonstrating rifampin exposures considerably lower (plasma-to-bone AUC ratio of 0.14) than previously thought, based on single time-point invasive measurements (plasma-to-bone ratio of 0.4) (Cluzel et al. 1984; Roth 1984; Sirot et al. 1983; 1977; Thabit et al. 2019; Iversen et al. 1983). This is relevant as AUC is most predictive of bactericidal activity for rifampin (Diacon et al. 2007; Chigutsa et al. 2015; J. G. Pasipanodya et al. 2013; Swaminathan et al. 2016). Similar ^{11}C -rifampin PET findings were noted in a mouse model of *S. aureus* orthopedic implant infection, where direct measurements of plasma rifampin were in agreement with previous reports (Jayaram et al. 2003; Jotam G Pasipanodya et al. 2018) and direct measurements of bone concentrations validated the imaging data. These concentrations led to higher bacterial killing and biofilm disruption in an in vitro *S. aureus* biofilm system (data not shown).

Three hypotheses were tested in the ^{11}C -rifampin microdose modeling. While we hypothesized that biodistribution of rifampin to bone tissue may be different between uninfected and infected bone tissue due to factors such as blood flow and inflammation, we were unable to identify any relationship either in mice or human PET imaging data. Additionally, we hypothesized that the PK between *S. aureus* and TB patients would be sufficiently similar so as to allow us to combine their data. While there are some reports that rifampin PK can be affected by disease states (Abdelgawad et al. 2024), we did not find substantial differences between *S. aureus* and TB patients, though our sample of *S.*

aureus patients was limited to three patients. Finally, we hypothesized that we could allometrically scale between mice and human rifampin PK. Mice clearance was found to be ten times lower than human clearance, however, indicating that scaling would not be possible. We attribute this difference largely to protein binding, with protein binding of approximately 97% in mice and 90% in humans (De Steenwinkel et al. 2013; Boman and Ringberger 1974; L. H.M. Te Brake et al. 2015; van Ewijk-Beneken Kolmer et al. 2017; Litjens et al. 2019; Alghamdi, Al-Shaer, and Peloquin 2018). The larger estimated bone penetration in mice of 15% as opposed to in humans of 10% may also be attributed to this difference in protein binding, as the partition coefficient is likely largely reflective of how much drug is available to the bone tissue.

The findings of this work are largely limited by limitations inherent to PET imaging studies (Wagner and Langer 2011; Lappin, Noveck, and Burt 2013). These limitations include the ability to monitor for only about 1-1.5 hours, due to the short radioactive half-life of ¹¹C-rifampin (DeMarco et al. 2015). Rifampin is reported to have a half life of approximately 2-3 hours in humans at steady state (Acocella 1978), so we were only able to capture a limited portion of the PK profile. Yet, rifampin follows 1-compartment kinetics (Svensson et al. 2018), increasing our confidence in our ability to adequately capture rifampin's PK with our microdose modeling. Microdosing may also not be reflective of therapeutic dosing due to dose disproportionality (Wagner and Langer 2011; Lappin, Noveck, and Burt 2013), and in particular, this has been reported previously for rifampin (Ordonez et al. 2020). Due to these limitations, we constrain our findings from the ¹¹C-rifampin microdose modeling primarily to the bone penetration-related findings.

3.5 References

- Abdelgawad, Noha, Maxwell Chirehwa, Charlotte Schutz, David Barr, Amy Ward, Saskia Janssen, Rosie Burton, et al. 2024. "Pharmacokinetics of Antitubercular Drugs in Patients Hospitalized with HIV-Associated Tuberculosis: A Population Modeling Analysis." *Wellcome Open Research* 7 (March):72. <https://doi.org/10.12688/wellcomeopenres.17660.3>.
- Acocella, G. 1978. "Clinical Pharmacokinetics of Rifampicin." *Clinical Pharmacokinetics* 3 (2): 108–27. <https://doi.org/10.2165/00003088-197803020-00002>.
- Alghamdi, Wael A, Mohammad H. Al-Shaer, and Charles A. Peloquin. 2018. "Protein Binding of First-Line Antituberculosis Drugs." *Antimicrobial Agents and Chemotherapy* 62 (7): 1–7. <https://doi.org/10.1128/AAC.00641-18>.
- Berenthal, Nicholas M., Alexandra I. Stavrakis, Fabrizio Billi, John S. Cho, Thomas J. Kremen, Scott I. Simon, Ambrose L. Cheung, et al. 2010. "A Mouse Model of Post-Arthroplasty Staphylococcus Aureus Joint Infection to Evaluate in Vivo the Efficacy of Antimicrobial Implant Coatings." *PLoS ONE* 5 (9): 1–11. <https://doi.org/10.1371/journal.pone.0012580>.
- Boman, G, and V. A. Ringberger. 1974. "Binding of Rifampicin by Human Plasma Proteins." *European Journal of Clinical Pharmacology* 7 (5): 369–73. <https://doi.org/10.1007/BF00558209>.
- Brake, L. H.M. Te, R. Ruslami, H. Later-Nijland, F. Mooren, M. Teulen, L. Apriani, J. B. Koenderink, et al. 2015. "Exposure to Total and Protein-Unbound Rifampin Is Not Affected by Malnutrition in Indonesian Tuberculosis Patients." *Antimicrobial Agents and Chemotherapy* 59 (6): 3233–39. <https://doi.org/10.1128/AAC.03485-14>.
- Chigutsa, Emmanuel, Jotam G. Pasipanodya, Marianne E. Visser, Paul D. van Helden, Peter J. Smith, Frederick A. Sirgel, Tawanda Gumbo, and Helen McIlleron. 2015. "Impact of Nonlinear Interactions of Pharmacokinetics and MICs on Sputum Bacillary Kill Rates as a Marker of Sterilizing Effect in Tuberculosis." *Antimicrobial Agents and Chemotherapy* 59 (1): 38–45. <https://doi.org/10.1128/AAC.03931-14>.
- Cluzel, R. A., R. Lopitiaux, J. Sirot, and S. Rampon. 1984. "Rifampicin in the Treatment of Osteoarticular Infections Due to Staphylococci." *Journal of Antimicrobial Chemotherapy* 13 (suppl C): 23–29. https://doi.org/10.1093/jac/13.suppl_C.23.
- DeMarco, Vincent P., Alvaro A. Ordonez, Mariah Klunk, Brendan Prideaux, Hui Wang, Zhang Zhuo, Peter J. Tonge, et al. 2015. "Determination of ¹¹C-Rifampin Pharmacokinetics within Mycobacterium Tuberculosis-Infected Mice by Using Dynamic Positron Emission Tomography Bioimaging." *Antimicrobial Agents and Chemotherapy* 59 (9): 5768–74. <https://doi.org/10.1128/AAC.01146-15>.

- Diacon, A. H., R. F. Patientia, A. Venter, P. D. van Helden, P. J. Smith, H. McIlleron, J. S. Maritz, and P. R. Donald. 2007. "Early Bactericidal Activity of High-Dose Rifampin in Patients with Pulmonary Tuberculosis Evidenced by Positive Sputum Smears." *Antimicrobial Agents and Chemotherapy* 51 (8): 2994–96. <https://doi.org/10.1128/AAC.01474-06>.
- Ewijk-Beneken Kolmer, Eleonora W.J. van, Marga J.A. Teulen, Erik C.A. van den Hombergh, Nielka E. van Erp, Lindsey H.M. te Brake, and Rob E. Aarnoutse. 2017. "Determination of Protein-Unbound, Active Rifampicin in Serum by Ultrafiltration and Ultra Performance Liquid Chromatography with UV Detection. A Method Suitable for Standard and High Doses of Rifampicin." *Journal of Chromatography B: Analytical Technologies in the Biomedical and Life Sciences* 1063 (April 2017): 42–49. <https://doi.org/10.1016/j.jchromb.2017.08.004>.
- Iversen, P, O S Nielsen, K M Jensen, and P O Madsen. 1983. "Comparison of Concentrations of Rifampin and a New Rifamycin Derivative, DL 473, in Canine Bone." *Antimicrobial Agents and Chemotherapy* 23 (2): 338–40. <https://doi.org/10.1128/AAC.23.2.338>.
- Jayaram, Ramesh, Sheshagiri Gaonkar, Parvinder Kaur, B. L. Suresh, B. N. Mahesh, R. Jayashree, Vrinda Nandi, et al. 2003. "Pharmacokinetics-Pharmacodynamics of Rifampin in an Aerosol Infection Model of Tuberculosis." *Antimicrobial Agents and Chemotherapy* 47 (7): 2118–24. <https://doi.org/10.1128/aac.47.7.2118-2124.2003>.
- Lappin, Graham, Robert Noveck, and Tal Burt. 2013. "Microdosing and Drug Development: Past, Present and Future." *Expert Opinion on Drug Metabolism & Toxicology* 9 (7): 817–34. <https://doi.org/10.1517/17425255.2013.786042>.
- Litjens, Carlijn H.C., Rob E. Aarnoutse, Eleonora W.J. Van Ewijk-Beneken Kolmer, Elin M. Svensson, Angela Colbers, David M. Burger, Martin J. Boeree, et al. 2019. "Protein Binding of Rifampicin Is Not Saturated When Using High-Dose Rifampicin." *Journal of Antimicrobial Chemotherapy* 74 (4): 986–90. <https://doi.org/10.1093/jac/dky527>.
- Merritt, Judith H., Daniel E. Kadouri, and George A. O'Toole. 2006. "Growing and Analyzing Static Biofilms." *Current Protocols in Microbiology* 00 (1). <https://doi.org/10.1002/9780471729259.mc01b01s00>.
- Ordonez, Alvaro A., Hechuan Wang, Gesham Magombedze, Camilo A. Ruiz-Bedoya, Shashikant Srivastava, Allen Chen, Elizabeth W. Tucker, et al. 2020a. "Dynamic Imaging in Patients with Tuberculosis Reveals Heterogeneous Drug Exposures in Pulmonary Lesions." *Nature Medicine* 26 (4): 529–34. <https://doi.org/10.1038/s41591-020-0770-2>.
- Pasipanodya, J. G., H. McIlleron, A. Burger, P. A. Wash, P. Smith, and T. Gumbo. 2013. "Serum Drug Concentrations Predictive of Pulmonary Tuberculosis Outcomes."

Journal of Infectious Diseases 208 (9): 1464–73.
<https://doi.org/10.1093/infdis/jit352>.

- Plaut, Roger D., Christopher P. Mocca, Ranjani Prabhakara, Tod J. Merkel, and Scott Stibitz. 2013. “Stably Luminescent *Staphylococcus Aureus* Clinical Strains for Use in Bioluminescent Imaging.” *PLoS ONE* 8 (3).
<https://doi.org/10.1371/journal.pone.0059232>.
- Pribaz, Jonathan R., Nicholas M. Bernthal, Fabrizio Billi, John S. Cho, Romela Irene Ramos, Y. Guo, Ambrose L. Cheung, Kevin P. Francis, and Lloyd S. Miller. 2012. “Mouse Model of Chronic Post-Arthroplasty Infection: Noninvasive in Vivo Bioluminescence Imaging to Monitor Bacterial Burden for Long-Term Study.” *Journal of Orthopaedic Research : Official Publication of the Orthopaedic Research Society* 30 (3): 335–40. <https://doi.org/10.1002/jor.21519>.
- Roth, B. 1984. “Penetration of Parenterally Administered Rifampicin into Bone Tissue.” *Chemotherapy* 30 (6): 358–65. <https://doi.org/10.1159/000238294>.
- Sirof, J, R Lopitiaux, R Cluzel, J J Delisle, and B Sauvezie. 1977. “[Rifampicin Diffusion in Non-Infected Human Bone (Author’s Transl)].” *Annales de Microbiologie* 128 (2): 229–36.
- Sirof, J, L Prive, R Lopitiaux, and Y Glanddier. 1983. “[Diffusion of Rifampicin into Spongy and Compact Bone Tissue during Total Hip Prosthesis Operation].” *Pathologie-Biologie* 31 (5): 438–41.
- Steenwinkel, Jurriaan E.M. De, Rob E. Aarnoutse, Gerjo J. De Knegt, Marian T. Ten Kate, Marga Teulen, Henri A. Verbrugh, Martin J. Boeree, Dick Van Soolingen, and Irma A.J.M. Bakker-Woudenberg. 2013. “Optimization of the Rifampin Dosage to Improve the Therapeutic Efficacy in Tuberculosis Treatment Using a Murine Model.” *American Journal of Respiratory and Critical Care Medicine* 187 (10): 1127–34. <https://doi.org/10.1164/rccm.201207-1210OC>.
- Svensson, Robin J., Rob E. Aarnoutse, Andreas H. Diacon, Rodney Dawson, Stephen H. Gillespie, Martin J. Boeree, and Ulrika S.H. Simonsson. 2018. “A Population Pharmacokinetic Model Incorporating Saturable Pharmacokinetics and Autoinduction for High Rifampicin Doses.” *Clinical Pharmacology and Therapeutics* 103 (4): 674–83. <https://doi.org/10.1002/cpt.778>.
- Swaminathan, Soumya, Jotam G. Pasipanodya, Geetha Ramachandran, A. K. Hemanth Kumar, Shashikant Srivastava, Devyani Deshpande, Eric Nuermberger, and Tawanda Gumbo. 2016. “Drug Concentration Thresholds Predictive of Therapy Failure and Death in Children With Tuberculosis: Bread Crumb Trails in Random Forests.” *Clinical Infectious Diseases* 63 (suppl 3): S63–74.
<https://doi.org/10.1093/cid/ciw471>.

- Thabit, Abrar K., Dania F. Fatani, Maryam S. Bamakhrama, Ola A. Barnawi, Lana O. Basudan, and Shahad F. Alhejaili. 2019. "Antibiotic Penetration into Bone and Joints: An Updated Review." *International Journal of Infectious Diseases* 81 (April):128–36. <https://doi.org/10.1016/j.ijid.2019.02.005>.
- Thompson, John M., Vikram Saini, Alyssa G. Ashbaugh, Robert J. Miller, Alvaro A. Ordonez, Roger V. Ortines, Yu Wang, Robert S. Sterling, Sanjay K. Jain, and Lloyd S. Miller. 2017. "Oral-Only Linezolid-Rifampin Is Highly Effective Compared with Other Antibiotics for Periprosthetic Joint Infection: Study of a Mouse Model." *Journal of Bone and Joint Surgery - American Volume*. Lippincott Williams and Wilkins. <https://doi.org/10.2106/JBJS.16.01002>.
- Tucker, Elizabeth W., Beatriz Guglieri-Lopez, Alvaro A. Ordonez, Brittaney Ritchie, Mariah H. Klunk, Richa Sharma, Yong S. Chang, et al. 2018a. "Noninvasive 11C-Rifampin Positron Emission Tomography Reveals Drug Biodistribution in Tuberculous Meningitis." *Science Translational Medicine* 10 (470): 1–12. <https://doi.org/10.1126/scitranslmed.aau0965>.
- Wagner, Claudia C., and Oliver Langer. 2011. "Approaches Using Molecular Imaging Technology — Use of PET in Clinical Microdose Studies." *Advanced Drug Delivery Reviews* 63 (7): 539–46. <https://doi.org/10.1016/j.addr.2010.09.011>.

Chapter 4: Separate Models Are Needed to Translate Findings from Microdose Modeling to Therapeutic Dosing

4.1 Introduction

Microdosing has been used within early drug development to explore pharmacokinetics (PK) (Lappin, Noveck, and Burt 2013; Wagner and Langer 2011). We utilized microdosing in conjunction with PET imaging to determine biodistribution of rifampin to bone tissue infected with *S. aureus* for orthopedic implant-associated infections (Gordon et al. 2021). Prior studies have indicated that rifampin penetration into bone tissue is substantial relative to plasma, with bone concentrations of about 20-50% of that of plasma (Roth 1984; Sirot et al. 1983; 1977). These values, however, were obtained from single time point experiments and were greatly variable, with difficulties in obtaining accurate and precise measurements due to the nature of the sample prep. Our PET imaging work indicated rifampin bone penetration may be much lower than previously thought, with estimates of 10 and 15% for mice and humans, respectively (Gordon et al. 2021).

Two concerns with microdosing PK studies are particularly relevant here with microdosing ^{11}C -rifampin in mice and humans. The first concern is regarding dose-proportionality, that is whether the PK from microdosing can be linearly extrapolated to that of therapeutic dosing, while the second concern is whether enough of the PK profile is captured during the short time allowed with PET imaging (Lappin, Noveck, and Burt 2013; Wagner and Langer 2011). These concerns were addressed earlier in Chapter 3. However, it is important to note that the PK in a prior ^{11}C -rifampin PET imaging study in humans with TB was noted to be different between microdosing and therapeutic dosing (Ordonez et al. 2020).

Due to these potential PK differences due to microdosing vs therapeutic dosing and mice vs human species differences, separate PK models from literature were pursued for therapeutic dosing. As information regarding PK parameters for bone is unavailable for therapeutic dosing, information from the ¹¹C-rifampin microdose modeling was borrowed and added to the therapeutic dose models.

4.2 Methods

- *Literature Review*

A literature review was conducted for rifampin PK models for both mouse and human models built on data where therapeutic dosing levels were given. A literature review was also conducted to find published rifampin PK profiles or PK summary statistics for both mice and humans. PK profiles found in the literature were digitized with WebPlotDigitizer (Automeris LLC) and utilized for either model building or validation. External validation of the literature models was performed by qualitatively comparing steady-state AUCs.

- *Rifampin Therapeutic Dose PK Model Development*

For the therapeutic dose mouse model, a subset of the digitized data was used for naïve-pooled modeling performed with Pumas 2.0 (Pumas-AI) (Rackauckas et al. 2020).. The model was qualified against the data used for model building and external data for model validation. For the therapeutic dose human model, a model was chosen from literature and validated against external data.

For both the therapeutic dose mouse and human models, the respective bone compartments with bone-related model parameter estimates were added from the ¹¹C-rifampin microdose modeling.

4.3 Results

- *Rifampin Therapeutic Dose PK Modeling*

A literature review was performed for published rifampin models for mice and humans built from therapeutic dosing levels. Two mouse models were found (Chunli Chen et al. 2016; Bartelink et al. 2017). However, both models failed to reproduce expected PK profiles, so a mouse model was built from data available in literature.

- *Mouse Model*

Through a literature review, ten publications were found with either PK profiles that could be digitized or with AUC_{0-24hr} summary statistics (Table 3). Five publications (Chao Chen et al. 2018; Maiga et al. 2015; Rosenthal et al. 2012; Almeida et al. 2011; Bruzzese et al. 2000) were used for model building and five publications (Y. Liu et al. 2018; Y. Hu et al. 2015; De Steenwinkel et al. 2013; Hosagrahara et al. 2013; Jayaram et al. 2003) were used for external validation. Doses ranged from 10-40 mg/kg given orally once daily in both the model-building and validation data sets. Neither accumulation nor autoinduction was found, so the single-dose and steady-state data were combined for the modeling and validation.

Table 3 Publications for Building and Validating Rifampin Therapeutic Dose Mouse Model

Publication	Dose (mg/kg)	Steady State (Y/N)	Data Set
Chen C, <i>et al. Antimicrob Agents Chemother.</i> 2018.	10	N	Model-building
Maiga M, <i>et al. EBioMedicine.</i> 2015.	10	Y	Model-building
Rosenthal IM, <i>et al. Antimicrob Agents Chemother.</i> 2012.	10, 20, 40	Y	Model-building
Almeida D, <i>et al. PLoS Negl Trop Dis.</i> 2011.	10	N	Model-building
Bruzzese T, <i>et al. Arzneimittelforschung.</i> 2000.	10	N	Model-building
Liu Y, <i>et al. J Antimicrob Chemother.</i> 2018.	10, 20, 30	Y	Validation
Hu Y, <i>et al. Front Microbiol.</i> 2015.	10, 20, 30, 40	N	Validation
de Steenwinkel JE, <i>et al. Am J Respir Crit Care Med.</i> 2013.	10	Y	Validation
Hosagrahara V, <i>et al. Eur J Pharm Sci.</i> 2013.	10	N, Y	Validation
Jayaram R, <i>et al. Antimicrob Agents Chemother.</i> 2003.	10	N	Validation

The final model structure was a 1-compartment model with first-order absorption (Figure 11). The parameter estimates are shown in Table 4. The model estimation was performed with allometric scaling to a 1-kg bodyweight and without the bone compartments. The bone-related parameter estimates from the ¹¹C-rifampin microdose modeling (Table 2) were added to Table 4 (Figure 12), as they were utilized for simulations for dose optimization.

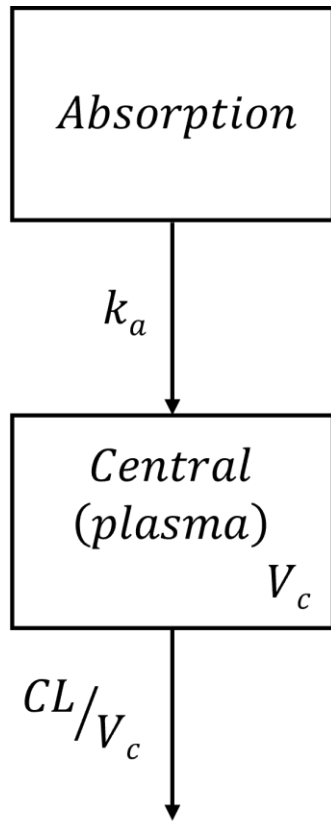


Figure 11 Rifampin Therapeutic Dose Mouse Model Structure

Table 4 Rifampin Therapeutic Dose Mouse Model Parameter Estimates

Parameter	Estimate
CL (L/h/kg)	0.033
Q _{b1} (L/h/kg)	10.3
Q _{b2} (L/h/kg)	61
V _c (L/kg)	0.51
V _{b1} (L/kg)	0.0036
V _{b2} (L/kg)	7
PC	0.10
k _a (h ⁻¹)	0.97

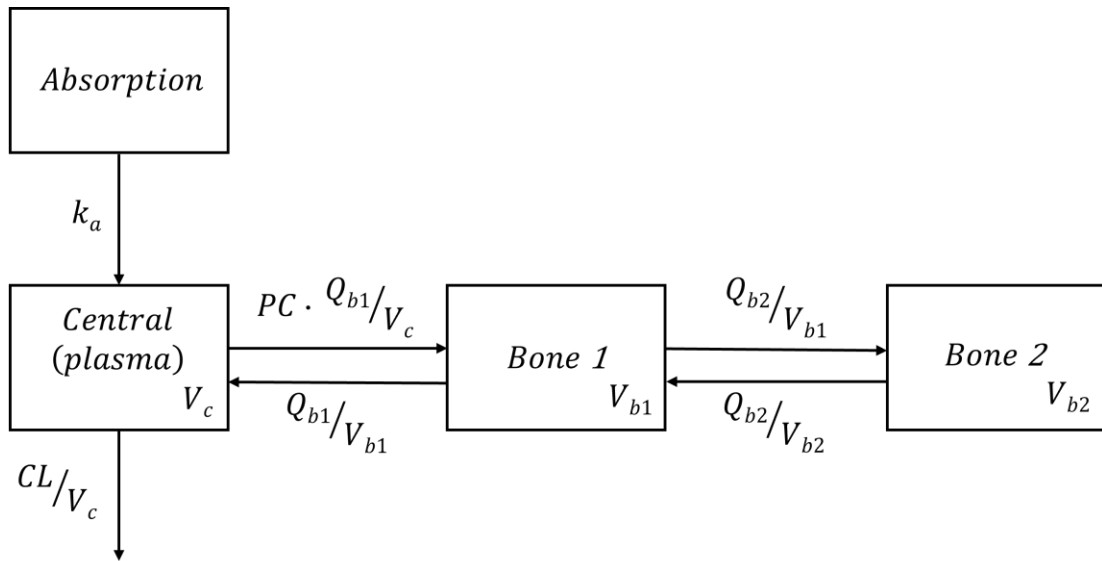


Figure 12 Rifampin Therapeutic Dose Mouse Model Structure with Bone Compartments

The rifampin therapeutic dose mouse model was qualified by evaluating the steady-state AUC at Day 7 with the different doses. The model was able to reasonably reproduce the AUCs from both the model-building and validation data sets across the entire range of doses from 10-40 mg/kg (Figure 13).

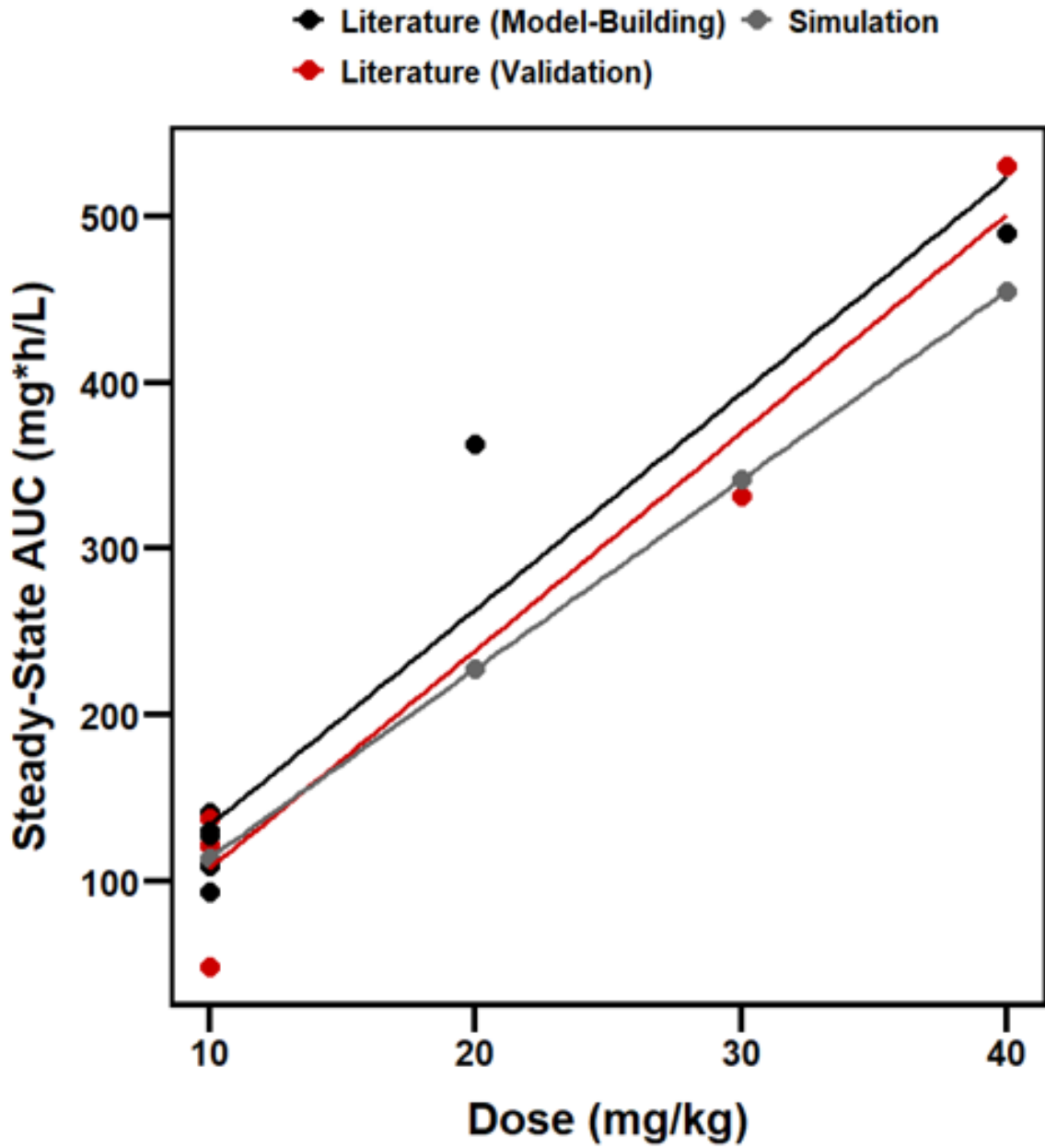


Figure 13 Validation of Rifampin Therapeutic Dose Mouse Model

- *Human Model*

A model built on data in TB patients with doses ranging from 10-40 kg/mg/day and sampling at Week 1 and Week 2 was chosen for the rifampin therapeutic dose human model (Svensson et al. 2018). The Svensson et al model was chosen as it was the only rifampin model to be able to characterize rifampin’s various PK non-linearities, particularly those that occur with high-dose rifampin regimens. The model included more than dose-proportional bioavailability, saturable elimination, and autoinduction (Figure 14). The parameter estimates are shown in Table 5, with the bone-related parameter estimates from the ¹¹C-rifampin microdose modeling (Table 2) added as they were utilized for simulations for dose optimization (Figure 15).

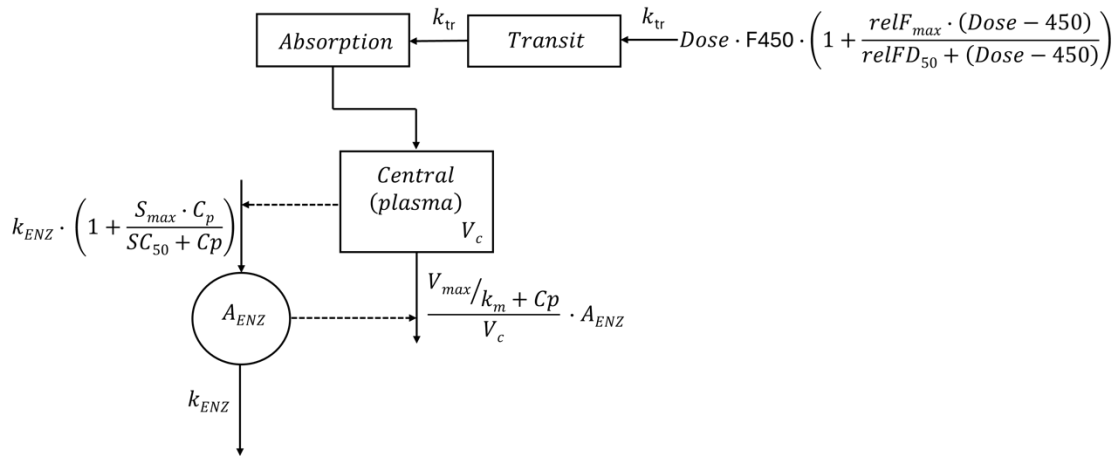


Figure 14 Rifampin Therapeutic Dose Human Model Structure

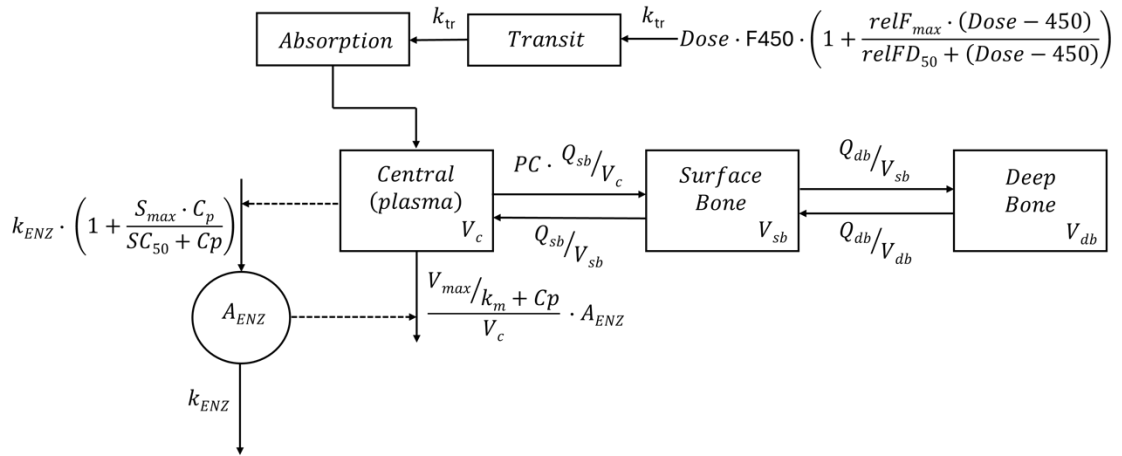


Figure 15 Rifampin Therapeutic Dose Human Model Structure with Bone Compartments

Table 5 Rifampin Therapeutic Dose Human Model Parameter Estimates

Parameter	Estimate
v_{\max} (mg/h/70kg)	525
k_m (mg/L)	35.3
Q_{b1} (L/h/70kg)	846
Q_{b2} (L/h/70kg)	2208
V_c (L/70kg)	87.2
V_{b1} (L/70kg)	0.86
V_{b2} (L/70kg)	226
PC	0.15
k_a (h^{-1})	1.77
MTT (h)	0.513
NN	23.8
S_{\max}	1.16
SC_{50} (mg/L)	0.0699
k_{enz} (h^{-1})	0.00603
$relF_{\max}$	0.504
$relFD_{50}$ (mg)	67

To validate the rifampin therapeutic dose human model, a literature search was conducted. Five publications (Aarnoutse et al. 2017; Boeree et al. 2017; Peloquin et al. 2017; Boeree et al. 2015; Ruslami et al. 2007) from a systematic review and meta-analysis (Stott et al. 2018) were chosen, with doses ranging from 7.5-35 mg/kg (Table 6).

Table 6 Publications for Validation of Rifampin Therapeutic Dose Human Model

Publication	Dose (mg/kg)
Aarnoutse RE, <i>et al. Antimicrob Agents Chemother.</i> 2017.	10, 15, 20
Boeree MJ, <i>et al. Lancet Infect Dis.</i> 2017.	10, 20, 35
Peloquin CA, <i>et al. Antimicrob Agents Chemother.</i> 2017.	10, 15, 20
Boeree MJ, <i>et al. Am J Respir Crit Care Med.</i> 2015.	10, 20, 25, 30, 35
Ruslami R, <i>et al. Antimicrob Agents Chemother.</i> 2007.	7.5, 13.3

The Svensson et al model was able to reproduce the AUCs from literature across all doses and the more than dose-proportional increase in exposure (Figure 16). Adding the bone compartments from the ¹¹C-rifampin microdosing model slightly decreased the plasma exposures at higher doses, but the literature plasma values were still matched reasonably well.

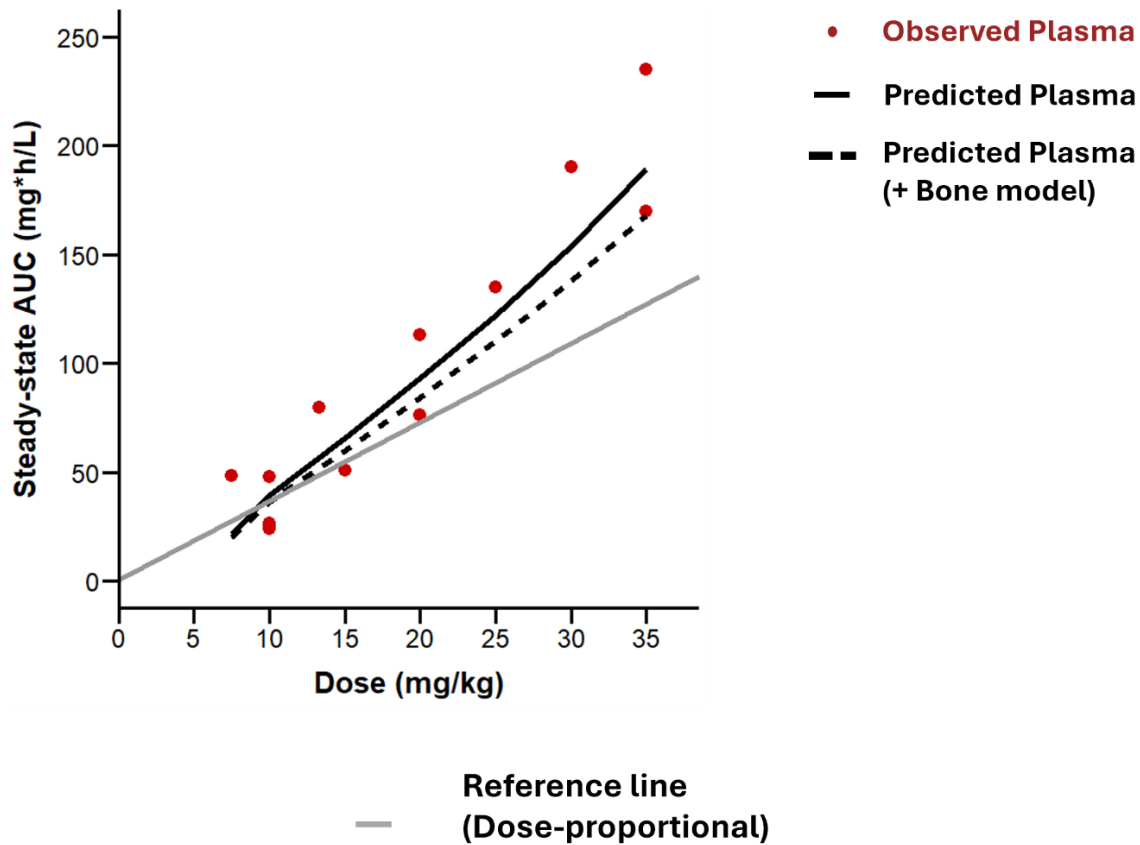


Figure 16 Validation of Rifampin Therapeutic Dose Human Model

4.4 Discussion

As several important differences in PK were suspected between microdosing and therapeutic dosing, separate therapeutic dosing PK models were pursued. For mice, two PK models were available in literature, yet both failed to reproduce rifampin PK reported in literature (Chao Chen et al. 2018; Bartelink et al. 2017), leading us to develop a therapeutic dose model from literature. For humans, Svensson et al’s model was chosen for the therapeutic dosing model, as it was able to characterize rifampin’s more than dose-proportional increase in bioavailability, autoinduction, and saturable clearance,

which are all important for simulating high-dose rifampin regimens out to steady state (Svensson et al. 2018).

While it is unclear why the therapeutic dose mouse models in literature failed to reproduce expected PK profiles, elements included in the structural models may be emblematic of fundamental confusions regarding rifampin PK in mice and humans. Bartelink et al's model included saturable absorption without explanation, which may be an attempt to mimic the more than dose-proportional increase in bioavailability in humans. However, this does not occur in mice, as is evident in Figure 13. Additionally, Chen et al attributed differences in clearance at Day 1 and Day 3 to autoinduction, yet autoinduction likely does not occur in mice due to a lack of sequence homology in PXR1 (Hosagrahara et al. 2013; LeCluyse 2001). Hosagrahara et al reported induction due to Pgp-mediated efflux, with lower exposures at Day 5 relative to Day 1 (Hosagrahara et al. 2013), yet this finding is inconsistent with our finding that single-dose and steady-state exposures are similar across literature (Table 3, Figure 13).

Some of these complexities in rifampin PK, with marked differences between species, highlight the need to investigate microdosing vs therapeutic dosing PK models. While one structural model was chosen for microdosing both mice and humans, markedly different structural models were chosen, with none of the PK non-linearities reported in humans being evident in mice. With a single microdose, the PK non-linearities in therapeutic dosing of humans cannot be investigated with the PET imaging experiments. Additionally, ¹¹C-rifampin being administered intravenously at a single microdose precludes the ability to investigate potential complexities in absorption, which is important as rifampin is most commonly administered orally.

4.5 References

- Aarnoutse, R. E., G. S. Kibiki, K. Reither, H. H. Semvua, F. Haraka, C. M. Mtabho, S. G. Mpagama, et al. 2017. "Pharmacokinetics, Tolerability, and Bacteriological Response of Rifampin Administered at 600, 900, and 1,200 Milligrams Daily in Patients with Pulmonary Tuberculosis." *Antimicrobial Agents and Chemotherapy* 61 (11): 1–13. <https://doi.org/10.1128/AAC.01054-17>.
- Almeida, Deepak, Paul J. Converse, Zahoor Ahmad, Kelly E. Dooley, Eric L. Nuermberger, and Jacques H. Grosset. 2011. "Activities of Rifampin, Rifapentine and Clarithromycin Alone and in Combination against Mycobacterium Ulcerans Disease in Mice." *PLoS Neglected Tropical Diseases* 5 (1). <https://doi.org/10.1371/journal.pntd.0000933>.
- Bartelink, I. H., N. Zhang, R. J. Keizer, N. Strydom, P. J. Converse, K. E. Dooley, E. L. Nuermberger, and R. M. Savic. 2017. "New Paradigm for Translational Modeling to Predict Long-Term Tuberculosis Treatment Response." *Clinical and Translational Science* 10 (5): 366–79. <https://doi.org/10.1111/cts.12472>.
- Boeree, Martin J., Andreas H. Diacon, Rodney Dawson, Kim Narunsky, Jeannine Du Bois, Amour Venter, Patrick P.J. Phillips, et al. 2015. "A Dose-Ranging Trial to Optimize the Dose of Rifampin in the Treatment of Tuberculosis." *American Journal of Respiratory and Critical Care Medicine* 191 (9): 1058–65. <https://doi.org/10.1164/rccm.201407-1264OC>.
- Boeree, Martin J., Norbert Heinrich, Rob Aarnoutse, Andreas H. Diacon, Rodney Dawson, Sunita Rehal, Gibson S. Kibiki, et al. 2017. "High-Dose Rifampicin, Moxifloxacin, and SQ109 for Treating Tuberculosis: A Multi-Arm, Multi-Stage Randomised Controlled Trial." *The Lancet Infectious Diseases* 17 (1): 39–49. [https://doi.org/10.1016/S1473-3099\(16\)30274-2](https://doi.org/10.1016/S1473-3099(16)30274-2).
- Bruzzese, Tiberio, Claudio Rimaroli, Angelo Bonabello, Giovanni Mozzi, Samyuktha Ajay, and Noshir D. Cooverj. 2000. "Pharmacokinetics and Tissue Distribution of Rifametan, a New 3- Azinomethyl-Rifamycin Derivative, in Several Animal Species." *Arzneimittel-Forschung/Drug Research* 50 (1): 60–71. <https://doi.org/10.1055/s-0031-1300165>.
- Chen, Chao, Susana Gardete, Robert Sander Jansen, Annanya Shetty, Thomas Dick, Kyu Y Rhee, and Véronique Dartois. 2018. "Verapamil Targets Membrane Energetics in Mycobacterium Tuberculosis." *Antimicrobial Agents and Chemotherapy* 62 (5): 11–13. <https://doi.org/10.1128/AAC.02107-17>.
- Chen, Chunli, Fatima Ortega, Laura Alameda, Santiago Ferrer, and Ulrika S.H. Simonsson. 2016. "Population Pharmacokinetics, Optimised Design and Sample Size Determination for Rifampicin, Isoniazid, Ethambutol and Pyrazinamide in the

- Mouse.” *European Journal of Pharmaceutical Sciences* 93:319–33.
<https://doi.org/10.1016/j.ejps.2016.07.017>.
- Gordon, Oren, Donald E Lee, Bessie Liu, Brooke Langevin, Alvaro A Ordonez, Dustin A Dikeman, Babar Shafiq, et al. 2021. “Dynamic PET-Facilitated Modeling and High-Dose Rifampin Regimens for Staphylococcus Aureus Orthopedic Implant–Associated Infections.” *Science Translational Medicine* 13 (622).
<https://doi.org/10.1126/scitranslmed.abl6851>.
- Hosagrahara, Vinayak, Jitendar Reddy, Samit Ganguly, Vijender Panduga, Vijaykamal Ahuja, Manish Parab, and Jayashree Giridhar. 2013. “Effect of Repeated Dosing on Rifampin Exposure in BALB/c Mice.” *European Journal of Pharmaceutical Sciences* 49 (1): 33–38. <https://doi.org/10.1016/j.ejps.2013.01.017>.
- Hu, Yanmin, Alexander Liu, Fatima Ortega-Muro, Laura Alameda-Martin, Denis Mitchison, and Anthony Coates. 2015. “High-Dose Rifampicin Kills Persisters, Shortens Treatment Duration, and Reduces Relapse Rate in Vitro and in Vivo.” *Frontiers in Microbiology* 6 (JUN): 1–10. <https://doi.org/10.3389/fmicb.2015.00641>.
- Jayaram, Ramesh, Sheshagiri Gaonkar, Parvinder Kaur, B. L. Suresh, B. N. Mahesh, R. Jayashree, Vrinda Nandi, et al. 2003. “Pharmacokinetics-Pharmacodynamics of Rifampin in an Aerosol Infection Model of Tuberculosis.” *Antimicrobial Agents and Chemotherapy* 47 (7): 2118–24. <https://doi.org/10.1128/aac.47.7.2118-2124.2003>.
- LeCluyse, Edward L. 2001. “Pregnane X Receptor: Molecular Basis for Species Differences in CYP3A Induction by Xenobiotics.” *Chemico-Biological Interactions* 134 (3): 283–89. [https://doi.org/10.1016/S0009-2797\(01\)00163-6](https://doi.org/10.1016/S0009-2797(01)00163-6).
- Liu, Yingjun, Henry Pertinez, Fatima Ortega-Muro, Laura Alameda-Martin, Thomas Harrison, Geraint Davies, Anthony Coates, and Yanmin Hu. 2018. “Optimal Doses of Rifampicin in the Standard Drug Regimen to Shorten Tuberculosis Treatment Duration and Reduce Relapse by Eradicating Persistent Bacteria.” *Journal of Antimicrobial Chemotherapy* 73 (3): 724–31. <https://doi.org/10.1093/jac/dkx467>.
- Maiga, Mamoudou, Bintou Ahmadou Ahidjo, Mariama C. Maiga, Laurene Cheung, Shaaretha Pelly, Shichun Lun, Flabou Bougoudogo, and William R. Bishai. 2015. “Efficacy of Adjunctive Tofacitinib Therapy in Mouse Models of Tuberculosis.” *EBioMedicine* 2 (8): 868–73. <https://doi.org/10.1016/j.ebiom.2015.07.014>.
- Ordonez, Alvaro A., Hechuan Wang, Gesham Magombedze, Camilo A. Ruiz-Bedoya, Shashikant Srivastava, Allen Chen, Elizabeth W. Tucker, et al. 2020. “Dynamic Imaging in Patients with Tuberculosis Reveals Heterogeneous Drug Exposures in Pulmonary Lesions.” *Nature Medicine* 26 (4): 529–34.
<https://doi.org/10.1038/s41591-020-0770-2>.
- Peloquin, C. A., G. E. Velásquez, L. Lecca, R. I. Calderón, J. Coit, M. Milstein, E. Osso, et al. 2017. “Pharmacokinetic Evidence from the HIRIF Trial To Support Increased

- Doses of Rifampin for Tuberculosis.” *Antimicrobial Agents and Chemotherapy* 61 (8): 1–6. <https://doi.org/10.1128/AAC.00038-17>.
- Rackauckas, Chris, Yingbo Ma, Andreas Noack, Vaibhav Dixit, Shubham Maddhashiya, Patrick Kofod Mogensen, José Bayoán Santiago Calderón, et al. 2020. “Accelerated Predictive Healthcare Analytics with Pumas, a High Performance Pharmaceutical Modeling and Simulation Platform.” *BioRxiv*. <https://doi.org/10.1101/2020.11.28.402297>.
- Rosenthal, Ian M., Rokeya Tasneen, Charles A. Peloquin, Ming Zhang, Deepak Almeida, Khisimuzi E. Mdluli, Petros C. Karakousis, Jacques H. Grosset, and Eric L. Nuermberger. 2012. “Dose-Ranging Comparison of Rifampin and Rifapentine in Two Pathologically Distinct Murine Models of Tuberculosis.” *Antimicrobial Agents and Chemotherapy* 56 (8): 4331–40. <https://doi.org/10.1128/AAC.00912-12>.
- Ruslami, Rovina, Hanneke M.J. Nijland, Bacht Alisjahbana, Ida Parwati, Reinout Van Crevel, and Rob E. Aarnoutse. 2007. “Pharmacokinetics and Tolerability of a Higher Rifampin Dose versus the Standard Dose in Pulmonary Tuberculosis Patients.” *Antimicrobial Agents and Chemotherapy* 51 (7): 2546–51. <https://doi.org/10.1128/AAC.01550-06>.
- Steenwinkel, Jurriaan E.M. De, Rob E. Aarnoutse, Gerjo J. De Knegt, Marian T. Ten Kate, Marga Teulen, Henri A. Verbrugh, Martin J. Boeree, Dick Van Soolingen, and Irma A.J.M. Bakker-Woudenberg. 2013. “Optimization of the Rifampin Dosage to Improve the Therapeutic Efficacy in Tuberculosis Treatment Using a Murine Model.” *American Journal of Respiratory and Critical Care Medicine* 187 (10): 1127–34. <https://doi.org/10.1164/rccm.201207-1210OC>.
- Stott, K. E., H. Pertinez, M. G.G. Sturkenboom, M. J. Boeree, R. Aarnoutse, G. Ramachandran, A. Requena-Méndez, et al. 2018. “Pharmacokinetics of Rifampicin in Adult TB Patients and Healthy Volunteers: A Systematic Review and Meta-Analysis.” *Journal of Antimicrobial Chemotherapy* 73 (9): 2305–13. <https://doi.org/10.1093/jac/dky152>.
- Svensson, Robin J., Rob E. Aarnoutse, Andreas H. Diacon, Rodney Dawson, Stephen H. Gillespie, Martin J. Boeree, and Ulrika S.H. Simonsson. 2018. “A Population Pharmacokinetic Model Incorporating Saturable Pharmacokinetics and Autoinduction for High Rifampicin Doses.” *Clinical Pharmacology and Therapeutics* 103 (4): 674–83. <https://doi.org/10.1002/cpt.778>.
- Wagner, Claudia C., and Oliver Langer. 2011. “Approaches Using Molecular Imaging Technology — Use of PET in Clinical Microdose Studies.” *Advanced Drug Delivery Reviews* 63 (7): 539–46. <https://doi.org/10.1016/j.addr.2010.09.011>.

Chapter 5: Simulations Suggest High-Dose Rifampin Regimens May Be Necessary for Adequate Bone Exposure

5.1 Introduction

With prolonged treatment duration and high failure and mortality rates with patients with prosthetic joint infections (Bernard et al. 2021; Zmistowski et al. 2013; Fischbacher and Borens 2019), there is a need to improve treatments. It is unclear whether adequate levels of rifampin are reaching infected bone tissue with standard dosing regimens (Sirot et al. 1983; 1977; Cluzel et al. 1984). Bacterial biofilm formation on the implant surface can also impede the penetration of immune cells and some antibiotics, though rifampin is reported to penetrate biofilm and have high bactericidal activity when tested *in vitro* (Zimmerli and Sendi 2019). The breakpoint, or concentration at which *S. aureus* is susceptible to rifampin treatment, in a biofilm environment is also unknown. IDSA established the breakpoint of 1 mg/L for planktonic, or free-floating, *S. aureus* (Osmon et al. 2013; Tunkel et al. 2017), yet it is unclear whether that is adequate for biofilm environments (Tang et al. 2013; Zimmerli and Sendi 2019).

To address these questions, an integrated approach was taken in which an *in vitro* biofilm assay was performed to obtain a rifampin concentration target, *in vivo* treatment-shortening efficacy experiments were performed in mice comparing standard-dose, 6-week regimens to high-dose, 4-week regimens, and PET imaging of ¹¹C-rifampin and PK modeling was performed to determine rifampin penetration into bone tissue.

As noted earlier, several differences exist between rifampin PK with microdosing and therapeutic dosing and also species differences between mice and humans, as well as differences attributed to oral dosing. Due to these differences, separate therapeutic dosing models were pursued (Chapter 4) with borrowing information from the microdosing

models to determine bone penetration. Here, we simulated bone exposures with standard- and high-dose regimens to assist with optimizing rifampin dosing for orthopedic implant-associated infections for *S. aureus*.

5.2 Methods

Simulations were performed with Pumas 2.0 (Pumas-AI) (Rackauckas et al. 2020). Multiple-dose simulations were performed with the rifampin therapeutic dose PK models and additional bone compartments and parameter estimates from the ¹¹C-rifampin microdose PK models, at standard- and high-dose regimens with rifampin given orally twice daily. 15 and 45 mg/kg/day were considered standard and high dose for mice, while 10 and 35 mg/kg/day were considered the equivalent doses for humans (De Steenwinkel et al. 2013; Boeree et al. 2015). As steady-state in humans is achieved after 7-14 days, simulations were performed for 14 days and steady-state C_{max} and steady-state 24hr AUC were assessed at Day 14.

5.3 Results

Simulations were performed for mouse and human standard- and high-dose regimens with twice daily dosing. Bone compartments were added to the structural models with bone-related parameter estimates from the ¹¹C-rifampin microdose modeling (Figure 12, Figure 15, Tables 4-5). Steady-state concentrations for bone tissue were higher for mice than humans for both standard- and high-dose regimens (Figure 17). Neither mouse nor human concentrations reached the 1mg/L breakpoint with a standard dose. With a high dose, mouse bone concentrations were maintained above the breakpoint, with a steady-state C_{max} of 2.66 mg/L (Table 7). Human bone concentrations

with a high dose (35mg/kg/day) reached the breakpoint ($C_{max,ss} = 1.71$), but were not maintained. Simulations were also performed at an additional high dose of 40 mg/kg/day for humans in which the bone $C_{max,ss}$ was 1.99 (Table 7). Additionally, human high doses were necessary to match the steady-state AUC from a mouse standard dose (Table 7).

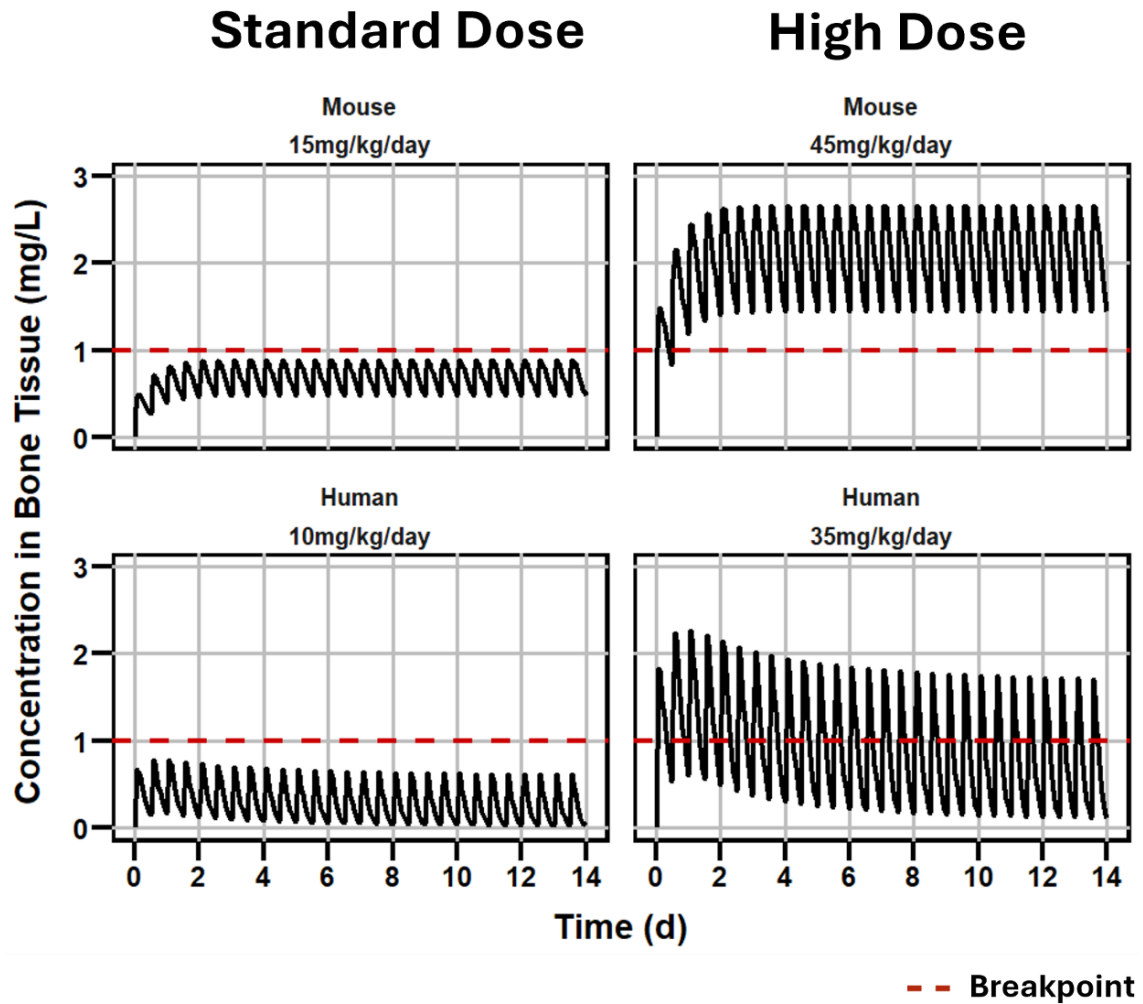


Figure 17 Simulations of Rifampin Concentrations in Bone Tissue with Standard- and High-Dose Regimens

Table 7 Simulated Steady-State Cmax and AUC for Bone Tissue with Standard- and High-Dose Rifampin Regimens

	Dose (mg/kg/day)	Cmax _{ss} (mg/L)	AUC _{ss} (mg*h/L)
Mouse	15	0.89	202
	45	2.66	607
Human	10	0.61	72
	35	1.71	211
	40	1.99	252

5.4 Discussion

From our therapeutic dose simulations with standard and high doses of rifampin, we found that bone exposures do not reach the 1 mg/L breakpoint for planktonic *S. aureus* with standard dosing for either mice or humans. However, markedly different exposures were observed between mice and humans at high dosing, while the dosing was presumed to be equivalent. Due to differences in exposures between mice and humans, results from the *in vivo* treatment shortening experiments are not shown here, as the high-dose exposures in mice are much higher than what is tolerable in humans (Lindsey H.M. te Brake et al. 2021).

In vitro biofilm assay results are also not shown here, as the results do not add to the body of evidence to determine a breakpoint in a biofilm environment. Several factors complicate this determination and have led to conflicting results (Zimmerli and Sendi 2019; Tang et al. 2013). This includes the maturity of the biofilm, as more mature biofilm have been reported to require higher minimum inhibitory concentration (MIC). Rifampin being given alone or in combination has also been shown to affect the results. *In vivo*

experiments have also given variable results, with also different infection models. Due to the inconsistency within literature as to what the breakpoint may be in a biofilm environment, including several results indicating no change from the planktonic 1 mg/L breakpoint, for this work we kept the target at 1 mg/L.

Given the 1 mg/L target, simulations indicated that the high-dose mouse regimen had bone exposures at steady state that remained above the target. For the human high-dose regimen, however, exposures fluctuated between above and below the target. Rifampin is considered to be primarily concentration-dependent, with AUC as the best predictor of bactericidal activity (Swaminathan et al. 2016; J. G. Pasipanodya et al. 2013; Chigutsa et al. 2015; Diacon et al. 2007). When considering 24hr AUC_{ss}, a high dose of 35 mg/kg in humans was needed to match the AUC of approximately 200 mg*h/L with standard dose in mice.

Such a discrepancy highlights marked differences in PK between mice and humans, as are evident in our therapeutic dose modeling. Human-equivalent dosing for the *in vivo* experiments were established based on publications that looked at AUC at Day 1 (De Steenwinkel et al. 2013; Ruslami et al. 2007; Thompson et al. 2017). Multiple dosing, however, leads to stark differences in PK profiles, as mice do not display the more than dose-proportional increases in exposure, autoinduction, or saturable clearance.

Of note, while it was mentioned that accumulation and induction were not observed to occur with mice multiple dosing in Chapter 4, accumulation is seen in our simulations due to rifampin being dosed twice daily here as opposed to once daily as is often the case for TB. Rifampin is dosed twice daily for prosthetic joint infections due to

the thought that more frequent administration is beneficial for eradicating bacteria within a biofilm environment.

Given these challenges with respects to the goals of the work in terms of integrating *in vitro*, *in vivo*, and human data with PK modeling and simulation to optimize rifampin dosing for orthopedic implant-associated infections, we conclude that current standard dosing regimens may be inadequate to provide sufficient exposures in bone tissue for some strains of *S. aureus*. The MIC for the strain used in *in vitro* and *in vivo* experiments here were ≤ 0.5 mg/L. Combination rifampin treatments are successful in 70-90% of cases (Zimmerli 1998), indicating that exposures are adequate in most cases. However, our work here suggests that higher dosing regimens could potentially improve cure rates, given rifampin's potentially limited penetration to bone tissue.

Additionally, due to rifampin's more than dose-proportional increase in exposures, a 14% increase in dose from 35 to 40 mg/kg leads to a 20% increase in steady-state AUC, highlighting the potential benefits of dosing to a maximal tolerable dose. Recently, 50 mg/kg was noted to be intolerable, while 40 mg/kg was well tolerated (Lindsey H.M. te Brake et al. 2021). Tolerability may further be improved by staggering dosing with a lower dose for a week before increasing to a higher dose (Susanto et al. 2023).

5.5 References

Bernard, Louis, Cédric Arvieux, Benoit Brunschweiler, Sophie Touchais, Séverine Ansart, Jean-Pierre Bru, Eric Oziol, et al. 2021. "Antibiotic Therapy for 6 or 12 Weeks for Prosthetic Joint Infection." *New England Journal of Medicine* 384 (21): 1991–2001. <https://doi.org/10.1056/NEJMoa2020198>.

- Boeree, Martin J., Andreas H. Diacon, Rodney Dawson, Kim Narunsky, Jeannine Du Bois, Amour Venter, Patrick P.J. Phillips, et al. 2015. "A Dose-Ranging Trial to Optimize the Dose of Rifampin in the Treatment of Tuberculosis." *American Journal of Respiratory and Critical Care Medicine* 191 (9): 1058–65. <https://doi.org/10.1164/rccm.201407-1264OC>.
- Brake, Lindsey H.M. te, Veronique de Jager, Kim Narunsky, Naadira Vanker, Elin M. Svensson, Patrick P.J. Phillips, Stephen H. Gillespie, et al. 2021. "Increased Bactericidal Activity but Dose-Limiting Intolerability at 50 Mg·kg⁻¹ Rifampicin." *European Respiratory Journal* 58 (1). <https://doi.org/10.1183/13993003.00955-2020>.
- Chigutsa, Emmanuel, Jotam G. Pasipanodya, Marianne E. Visser, Paul D. van Helden, Peter J. Smith, Frederick A. Sirgel, Tawanda Gumbo, and Helen McIlleron. 2015. "Impact of Nonlinear Interactions of Pharmacokinetics and MICs on Sputum Bacillary Kill Rates as a Marker of Sterilizing Effect in Tuberculosis." *Antimicrobial Agents and Chemotherapy* 59 (1): 38–45. <https://doi.org/10.1128/AAC.03931-14>.
- Cluzel, R. A., R. Lopitiaux, J. Sirot, and S. Rampon. 1984. "Rifampicin in the Treatment of Osteoarticular Infections Due to Staphylococci." *Journal of Antimicrobial Chemotherapy* 13 (suppl C): 23–29. https://doi.org/10.1093/jac/13.suppl_C.23.
- Diacon, A. H., R. F. Patientia, A. Venter, P. D. van Helden, P. J. Smith, H. McIlleron, J. S. Maritz, and P. R. Donald. 2007. "Early Bactericidal Activity of High-Dose Rifampin in Patients with Pulmonary Tuberculosis Evidenced by Positive Sputum Smears." *Antimicrobial Agents and Chemotherapy* 51 (8): 2994–96. <https://doi.org/10.1128/AAC.01474-06>.
- Fischbacher, Arnaud, and Olivier Borens. 2019. "Prosthetic-Joint Infections: Mortality Over The Last 10 Years." *Journal of Bone and Joint Infection* 4 (4): 198–202. <https://doi.org/10.7150/jbji.35428>.
- Osmon, Douglas R, Elie F Berbari, Anthony R Berendt, Daniel Lew, Werner Zimmerli, James M Steckelberg, Nalini Rao, Arlen Hanssen, and Walter R Wilson. 2013. "Diagnosis and Management of Prosthetic Joint Infection: Clinical Practice Guidelines by the Infectious Diseases Society of America." *Clinical Infectious Diseases* 56 (1): e1–25. <https://doi.org/10.1093/cid/cis803>.
- Pasipanodya, J. G., H. McIlleron, A. Burger, P. A. Wash, P. Smith, and T. Gumbo. 2013. "Serum Drug Concentrations Predictive of Pulmonary Tuberculosis Outcomes." *Journal of Infectious Diseases* 208 (9): 1464–73. <https://doi.org/10.1093/infdis/jit352>.
- Rackauckas, Chris, Yingbo Ma, Andreas Noack, Vaibhav Dixit, Shubham Maddhashiya, Patrick Kofod Mogensen, José Bayoán Santiago Calderón, et al. 2020. "Accelerated Predictive Healthcare Analytics with Pumas, a High Performance Pharmaceutical

Modeling and Simulation Platform.” *BioRxiv*.
<https://doi.org/10.1101/2020.11.28.402297>.

- Sirot, J, R Lopitiaux, R Cluzel, J J Delisle, and B Sauvezie. 1977. “[Rifampicin Diffusion in Non-Infected Human Bone (Author’s Transl)].” *Annales de Microbiologie* 128 (2): 229–36.
- Sirot, J, L Prive, R Lopitiaux, and Y Glanddier. 1983. “[Diffusion of Rifampicin into Spongy and Compact Bone Tissue during Total Hip Prosthesis Operation].” *Pathologie-Biologie* 31 (5): 438–41.
- Tunkel, Allan R, Rodrigo Hasbun, Adarsh Bhimraj, Karin Byers, Sheldon L Kaplan, W Michael Scheld, Diederik van de Beek, Thomas P Bleck, Hugh J.L. Garton, and Joseph R Zunt. 2017. “2017 Infectious Diseases Society of America’s Clinical Practice Guidelines for Healthcare-Associated Ventriculitis and Meningitis*.” *Clinical Infectious Diseases* 64 (6): e34–65. <https://doi.org/10.1093/cid/ciw861>.
- Steenwinkel, Jurriaan E.M. De, Rob E. Aarnoutse, Gerjo J. De Knegt, Marian T. Ten Kate, Marga Teulen, Henri A. Verbrugh, Martin J. Boeree, Dick Van Soolingen, and Irma A.J.M. Bakker-Woudenberg. 2013. “Optimization of the Rifampin Dosage to Improve the Therapeutic Efficacy in Tuberculosis Treatment Using a Murine Model.” *American Journal of Respiratory and Critical Care Medicine* 187 (10): 1127–34. <https://doi.org/10.1164/rccm.201207-1210OC>.
- Susanto, Budi O., Elin M. Svensson, Lindsey te Brake, Rob E. Aarnoutse, Martin J. Boeree, and Ulrika S.H. Simonsson. 2023. “Model-Based Analysis of Bactericidal Activity and a New Dosing Strategy for Optimised-Dose Rifampicin.” *International Journal of Antimicrobial Agents* 61 (6).
<https://doi.org/10.1016/j.ijantimicag.2023.106813>.
- Swaminathan, Soumya, Jotam G. Pasipanodya, Geetha Ramachandran, A. K. Hemanth Kumar, Shashikant Srivastava, Devyani Deshpande, Eric Nuermberger, and Tawanda Gumbo. 2016. “Drug Concentration Thresholds Predictive of Therapy Failure and Death in Children With Tuberculosis: Bread Crumb Trails in Random Forests.” *Clinical Infectious Diseases* 63 (suppl 3): S63–74.
<https://doi.org/10.1093/cid/ciw471>.
- Zimmerli, Werner. 1998. “Role of Rifampin for Treatment of Orthopedic Implant–Related Staphylococcal Infections: A Randomized Controlled Trial.” *JAMA* 279 (19): 1537.
<https://doi.org/10.1001/jama.279.19.1537>.
- Zimmerli, Werner, and Parham Sendi. 2019. “Role of Rifampin against Staphylococcal Biofilm Infections in Vitro, in Animal Models, and in Orthopedic-Device-Related Infections.” *Antimicrobial Agents and Chemotherapy*. American Society for Microbiology. <https://doi.org/10.1128/AAC.01746-18>.

Zmistowski, Benjamin, Joseph A. Karam, Joel B. Durinka, David S. Casper, and Javad Parvizi. 2013. "Periprosthetic Joint Infection Increases the Risk of One-Year Mortality." *The Journal of Bone & Joint Surgery* 95 (24): 2177–84. <https://doi.org/10.2106/JBJS.L.00789>.

Chapter 6: There Is a Need for a Model-Integrated Bioequivalence Framework to Facilitate Generic Drug Development for Long-Acting Injectables

Nine out of ten prescriptions currently filled in the United States are for generic drugs. Generic drugs are important options that allow greater access to health care for all Americans. All generic drugs approved by the U.S. Food and Drug Administration (FDA) have the same high quality, strength, purity and stability as brand-name drugs. As of today, however, approximately 80% of long-acting injectable (LAI) products do not have an FDA-approved generic (O'Brien et al. 2021). LAIs are available in therapeutic areas such as antipsychotics, cancer, hormonal therapy, and addiction. LAI formulations possess many advantages when compared to conventional formulations by having 1) a predictable drug-release profile, 2) improved patient adherence because of reduced dosing frequency, 3) decreased incidence of side effects, and 4) overall cost reduction of medical care (Brissos et al. 2014; Stevens, Dawson, and Zummo 2016; Creinin et al. 2016).

However, LAIs can also pose challenges for generic drug development, due to often complex absorption profiles and long apparent half-lives. Complex absorption profiles can make establishing bioequivalence (BE) with pharmacokinetics (PK) studies more difficult with often an immediate release followed by a slow release that may last weeks or months (Figure 18) and may necessitate additional partial AUC (pAUC) BE endpoints be met (Table 8) (Lee, Gong, et al. 2020; Fang et al. 2021). Additionally, with complex absorption C_{max} for some products may occur at either the immediate or slow release phase, adding to the variability and thereby increasing the difficulty in passing the 80-125% GMR criteria for passing BE (Figure 19) (Laffont et al. 2015).

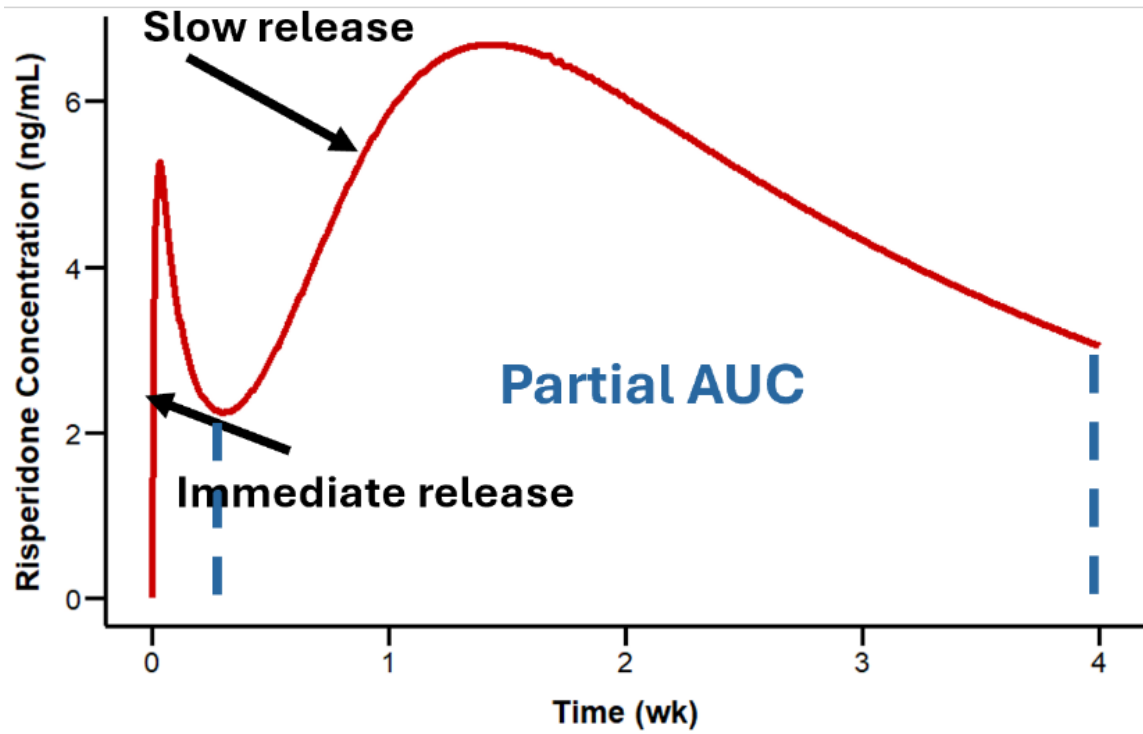


Figure 18 Complex Absorption with Long-Acting Injectables

Table 8 Representative Long-Acting Injectables with Product-Specific Guidances Recommending Partial AUCs

Active Ingredient	Dosage Form	Partial AUC Recommended
Naltrexone	ER suspension	$AUC_{1-10days}$, $AUC_{10-28days}$
Leuprolide acetate	Injectable and injectable depot	$AUC_{7days-t}$
Leuprolide acetate, Norethindrone acetate	Injectable depot/tablet	$AUC_{7days-t}$
Triptorelin pamoate	Injectable	$AUC_{7days-t}$
Buprenorphine	Injectable	$AUC_{3-4weeks}$
Octreotide acetate	Injectable	$AUC_{0-28days}$, $AUC_{10-28days}$

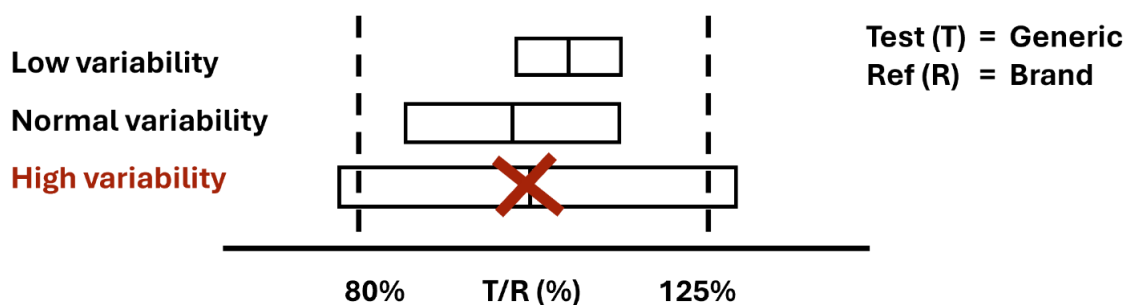


Figure 19 Consequences of Variability on Bioequivalence Determination

Long apparent half-lives (Table 9) can also make conventional BE trials (i.e., parallel and crossover) long and suffer from high dropout rates, while making rich PK sampling infeasible (Sharan et al. 2021). While single-dose parallel design trials suffer from low power, they are also often not recommended due to safety concerns (Sharan et al. 2021; Gong et al. 2023). LAIs are mostly unable to be given safely to healthy

volunteers, making single-dose parallel design infeasible for most LAIs (Figure 20). Because LAIs are mostly not safe for healthy volunteers, product-specific guidances (PSG) often recommend patients stable on the reference product and a multiple-dose steady state crossover design. Such a design poses several challenges, including difficulty in recruiting patients, high dropout rates due to steady state studies being extremely long, and the challenge in determining steady state (Sharan et al. 2021).

Table 9 Half-Lives and Times to Steady State for Representative Immediate Release and Long-Acting Product Counterparts

Active Ingredient	Immediate-Release Oral Product		Long-Acting Injectable	
	t_{1/2}	t_{ss, washout}	t_{1/2}	t_{ss, washout}
Risperidone	3 hrs	12 hrs	17 hrs	3 days
Medroxy-progesterone acetate	45 hrs	7.5 days	10 days	40 days
Leuprolide acetate	3 hrs	12 hrs	23 days	92 days

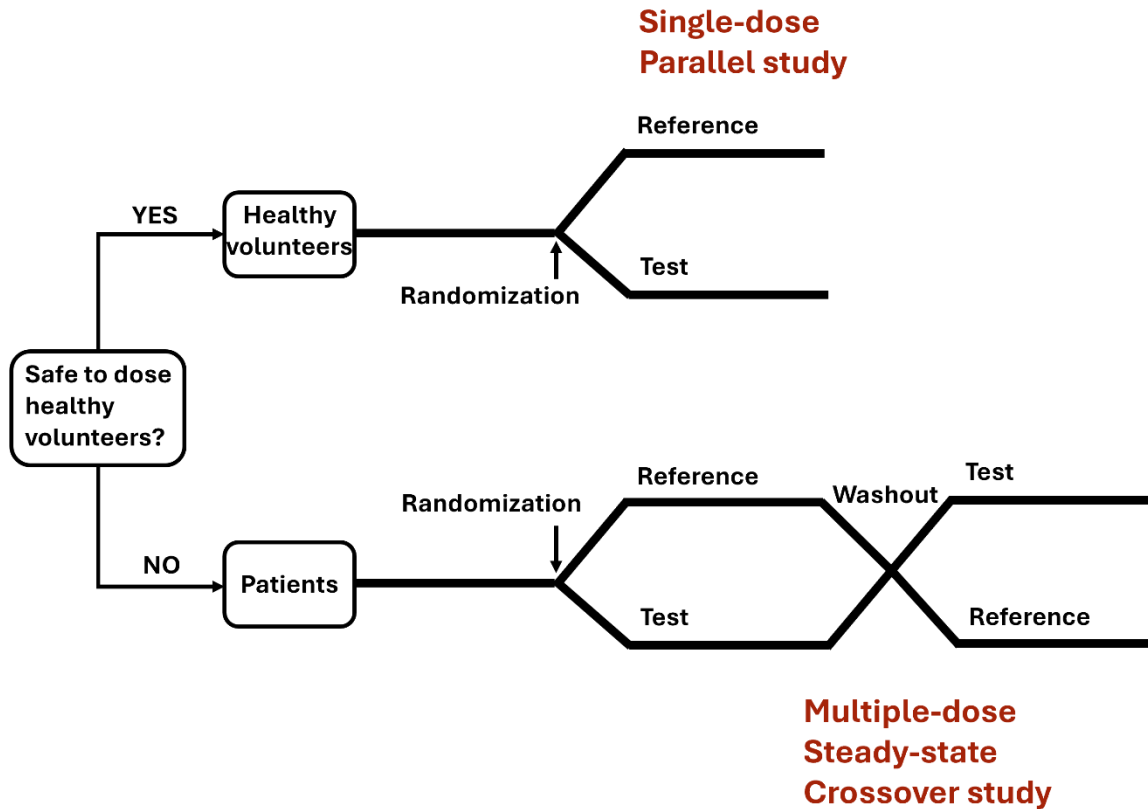


Figure 20 Conventional Study Designs to Establish Bioequivalence with Long-Acting Injectables

To make BE trials more manageable, innovative approaches such as adaptive design have been proposed (Lee, Feng, et al. 2020). Yet, more traction has been gained with utilizing model-integrated approaches to overcome the challenges in establishing BE for LAIs (Sharan et al. 2021; Zhao et al. 2019; Fang et al. 2018; Administration, n.d.). Model qualification, however, remains a major challenge for acceptance of model-informed and model-integrated BE approaches (Fang et al. 2018). Several model qualification approaches are commonly utilized during model development, including both graphical and numerical approaches. Currently, no standard exists for model qualification, and using a model to simulate trials necessitates more rigorous model qualification. For BE, models must be able to accurately and precisely estimate C_{max}

and AUC metrics. A qualified model should therefore be able to reproduce reported BE metrics for the reference product. Additionally, for virtual BE assessment, the MIBE approach must maintain acceptable Type I error rate (Gong et al. 2023) to protect against non-generics being approved due to application of a novel approach.

Here, we propose a model-integrated bioequivalence (MIBE) approach that can be applied to reduce the size of bioequivalence trials, thereby reducing costs and barriers to generic drug companies in establishing bioequivalence for complex drug products. This approach consists of a smaller abbreviated BE trial on which population PK (pop-PK) modeling is performed and BE is assessed virtually on larger simulated full BE trials. Pilot BE trials are smaller than may be necessary to establish BE by conventional approaches, such as parallel or crossover trial design and analysis with a non-compartmental analysis (NCA)-based average bioequivalence approach. Full BE trials are larger trials that may be prohibitively costly or infeasible to perform. With our proposed MIBE approach, full BE trials are simulated, and BE is assessed virtually.

To assist generic companies with the application of MIBE, we provide a framework with which the sponsors can consider and plan for an MIBE approach to take to regulatory agencies for agreement. This involves thorough evaluation of the MIBE approach and an application of a credibility assessment framework that has been advocated for within pharmacometrics in recent years at the FDA (ASME 2018; U.S. Food and Drug Administration 2023; Kuemmel et al. 2020).

References

Administration, U.S. Food and Drug. n.d. “Model-Integrated Evidence (MIE) Industry Meeting Pilot Between FDA and Generic Drug Applicants.” Accessed February 2,

2024. <https://www.fda.gov/drugs/abbreviated-new-drug-application-anda/model-integrated-evidence-mie-industry-meeting-pilot-between-fda-and-generic-drug-applicants>.
- ASME. 2018. “V V - Assessing Credibility of Computational Modeling through Verification and Validation: Application to Medical Devices.” 2018. <https://www.asme.org/codes-standards/find-codes-standards/assessing-credibility-of-computational-modeling-through-verification-and-validation-application-to-medical-devices>.
- Brissos, Sofia, Miguel Ruiz Veguilla, David Taylor, and Vicent Balanzá-Martinez. 2014. “The Role of Long-Acting Injectable Antipsychotics in Schizophrenia: A Critical Appraisal.” *Therapeutic Advances in Psychopharmacology* 4 (5): 198–219. <https://doi.org/10.1177/2045125314540297>.
- Creinin, Mitchell D., Rolf Jansen, Robert M. Starr, Joga Gobburu, Mathangi Gopalakrishnan, and Andrea Olariu. 2016. “Levonorgestrel Release Rates over 5 Years with the Liletta® 52-Mg Intrauterine System.” *Contraception* 94 (4): 353–56. <https://doi.org/10.1016/j.contraception.2016.04.010>.
- Fang, Lanyan, Myong Jin Kim, Zhichuan Li, Yaning Wang, Charles E. DiLiberti, Jessie Au, Andrew Hooker, Murray P. Ducharme, Robert Lionberger, and Liang Zhao. 2018. “Model-Informed Drug Development and Review for Generic Products: Summary of FDA Public Workshop.” *Clinical Pharmacology and Therapeutics* 104 (1): 27–30. <https://doi.org/10.1002/cpt.1065>.
- Fang, Lanyan, Ramana Uppoor, Mingjiang Xu, Satish Sharan, Hao Zhu, Nilufer Tampal, Bing Li, Lei Zhang, Robert Lionberger, and Liang Zhao. 2021. “Use of Partial Area Under the Curve in Bioavailability or Bioequivalence Assessments: A Regulatory Perspective.” *Clinical Pharmacology and Therapeutics* 0 (0): 1–8. <https://doi.org/10.1002/cpt.2174>.
- Gong, Yuqing, Peijue Zhang, Miyoung Yoon, Hao Zhu, Ameya Kohojkar, Andrew C. Hooker, Murray P. Ducharme, et al. 2023. “Establishing the Suitability of Model-Integrated Evidence to Demonstrate Bioequivalence for Long-Acting Injectable and Implantable Drug Products: Summary of Workshop.” *CPT: Pharmacometrics and Systems Pharmacology*. American Society for Clinical Pharmacology and Therapeutics. <https://doi.org/10.1002/psp4.12931>.
- Kuettel, Colleen, Yuching Yang, Xinyuan Zhang, Jeffry Florian, Hao Zhu, Million Tegenge, Shiew Mei Huang, Yaning Wang, Tina Morrison, and Issam Zineh. 2020. “Consideration of a Credibility Assessment Framework in Model-Informed Drug Development: Potential Application to Physiologically-Based Pharmacokinetic Modeling and Simulation.” *CPT: Pharmacometrics and Systems Pharmacology* 9 (1): 21–28. <https://doi.org/10.1002/psp4.12479>.

- Laffont, Celine M., Roberto Gomeni, Bo Zheng, Christian Heidebreder, Paul J. Fudala, and Azmi F. Nasser. 2015. "Population Pharmacokinetic Modeling and Simulation to Guide Dose Selection for RBP-7000, a New Sustained-Release Formulation of Risperidone." *Journal of Clinical Pharmacology* 55 (1): 93–103. <https://doi.org/10.1002/jcph.366>.
- Lee, Jieon, Kairui Feng, Mingjiang Xu, Xiajing Gong, Wanjie Sun, Jessica Kim, Zhen Zhang, Meng Wang, Lanyan Fang, and Liang Zhao. 2020. "Applications of Adaptive Designs in Generic Drug Development." *Clinical Pharmacology and Therapeutics*. <https://doi.org/10.1002/cpt.2050>.
- Lee, Jieon, Yuqing Gong, Sid Bhoopathy, Charles E. DiLiberti, Andrew C. Hooker, Amin Rostami-Hodjegan, Stephan Schmidt, et al. 2020. "Public Workshop Summary Report on Fiscal Year 2021 Generic Drug Regulatory Science Initiatives: Data Analysis and Model-Based Bioequivalence." *Clinical Pharmacology and Therapeutics* 0 (0): 1–6. <https://doi.org/10.1002/cpt.2120>.
- O'Brien, Matthew N., Wenlei Jiang, Yan Wang, and David M. Loffredo. 2021. "Challenges and Opportunities in the Development of Complex Generic Long-Acting Injectable Drug Products." *Journal of Controlled Release* 336 (June): 144–58. <https://doi.org/10.1016/j.jconrel.2021.06.017>.
- Sharan, Satish, Lanyan Fang, Viera Lukacova, Xiaomei Chen, Andrew C. Hooker, and Mats O. Karlsson. 2021. "Model-Informed Drug Development for Long-Acting Injectable Products: Summary of American College of Clinical Pharmacology Symposium." *Clinical Pharmacology in Drug Development* 10 (3): 220–28. <https://doi.org/10.1002/cpdd.928>.
- Stevens, Georgia L., Gail Dawson, and Jacqueline Zummo. 2016. "Clinical Benefits and Impact of Early Use of Long-Acting Injectable Antipsychotics for Schizophrenia." *Early Intervention in Psychiatry* 10 (5): 365–77. <https://doi.org/10.1111/eip.12278>.
- U.S. Food and Drug Administration. 2023. "Assessing the Credibility of Computational Modeling and Simulation in Medical Device Submissions - Guidance for Industry and Food and Drug Administration Staff." <https://www.regulations.gov>.
- Zhao, Liang, Myong Jin Kim, Lei Zhang, and Robert Lionberger. 2019. "Generating Model Integrated Evidence for Generic Drug Development and Assessment." *Clinical Pharmacology and Therapeutics* 105 (2): 338–49. <https://doi.org/10.1002/cpt.1282>.

Chapter 7: With Model-Integrated Bioequivalence, Bioequivalence Can Be Assessed through a Simulation-Based Approach

Over the past two decades, various model-informed approaches have been proposed to facilitate BE assessment. Conventionally, BE is assessed on the geometric mean ratio (GMR) of PK metrics (i.e., C_{max}, AUC) for reference vs test product based on the two one-sided t-test (TOST) (Schuirmann 1987). Average BE is considered to have passed if the 90% confidence interval (CI) of the GMR is within 80-125%. The most straight-forward of model-informed approaches involves performing the TOST procedure on NCA parameters derived from individual model predictions (Dubois et al. 2010; 2011) as opposed to directly from the observed data. Such a procedure, however, has been shown to inflate Type I error rate when PK sampling is relatively sparse, even more so than the standard NCA-based approach. Another model-informed approach that has been proposed is to perform TOST directly on the treatment effect estimate using a model-derived standard error estimate (Loingeville et al. 2020).

Simulation-based approaches, however, have also been proposed to assess bioequivalence virtually. These methods include nonparametric bootstrapping or parametric approaches. Virtual bioequivalence assessment via parametric simulations has been commonly proposed for physiologically-based pharmacokinetic (PBPK) modeling, where its use could be applicable to complex or locally-acting generics (Tsakalozou, Babiskin, and Zhao 2021; van Borselen et al. 2024; Pal et al. 2024; Lee, Gong, et al. 2020). For non-linear mixed effects (NLME) modeling, a simulation-based approach has been proposed with simulations with parameter and structural model uncertainty to generate confidence intervals of the GMRs for the BE endpoints (X. Chen et al. 2024; Bjugård Nyberg et al. 2024; Fang et al. 2018; Gong et al. 2023).

In our work, we propose an NLME modeling and simulation approach that does not involve simulations with parameter or structural model uncertainty (Figure 21). To assess BE with our approach, a pivotal abbreviated BE trial must first be conducted by the sponsor. NLME modeling is performed on the abbreviated pivotal trial data. After the model is qualified for the MIBE application, a large number (e.g., Nreps = 1000) of full BE trials are simulated, and NCA is performed on the simulations. From the distribution of GMRs for the BE endpoints, if the 5th and 95th percentiles are within 80-125%, the trial is considered to have passed BE. With this MIBE approach we can increase BE power compared to the conventional NCA and TOST procedure, while also maintaining quality. Application of this simulation-based BE assessment will be demonstrated in subsequent chapters.

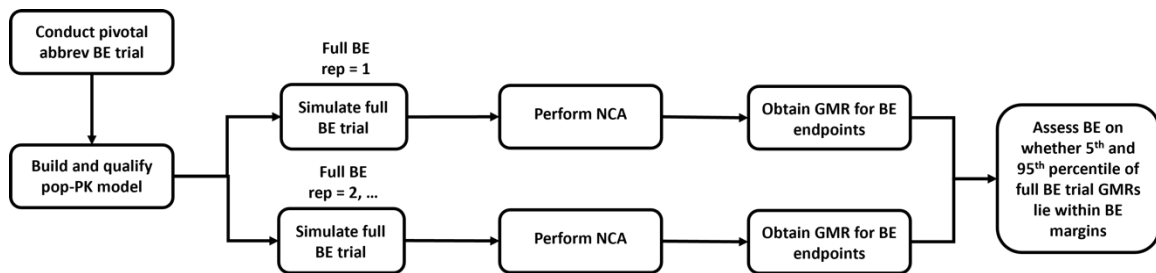


Figure 21 Simulation-Based Bioequivalence Assessment

References

- Bjugård Nyberg, Henrik, Xiaomei Chen, Mark Donnelly, Lanyan Fang, Liang Zhao, Mats O. Karlsson, and Andrew C. Hooker. 2024. "Evaluation of Model-integrated Evidence Approaches for Pharmacokinetic Bioequivalence Studies Using Model Averaging Methods." *CPT: Pharmacometrics & Systems Pharmacology*, August. <https://doi.org/10.1002/psp4.13217>.

- Borselen, Marjolein D. van, Laurens Auke Aemiel Sluijterman, Rick Greupink, and Saskia N. de Wildt. 2024. “Towards More Robust Evaluation of the Predictive Performance of Physiologically Based Pharmacokinetic Models: Using Confidence Intervals to Support Use of Model-Informed Dosing in Clinical Care.” *Clinical Pharmacokinetics* 63 (3): 343–55. <https://doi.org/10.1007/s40262-023-01326-3>.
- Chen, Xiaomei, Henrik B. Nyberg, Mark Donnelly, Liang Zhao, Lanyan Fang, Mats O. Karlsson, and Andrew C. Hooker. 2024. “Development and Comparison of Model-integrated Evidence Approaches for Bioequivalence Studies with Pharmacokinetic End Points.” *CPT: Pharmacometrics & Systems Pharmacology*, August. <https://doi.org/10.1002/psp4.13216>.
- Dubois, Anne, Sandro Gsteiger, Etienne Pigeolet, and France Mentré. 2010. “Bioequivalence Tests Based on Individual Estimates Using Non-Compartmental or Model-Based Analyses: Evaluation of Estimates of Sample Means and Type I Error for Different Designs.” *Pharmaceutical Research* 27 (1): 92–104. <https://doi.org/10.1007/s11095-009-9980-5>.
- Dubois, Anne, Marc Lavielle, Sandro Gsteiger, Etienne Pigeolet, and France Mentré. 2011. “Model-Based Analyses of Bioequivalence Crossover Trials Using the Stochastic Approximation Expectation Maximisation Algorithm.” *Statistics in Medicine* 30 (21): 2582–2600. <https://doi.org/10.1002/sim.4286>.
- Fang, Lanyan, Myong Jin Kim, Zhichuan Li, Yaning Wang, Charles E. DiLiberti, Jessie Au, Andrew Hooker, Murray P. Ducharme, Robert Lionberger, and Liang Zhao. 2018. “Model-Informed Drug Development and Review for Generic Products: Summary of FDA Public Workshop.” *Clinical Pharmacology and Therapeutics* 104 (1): 27–30. <https://doi.org/10.1002/cpt.1065>.
- Gong, Yuqing, Peijue Zhang, Miyoung Yoon, Hao Zhu, Ameya Kohojkar, Andrew C. Hooker, Murray P. Ducharme, et al. 2023. “Establishing the Suitability of Model-Integrated Evidence to Demonstrate Bioequivalence for Long-Acting Injectable and Implantable Drug Products: Summary of Workshop.” *CPT: Pharmacometrics and Systems Pharmacology*. American Society for Clinical Pharmacology and Therapeutics. <https://doi.org/10.1002/psp4.12931>.
- Lee, Jieon, Yuqing Gong, Sid Bhoopathy, Charles E. DiLiberti, Andrew C. Hooker, Amin Rostami-Hodjegan, Stephan Schmidt, et al. 2020. “Public Workshop Summary Report on Fiscal Year 2021 Generic Drug Regulatory Science Initiatives: Data Analysis and Model-Based Bioequivalence.” *Clinical Pharmacology and Therapeutics* 0 (0): 1–6. <https://doi.org/10.1002/cpt.2120>.
- Pal, Arindom, Fang Wu, Ross Walenga, Eleftheria Tsakalozou, Khondoker Alam, Yuqing Gong, Liang Zhao, and Lanyan Fang. 2024. “Leveraging Modeling and Simulation to Enhance the Efficiency of Bioequivalence Approaches for Generic Drugs: Highlights from the 2023 Generic Drug Science and Research Initiatives Public

Workshop.” *The AAPS Journal* 26 (3): 45. <https://doi.org/10.1208/s12248-024-00916-8>.

Schuirmann, Donald J. 1987. “A Comparison of the Two One-Sided Tests Procedure and the Power Approach for Assessing the Equivalence of Average Bioavailability.” *Journal of Pharmacokinetics and Biopharmaceutics* 15 (6): 657–80. <https://doi.org/10.1007/BF01068419>.

Tsakalozou, Eleftheria, Andrew Babiskin, and Liang Zhao. 2021. “Physiologically-Based Pharmacokinetic Modeling to Support Bioequivalence and Approval of Generic Products: A Case for Diclofenac Sodium Topical Gel, 1%.” *CPT: Pharmacometrics and Systems Pharmacology*. American Society for Clinical Pharmacology and Therapeutics. <https://doi.org/10.1002/psp4.12600>.

Chapter 8: Successful Application of Model-Integrated Bioequivalence Is Predicated on Thorough Planning Using Modeling and Simulation

Research into MIBE applications has been abundant in the last decade, with funding from and workshops organized by the FDA (Fang et al. 2018; Lee, Gong, et al. 2020; Gong et al. 2023; Pal et al. 2024). From this effort, the Model-Integrated Evidence (MIE) Pilot Program was launched in 2023 to facilitate interactions with sponsors and FDA on model-informed approaches for ANDA applications (U.S. Food and Drug Administration, n.d.-c). Still, much uncertainty exists with respect to how to apply MIBE and how it will be regulated by regulatory bodies, as a guidance is not yet available.

For PBPK applications to MIBE, however, the FDA has published on the first use of dermal PBPK modeling and simulation in determining BE virtually, which led to a successful generic approval (Tsakalozou, Babiskin, and Zhao 2021). Additionally, regulatory considerations and application of ASME V&V 40 for model-integrated evidence have been published for PBPK modeling (Pal et al. 2024; Kuemmel et al. 2020; ASME 2018). Such recommendations or examples for application of MIBE for non-PBPK applications, however, have not been published. We propose here in our work a general MIBE framework that sponsors can follow to guide the implementation of MIBE for their products (Figure 22).

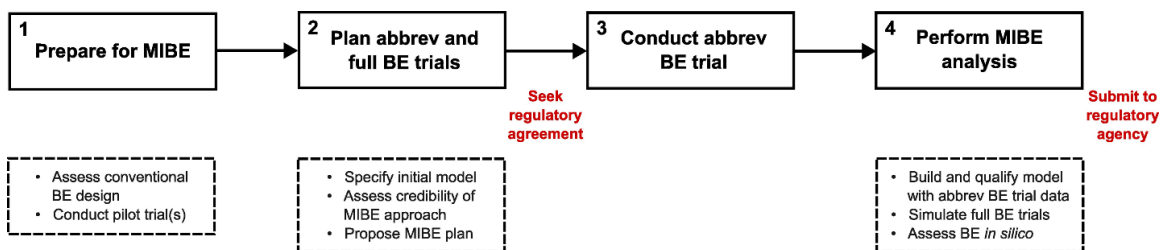


Figure 22 Model-Integrated Bioequivalence Framework

The first stage we propose is the preparation phase for MIBE. Here, we presume that in vitro formulation-related checks have been performed and that Q1/Q2 are met. Conventional BE designs will be assessed, meaning exploration of the feasibility of parallel and crossover designs and the requisite sample sizes with conventional BE assessment (i.e., NCA and TOST). This assessment should be done prior to and after the conduct of pilot trial(s). If a need for MIBE is determined from this assessment, an MIBE plan is then developed.

The second stage involves planning the abbreviated and full BE trials through a thorough investigation of the MIBE approach and then presenting the final plan to the regulatory agency. To begin this planning stage, we develop a model on the pilot data. Through model development we will arrive at a final model that will be qualified. However, we refer to this final model as the initial model, as it is the model developed on pilot data. For model qualification, along with standard evaluation of model diagnostics and goodness-of-fit plots, the final model should be qualified with quantitative predictive checks (QPC) that ensure that the model can reproduce the expected central tendency and variability in the PK metrics of interest for BE determination. After qualifying the model, the MIBE plan is developed and the credibility of the MIBE plan is assessed. Application of the planning stage for MIBE with Depo-SubQ Provera 104 will be demonstrated in Chapter 9.

References

- ASME. 2018. “V V - Assessing Credibility of Computational Modeling through Verification and Validation: Application to Medical Devices.” 2018. <https://www.asme.org/codes-standards/find-codes-standards/assessing-credibility-of-computational-modeling-through-verification-and-validation-application-to-medical-devices>.
- Fang, Lanyan, Myong Jin Kim, Zhichuan Li, Yaning Wang, Charles E. DiLiberti, Jessie Au, Andrew Hooker, Murray P. Ducharme, Robert Lionberger, and Liang Zhao. 2018. “Model-Informed Drug Development and Review for Generic Products: Summary of FDA Public Workshop.” *Clinical Pharmacology and Therapeutics* 104 (1): 27–30. <https://doi.org/10.1002/cpt.1065>.
- Gong, Yuqing, Peijue Zhang, Miyoung Yoon, Hao Zhu, Ameya Kohojkar, Andrew C. Hooker, Murray P. Ducharme, et al. 2023. “Establishing the Suitability of Model-Integrated Evidence to Demonstrate Bioequivalence for Long-Acting Injectable and Implantable Drug Products: Summary of Workshop.” *CPT: Pharmacometrics and Systems Pharmacology*. American Society for Clinical Pharmacology and Therapeutics. <https://doi.org/10.1002/psp4.12931>.
- Kuemmel, Colleen, Yuching Yang, Xinyuan Zhang, Jeffry Florian, Hao Zhu, Million Tegenge, Shiew Mei Huang, Yaning Wang, Tina Morrison, and Issam Zineh. 2020. “Consideration of a Credibility Assessment Framework in Model-Informed Drug Development: Potential Application to Physiologically-Based Pharmacokinetic Modeling and Simulation.” *CPT: Pharmacometrics and Systems Pharmacology* 9 (1): 21–28. <https://doi.org/10.1002/psp4.12479>.
- Lee, Jieon, Yuqing Gong, Sid Bhoopathy, Charles E. DiLiberti, Andrew C. Hooker, Amin Rostami-Hodjegan, Stephan Schmidt, et al. 2020. “Public Workshop Summary Report on Fiscal Year 2021 Generic Drug Regulatory Science Initiatives: Data Analysis and Model-Based Bioequivalence.” *Clinical Pharmacology and Therapeutics* 0 (0): 1–6. <https://doi.org/10.1002/cpt.2120>.
- Pal, Arindom, Fang Wu, Ross Walenga, Eleftheria Tsakalozou, Khondoker Alam, Yuqing Gong, Liang Zhao, and Lanyan Fang. 2024. “Leveraging Modeling and Simulation to Enhance the Efficiency of Bioequivalence Approaches for Generic Drugs: Highlights from the 2023 Generic Drug Science and Research Initiatives Public Workshop.” *The AAPS Journal* 26 (3): 45. <https://doi.org/10.1208/s12248-024-00916-8>.
- Tsakalozou, Eleftheria, Andrew Babiskin, and Liang Zhao. 2021. “Physiologically-Based Pharmacokinetic Modeling to Support Bioequivalence and Approval of Generic Products: A Case for Diclofenac Sodium Topical Gel, 1%.” *CPT: Pharmacometrics and Systems Pharmacology*. American Society for Clinical Pharmacology and Therapeutics. <https://doi.org/10.1002/psp4.12600>.

———. n.d.-c. “Model-Integrated Evidence (MIE) Industry Meeting Pilot Between FDA and Generic Drug Applicants.” Accessed September 17, 2024.
<https://www.fda.gov/drugs/abbreviated-new-drug-application-anda/model-integrated-evidence-mie-industry-meeting-pilot-between-fda-and-generic-drug-applicants>.

Chapter 9: The Credibility of a Model-Integrated Bioequivalence Plan Should Be Thoroughly Assessed to Enhance Confidence

9.1 Introduction

Model qualification remains a major challenge for acceptance of model-informed and model-integrated BE approaches (Fang et al. 2018; Kuemmel et al. 2020). While general best practices for model qualification with pop-PK and exposure-response modeling have been established (U.S. Food and Drug Administration 2022a; 2003), currently no standard exists to assess the credibility of modeling and simulation for which the modeling provides substantial evidence to support a regulatory decision. From the FDA, there has been a push to implement the V&V 40 framework from the medical device space and adapt it for MIDD and MIE applications (U.S. Food and Drug Administration 2023; Kuemmel et al. 2020). This involves establishing the question of interest and the context of use for the model and then assessing the model risk and establishing a qualification plan to assess the credibility, given the context of use and model risk.

Importantly, the qualification should be tailored to the context of use. The rigor of the qualification will be determined by the model risk, with higher risk necessitating more rigorous qualification. Model risk is composed of two factors—model influence and decision consequence—and each factor can be characterized as low, medium, or high. Model influence is the degree to which the model contributes to making a decision, while decision consequence is the severity of the negative consequences of making an incorrect decision. The modeling approach is deemed credible if the approach is sufficiently qualified for the context of use.

To demonstrate the credibility assessment framework for MIBE, we apply it to the contraceptive Depo-SubQ Provera 104, a long-acting injectable administered subcutaneously every three months, as the reference drug product. While there are several approved generics for Depo Provera, an intramuscular LAI with the same active ingredient medroxyprogesterone acetate (MPA), no generic for Depo-SubQ Provera 104 has been approved. For in vivo BE, the FDA product-specific guidance for medroxyprogesterone acetate recommends a single-dose parallel design (U.S. Food and Drug Administration, n.d.-b). We demonstrate here how to plan your MIBE approach (i.e., planning stage of MIBE framework in Figure 22) for a generic for Depo-SubQ Provera 104 with the simulation-based BE assessment described in Chapter 7.

9.2 Methods

- *Model Development and Qualification*

A literature review of PubMed, Scopus, and regulatory databases was performed for pop-PK models of Depo-SubQ Provera 104. As a published pop-PK model was unavailable, a model was developed from digitized PK data and summary statistics from the FDA Clinical Pharmacology Review (Jain et al. 2004; U.S. Food and Drug Administration, n.d.-a). Mean PK values from Study 272, a single-dose 3-month PK study with 42 subjects, were digitized with WebPlotDigitizer 4.5.

A naïve-averaged analysis was performed on the digitized PK data in Pumas 2.1 software (Rackauckas et al. 2020) to develop the structural model. A visual inspection of simulation with the fixed effects parameter estimates was performed to qualify the naïve-averaged model. To develop a non-linear mixed effects model (NLME), estimates of

between-subject variability were derived from Table 1 summary statistics from the FDA Clinical Pharmacology Review. The residual error model estimates were taken from Francis, et al's model of depot medroxyprogesterone acetate (Francis et al. 2021).

The NLME model was qualified with QPC. Percentiles (25, 50, 75%) for BE parameters (i.e., C_{max}, AUC_{inf}) were derived from the reported summary statistics with the assumption of a lognormal distribution in BE parameters. A large number of subjects (i.e., 200) was used in the simulations to get an accurate assessment of the BE parameters. Adjustments to the original parameter estimates were made to adequately match the central tendency and spread in BE parameters (i.e., C_{max}, AUC_{inf}).

- *MIBE Evaluation*

The MIBE plan was developed and evaluated within the V&V 40 credibility assessment framework according to the four steps laid out below.

o *Assessment of Conventional BE Power and Type I Error Rate*

Single-dose, parallel BE trials were simulated (Nreps = 500) with 24-96 subjects (12-48 subjects per arm) and 72-312 subjects for low and high variability scenarios, respectively. Between-subject variability (BSV) for CL and V_c were set to 25% and 50% CV for low and high variability, respectively. Power was assessed by simulating a test-to-reference (T/R) ratio of 0.95 on relative bioavailability, while Type I error rate was assessed with a T/R ratio of 0.80. Noncompartmental analysis (NCA) was performed with Pumas 2.1, and bioequivalence analysis was performed for C_{max} and AUC with the Bioequivalence.jl package.

- *Assessment of Reliability of Parameter Estimates*

The reliability of the parameter estimates (i.e., bias and precision) were assessed by evaluating the percent error of the parameter estimates (Equation 1).

$$\text{Percent Error (\%)} = \frac{\text{Estimate} - \text{True Value}}{\text{True Value}} \cdot 100 \quad (\text{Equation 1})$$

Simulations (Nreps = 200) were performed at several number of subjects. Bias was determined by evaluating deviation of the median of the 200 simulation repetitions from 0% error, while precision was determined by evaluating the 5th and 95th percentiles.

- *Assessment of Full BE Power and Type I Error Rate*

To assess full BE power and Type I error rate, first the number of subjects needed to power the trial by conventional BE analysis was determined. 33, 50, and 67% of the trial size to power by conventional analysis were explored for the abbreviated BE trial (Nreps = 200). Estimation was performed on the abbreviated BE trial simulations. Full BE trials (Nreps = 100) were simulated from the abbreviated BE trial estimates with number of subjects up to 100% of the conventional BE trial size. BE was assessed virtually on the full BE trials simulations from the 5th and 95th percentile of the geometric mean ratios (GMR) (Figure 21). The overall workflow is shown in Figure 23.

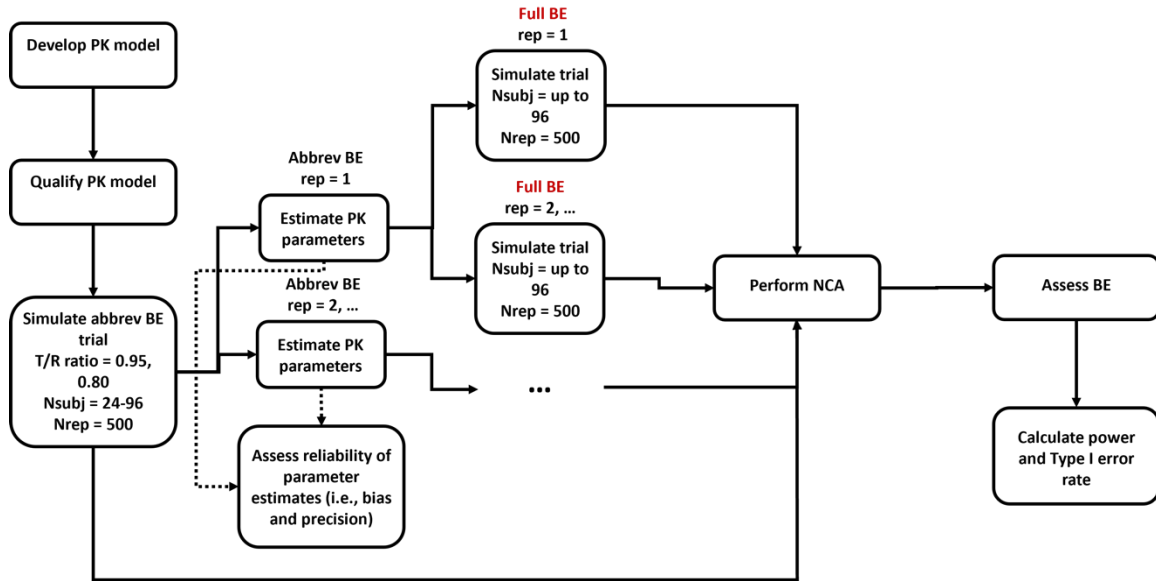


Figure 23 Model-Integrated Bioequivalence Planning Simulation Framework

The final MIBE plan is determined by minimizing the abbreviated BE trial size while maximizing full BE power and maintaining full BE Type I error rate of 5%.

- *Sensitivity Analyses*

Sensitivity analyses were performed for three potential scenarios to determine the robustness of the MIBE approach. The first scenario entailed a large discrepancy between the variability assumed while planning and observed from the abbreviated pivotal trial (e.g., 25% BSV planned vs 50% BSV observed or vice versa). For the second and third scenarios, only the low variability (i.e., 25% BSV) scenario was considered. For the second scenario, the impacts of bias and imprecision in parameter estimates were determined by simulating sparse sampling trials (i.e., 25% of the rich sampling) and assessing full BE power and Type I error rate. The third scenario assessed the impact of performing full BE trial simulations with parameter uncertainty. Parameter uncertainty

was obtained from the variance-covariance matrix, with simulations including not only the variances but also the covariances to include correlations between parameters.

9.3 Results

- MIBE Credibility Assessment Framework

The MIBE credibility assessment framework that guided our work in the planning stage is shown in Table 10. Even though BE will be assessed virtually from modeling and simulation, the model influence was deemed to be medium due to rich empiric data still being generated with our MIBE approach. The decision consequence was high because an ineffective generic being approved could result in unwanted pregnancies or unmanaged pain for an endometriosis indication. Overall, the model risk here was deemed medium-high, necessitating a robust four-step qualification plan to evaluate the MIBE approach.

Table 10 Assessment of Credibility of Model-Integrated Bioequivalence Approach

Question of interest	Is the test formulation bioequivalent to the reference Depo-SubQ Provera 104?
Context of use	The model will be used to assess BE virtually from an abbreviated BE trial.
Model risk	Medium-High
<ul style="list-style-type: none"> • Model influence 	<p>Medium</p> <ul style="list-style-type: none"> • Rich empiric BE data is available from the pivotal abbreviated BE trial. • BE will be assessed virtually on full BE trial simulations.
<ul style="list-style-type: none"> • Decision consequence 	<p>High</p> <ul style="list-style-type: none"> • Incorrect decision could result in a non-generic entering the market and could result in inadequate efficacy or mild adverse events.
Qualification plan	
<ul style="list-style-type: none"> • Planning stage 	<ul style="list-style-type: none"> • Model development <ol style="list-style-type: none"> 1. Diagnostics according to good practices recommended in regulatory guidances 2. Quantitative predictive checks (QPC) to ensure model is reproducing the distribution of PK metrics (e.g., Cmax and AUC) • MIBE evaluation <ol style="list-style-type: none"> 1. Assessment of conventional BE power and Type I error rate 2. Assessment of reliability of parameter estimates (i.e., bias and precision) 3. Assessment of full BE power and Type I error rate 4. Sensitivity analyses to determine robustness of MIBE plan
<ul style="list-style-type: none"> • MIBE analysis stage 	<ul style="list-style-type: none"> • Model development <ol style="list-style-type: none"> 1. Diagnostics according to good practices recommended in regulatory guidances 2. Quantitative predictive checks (QPC) to ensure model is reproducing the distribution of PK metrics (e.g., Cmax and AUC) 3. Sensitivity analyses deemed necessary if final model different from planning stage model

- *Model Development and Qualification*

MPA from Depo-SubQ Provera 104 is absorbed rapidly, without an apparent delay or multiphasic features, so first-order and zero-order absorption models were considered (Jain et al. 2004). A zero-order absorption model was chosen, as an assumed lognormal distribution in the zero-order parameter, duration, matched the skew in t_{max} from the summary statistics (U.S. Food and Drug Administration, n.d.-a). A zero-order, one-compartment model was able to reproduce the central tendency and variability from Study 272 (Figure 24). BSV in the duration parameter was unable to be estimated.

However, we were still able to reasonably reproduce the observed C_{max} .

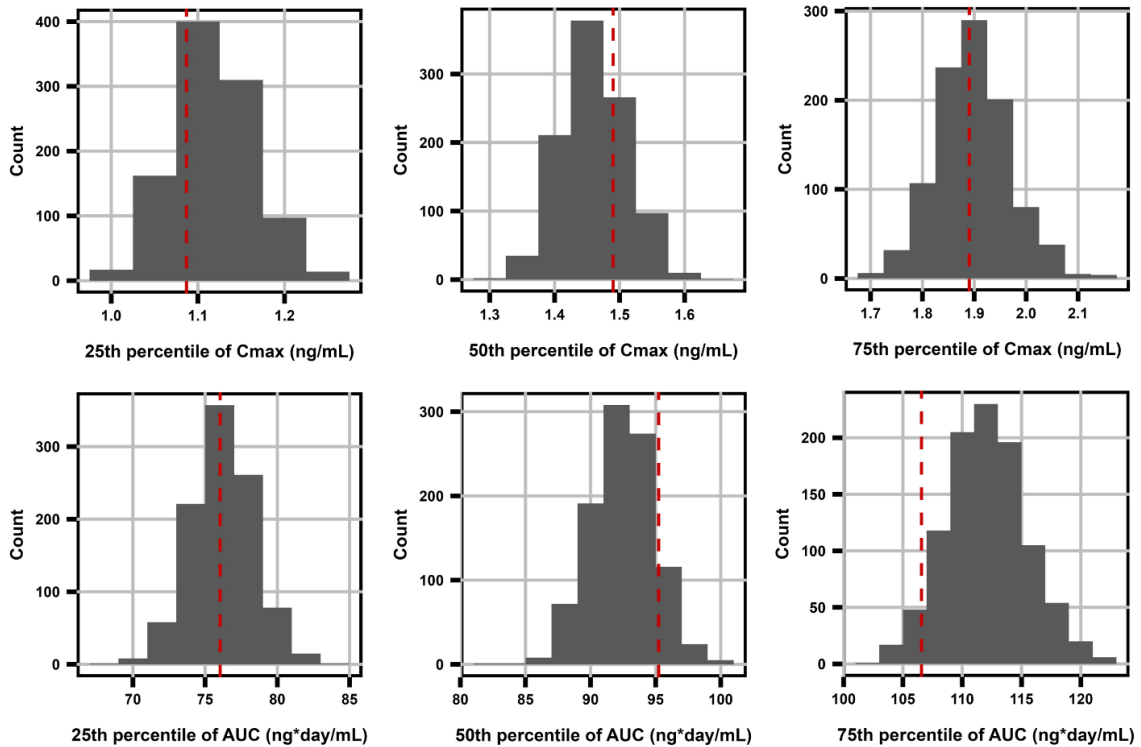


Figure 24 *Quantitative Predictive Check of the PK Model for Depo-SubQ Provera 104*

- *MIBE Evaluation*

The MIBE approach was developed and evaluated in four steps (Table 10).

o *Assessment of Conventional BE Power and Type I Error Rate*

With our Depo-SubQ Provera 104 example, we demonstrate BE power and Type I error rate by conventional analysis for low and high variability scenarios (25 and 50% BSV) (Figure 25). We demonstrate that by conventional analysis approximately 72 and 264 subjects are needed to achieve an overall target power of 80% for variability of 25 and 50%, respectively. We also demonstrate that the expected Type I error rate of approximately 5% is maintained in both Cmax and AUC.

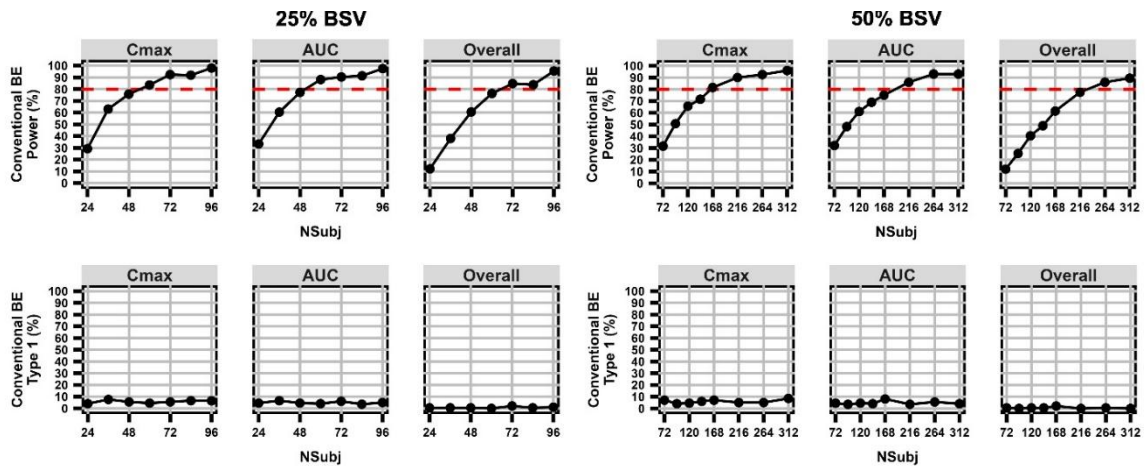


Figure 25 Bioequivalence Power and Type I Error Rate with Conventional BE Analysis

○ *Assessment of Reliability of Parameter Estimates*

Reliability of parameter estimates was assessed by evaluating percent error (Equation 1, Figure 26). Bias is minimal in the parameters T/R, CL, Vc, ω CL, and ω Vc. Precision is also reasonable on these parameters, with 95% of estimates within approximately 10% of the true values for the typical values and within approximately 30% for the between-subject variability estimates. The duration and proportional error estimates are positively biased (20%), however, presumably due to the sampling around Cmax and inability to estimate between-subject variability in the duration parameter.

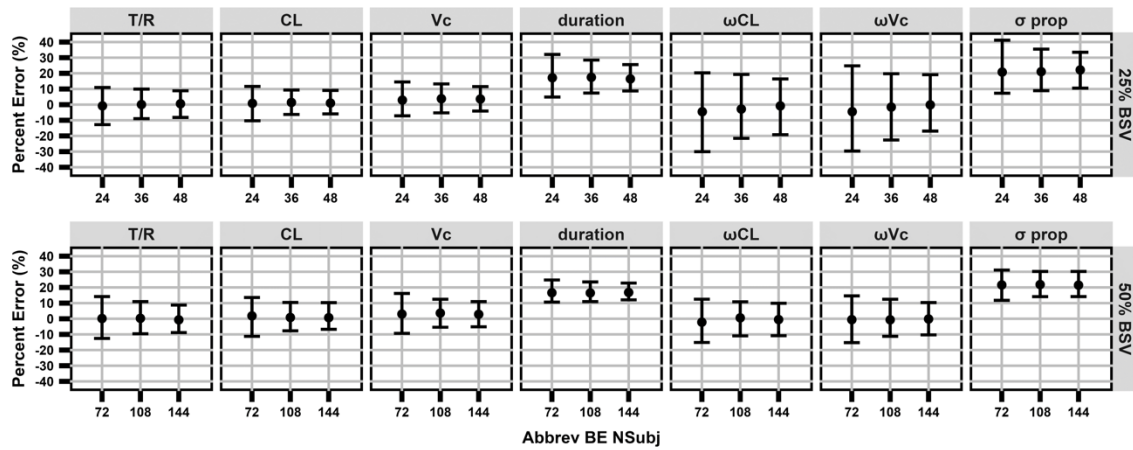


Figure 26 Bias and Precision in Parameter Estimates of Abbreviated BE Trials

Dot represents 50th percentile, and error bars represent 5th and 95% percentiles.

○ *Assessment of Full BE Power and Type I Error Rate*

Full BE power with the simulation-based approach was higher than the conventional TOST approach for every full BE trial size (Figure 27). Power and Type I error rate increased with full BE trial sizes, as expected due to shrinking lower and upper bounds on the GMRs. Adequate full BE Type I error rate, however, was better maintained at higher abbreviated BE trial sizes.

The following criteria were used to determine the final abbreviated and full be trial sizes—minimizing abbreviated BE trial size, while maximizing full BE power and maintaining adequate Type I error rate. The final proposal for the low variability scenario is 36 and 72 subjects for abbreviated and full BE trials, respectively. The final proposal for the high variability scenario is 144 and 216 subjects. Thus, we propose a 50% and 33% reduction in trial size with the MIBE approach for low and high variability, respectively.

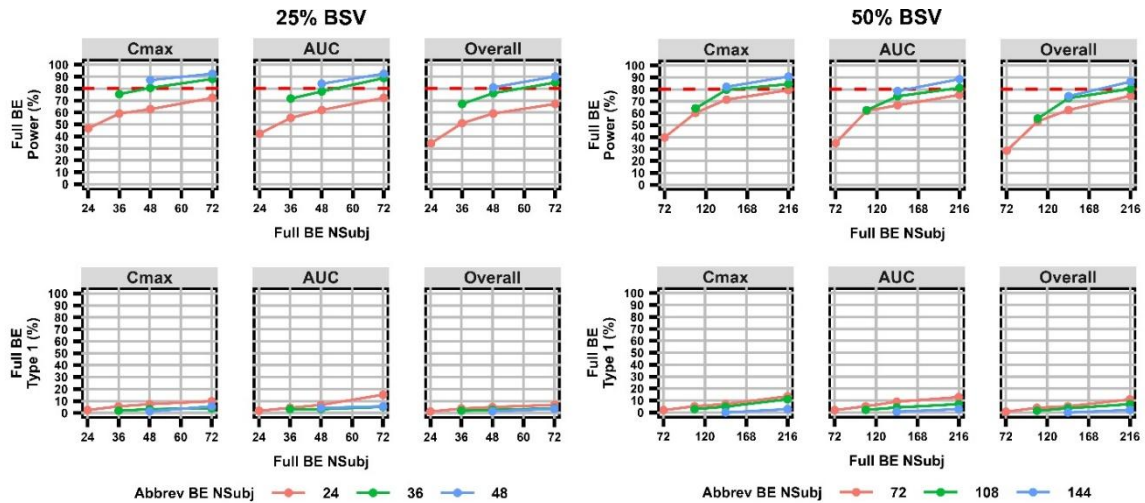


Figure 27 Bioequivalence Power and Type I Error Rate with MIBE

- *Sensitivity Analyses*

- 1. *Large Disparity Between Planned and Observed Pivotal Trial Variability*

If MIBE planning were to be performed with an assumed 25% BSV, then the resulting abbreviated and full BE trial sizes would be 36 and 72 subjects, respectively (Figure 27). As opposed to a full BE overall power of approximately 85% with matching variability between planned and observed in the pivotal trial, the full BE power would be much lower at approximately 30% if the pivotal abbreviated BE trial were to have 50% BSV (Figure 28). With the observed pivotal trial variability being much higher than planned, the full BE Type I error rate would be maintained at 5% or lower. For the opposite scenario in which the observed pivotal trial variability is much lower than planned, the full BE power would be nearly 100%, while Type I error rate would be much lower than the nominal 5%.

number of abbreviated subjects. Importantly, the sparse sampling had no impact on the bias of the T/R estimate. Sparse sampling had minimal impact on the BSV estimates for CL and V_c , but caused the bias in the proportional error estimate to increase from approximately 20% to 50%.

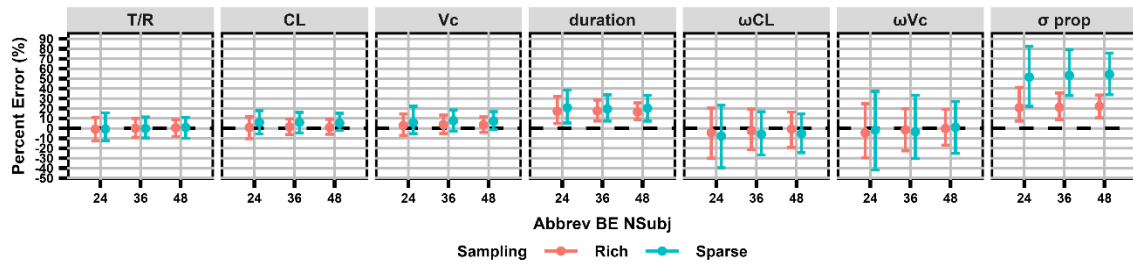


Figure 29 Bias and Precision of Parameter Estimates with Rich and Sparse Sampling

With the confirmation that our sparse sampling impacts the reliability of the parameter estimates, we evaluated the ultimate impact of the bias and imprecision on full BE power and Type I error rates. Sparse sampling reduced full BE power, but the power for rich and sparse sampling tended to converge as full BE trial subjects increased to 72 subjects (i.e., number of subjects needed to power by conventional analysis) (Figure 30). The impact of sparse sampling on full BE Type I error rate was less clear, with potentially a slight inflation of Type I with more abbreviated BE trial subjects. Ultimately, even with sparse sampling here, the choice of 36 and 72 abbreviated and full BE trial subjects, respectively, may be unaffected, as Type I error rate is still around 5% and power is still above 80%.

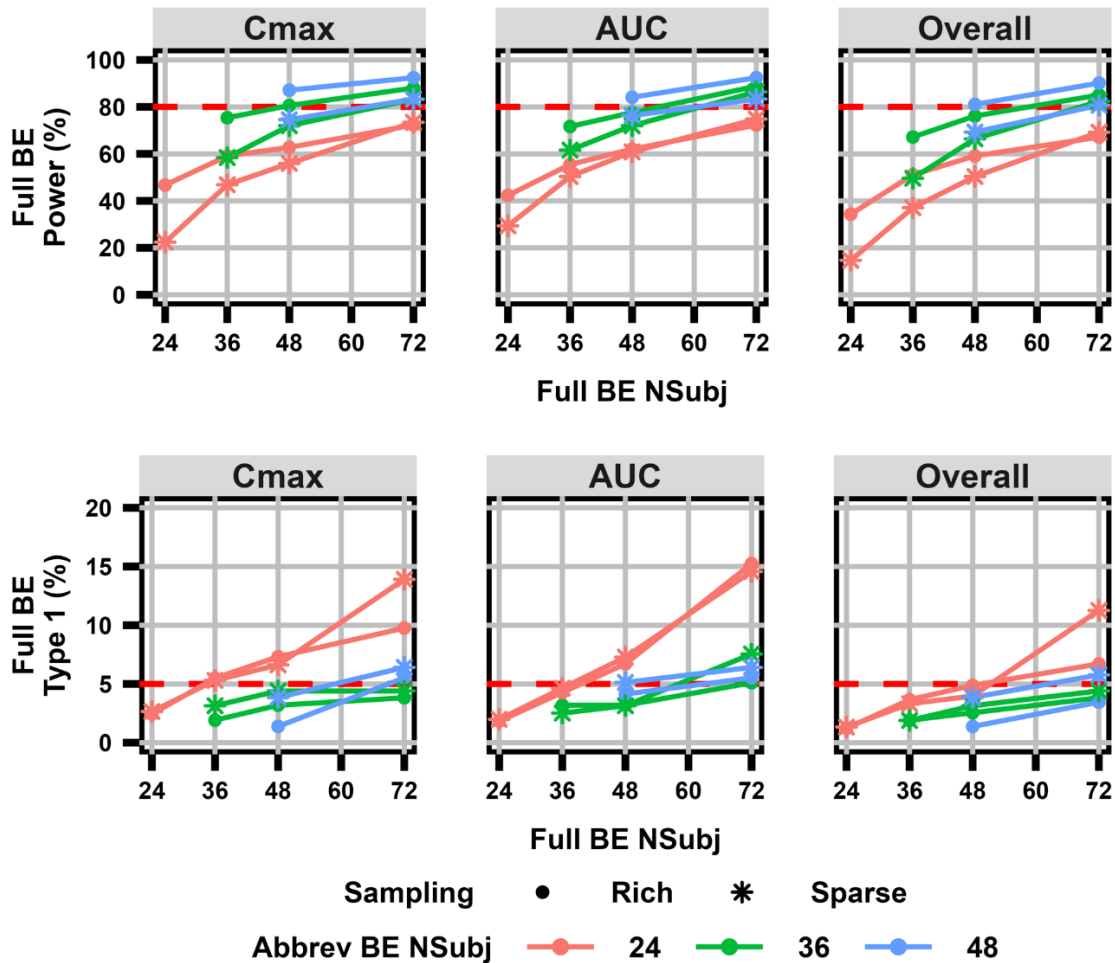


Figure 30 Bioequivalence Power and Type I Error Rate with Rich and Sparse Sampling

3. Full BE Trial Simulations with Parameter Uncertainty

Because our simulation-based approach to assess BE does not simulate with parameter uncertainty (Figure 21), the impact of simulating full BE trials with parameter uncertainty was assessed, with the pass rates for both full BE power and Type I error rates decreasing (Figure 31). Without simulating with parameter uncertainty, given our framework for deciding on abbreviated and full BE trial sizes, abbreviated and full BE

trial sizes are 36 and 72 subjects, respectively, resulting in an overall BE power of approximately 85%. With simulating with parameter uncertainty, however, 36 and 72 subjects (abbreviated and full BE trial sizes) results in a reduced overall power of approximately 70%, which does not achieve the 80% target. An abbreviated BE trial size of 48 subjects with simulating with parameter uncertainty marginally improves the overall power to nearly 80%.

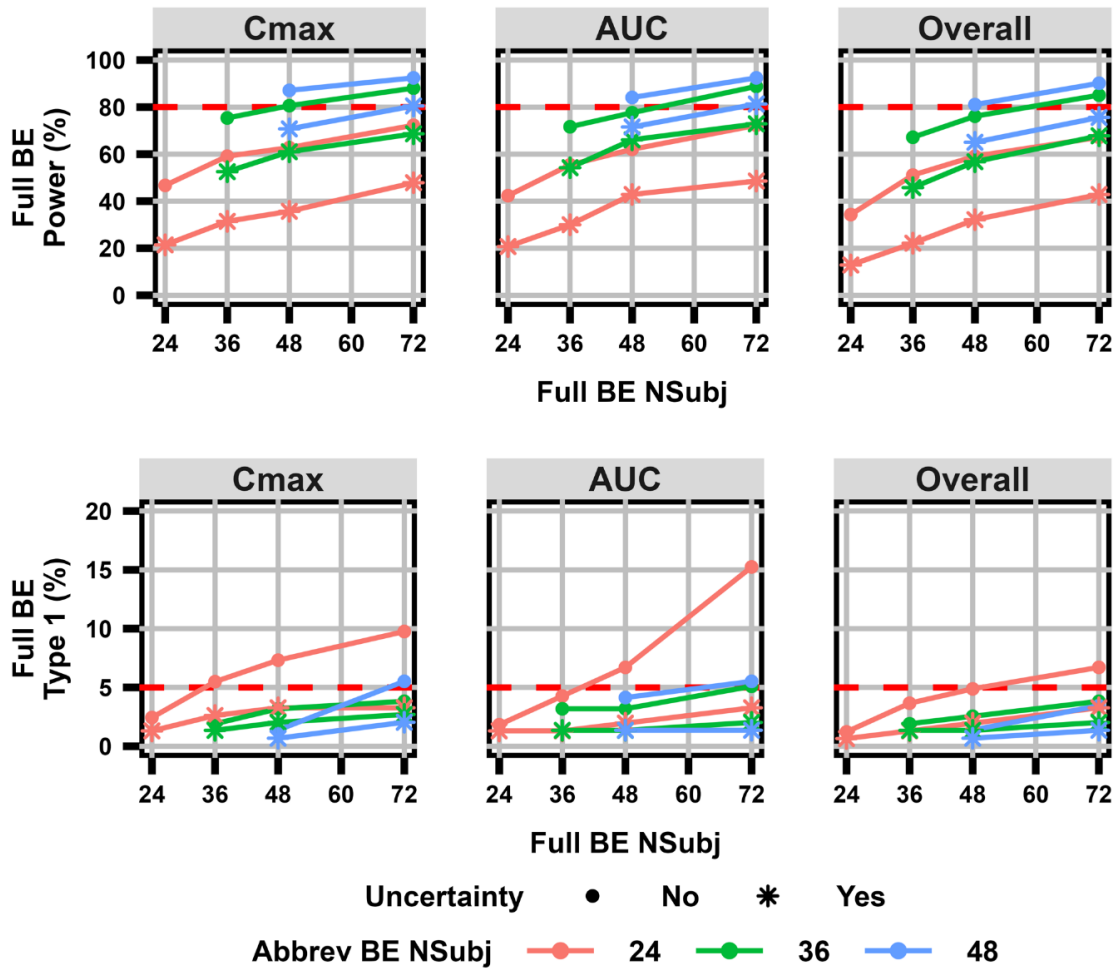


Figure 31 Bioequivalence Power and Type I Error Rate with and without Simulations with Parameter Uncertainty

9.4 Discussion

Modeling is often recommended by regulatory agencies to address challenges within generic drug development. In particular, with products like long-acting injectables (LAIs), due to the challenging nature of conducting long trials in patients, the ability to abbreviate trials with MIBE may facilitate more generics entering the market. We demonstrated here with the Depo-SubQ Provera 104 example that MIBE offers a more efficient pathway to establishing BE without compromising quality.

- *Power and Type I Error Rate with Conventional Analysis*

With our Depo-SubQ Provera 104 example, we demonstrated BE power and Type I error rate by conventional analysis for low and high variability scenarios (25 and 50% BSV) (Figure 27). This power analysis can be part of the assessment of the need for MIBE in the planning stage (Figure 22). However, the power analysis can also be done without PK modeling and simulation with conventional statistical methods (Labes 2024).

Concerns at this stage for Type I error rate not being maintained at approximately 5% would primarily come from potential deficiencies in sampling or bioanalysis (Dubois et al. 2010). If sampling is inadequate around C_{max} , Type I error rate can be impacted. With below limit of quantification (BLQ) samples, Type I error rate can also be impacted for AUC or partial AUC. Of note, these potential concerns require PK modeling and simulation to be identified and cannot be identified with conventional statistical analysis.

- *The Pivotal Trial Should Be Designed to Estimate Sensitive Formulation-Related Model Parameters Reasonably Well*

The most sensitive parameters for MIBE are the absorption and bioavailability-related parameters on which T/R ratios are applied. If bias or imprecision are noted in parameter estimates, judgment should be used in determining whether adjustments may be necessary in the modeling, sampling, or trial design. In our Depo-SubQ Provera 104 example, bias was noted in the duration and proportional error estimates (Figure 26). Yet, the QPC in Figure 24 indicates that the model is still able to reproduce the expected central tendency and variability in both C_{max} and AUC, providing confidence in the model's use for MIBE.

Precision of parameter estimates can be influenced by the number of subjects, yet the determination of the abbreviated and full BE trial sizes based on preserving Type I error rate implicitly evaluates whether the precision of parameter estimates is adequate. This is evident in that full BE Type I error rate increases at a greater rate with more full BE subjects when the abbreviated BE trial has fewer subjects (Figure 27), confirming that the parameters are estimated more precisely with more abbreviated BE trial subjects.

We demonstrated here how to assess the impact of bias and imprecision in parameter estimates due to sparse sampling. Even with sparse sampling, however, the estimate of the formulation effect remained unbiased with all abbreviated trial sizes and precision was only affected at the smallest trial size (Figure 29). The final MIBE plan and overall BE power was also unaffected by the sparse sampling (Figure 30). Thus, this overall MIBE approach appears to be resilient to bias and imprecision as long as the formulation effect is estimated reliably.

- *The Final MIBE Plan Can Be Designed to Preserve Type I Error Rate*

Virtual BE methodology has not been well established, with more advancement within the PBPK realm (van Borselen et al. 2024). Recently, a Bayesian virtual BE framework was proposed, but we are not aware of any proposed framework for virtual BE with NLME and maximum likelihood estimation (Bois and Brochet 2024). Here, we demonstrated how to design the MIBE plan in a manner that maximizes power and maintains adequate Type I error rate.

First, we establish the number of subjects required to power the study by conventional analysis. Our target here is the traditional 80% power. However, we aim for an overall model-derived power, as opposed to an 80% power on an individual rate-limiting BE endpoint. For our low and high variability scenarios, approximately 72 and 216 subjects, respectively, were needed to achieve an overall 80% power.

Of note, while I mentioned earlier that the power analysis as part of assessing the need for MIBE (Figure 25) could be performed without modeling and simulation, it is strongly recommended that the overall 80% power target by conventional analysis be performed through modeling and simulation for two reasons. First, it is desirable to match the powering for the full BE simulations to a model-derived powering to make them more comparable. Second, comparing a model-derived power, especially overall power, to a conventional statistically-derived power may not be straightforward. For a conventional sample size determination, an analytical solution will likely be utilized for the more standard trial designs (U.S. Food and Drug Administration 2022b). The highest variability derived from conventional analysis of BE endpoints on pilot data is commonly chosen for sample size determination for the pivotal trial, rather than a composite analysis

of all the BE endpoints together. This is due to the interdependence of all the BE endpoints not being straightforward, and thus, requiring simulations to derive sample sizes based on true overall power.

After establishing the number of subjects needed to power the study by conventional analysis, set percentages of this number of subjects are explored for MIBE planning. Given the 72 and 216 subjects to achieve 80% power by conventional analysis in our example, 33, 50, and 67% of 72 and 216 subjects (i.e., 24, 36, 48 subjects; 72, 108, 144 subjects) were chosen as the number of abbreviated BE trial subjects to investigate. For full BE simulations, the number of subjects simulated were up to the 72 and 216 subjects to power by conventional analysis. For example, for evaluation of 24 subjects in the abbreviated BE trial, 24, 36, 48, and 72 subjects (i.e., 33, 50, 67, and 100% of subjects to achieve 80% power by conventional analysis) would be simulated for the full BE trials. For evaluation of 36 subjects in the abbreviated BE trial, 36 to 72 subjects would be simulated, and so forth.

To evaluate the scenarios in determining the final recommendation, two criteria were used to maximize full BE power while maintaining acceptable full BE Type I error rate. The first criteria is to minimize the number of subjects in the abbreviated BE trial that can still lead to the target of 80% overall power, and the second criteria is to only consider full BE trials that maintain acceptable Type I error.

Within this framework, if we were to evaluate 24 subjects in the abbreviated trial (i.e., 67% reduction in trial size), we would stop at either 36 or 48 subjects for the full BE trial, as the full BE Type I error rate is approximately 10% and 13% for C_{max} and AUC at 72 subjects. With abbreviated BE trial size of 24 subjects and full BE trial size of 36 or

48 subjects, overall power is approximately 50 or 60%, respectively. Thus, an abbreviated BE trial with 24 subjects would be inadequate to power the study. The same evaluation for 36 subjects results in full BE simulations with 72 subjects and overall power of approximately 85%. Therefore, for the low variability scenario, the final recommendation would be 36 and 72 subjects for the abbreviated and full BE trials, respectively, providing a 50% reduction in the pivotal trial size.

However, for the high variability scenario, the final recommendation results in a 33% reduction. The inability to achieve the same 50% reduction as in the low variability scenario is due to two factors. The first factor is that a 50% reduction (i.e., 108 subjects) results in inflated full BE Type I error rate in C_{max} at 216 subjects, which limits the evaluation of 108 abbreviated BE trial subjects to 144 full BE trial subjects. The second factor is that this pairing results in an overall full BE power of approximately 72%, which is less than the target of 80%. This necessitates the evaluation of a greater number of subjects than 108. With 144 abbreviated BE trial subjects, full BE Type I error is maintained at 216 subjects (i.e., number of subjects to power by conventional analysis) and results in an overall full BE power of nearly 90%. The final recommendation, therefore, would be 144 abbreviated BE trial subjects and 216 abbreviated BE trials. Given that the overall full BE power is nearly 90%, additional analysis could be performed by the sponsor to further reduce the size of the abbreviated BE trial if even 144 subjects could be deemed too large from cost, recruitment and timeline perspectives.

To summarize, virtual BE simulations with larger trial sizes can be designed based on evaluating abbreviated and full BE trial sizes that maximize full BE power while

preserving Type I error rate. As a rule of thumb, we propose the trial size needed to power the trial by conventional analysis as the upper limit for the simulated full BE trial size.

- *Our MIBE Approach Is Robust to a Large Disparity Between Planned and Observed Variability*

When planning the MIBE approach, much of the assumptions will come from pilot data, including assumptions regarding the model structure and parameter estimates. Additional assumptions may include the T/R ratio of the final test formulation and the variability, which will largely be a consequence of BSV for a parallel design and BOV for a crossover design. While pilot data should be robust to have more confidence while planning the MIBE approach, due to inherent variability from various sources, the variability assumptions used to plan the final MIBE approach could end up being very disparate from the resulting variability in the pivotal abbreviated trial.

The likelihood of this occurring can be mitigated by several factors. First, pilot data should be robust, meaning there should be sufficient information to make reasonable assessments of T/R and variability. This includes adequate number of subjects in pilot data for both reference and test formulations, as well as adequate PK sampling, as the sampling may impact several factors, such as the GMR and CV of C_{max} or partial AUC. Ideally, the sampling in the pilot trial(s) should closely match that which is planned for the pivotal trial to mitigate risks and additional sensitivity analyses. Second, the pilot data should include PK data on the final test formulation. While information on several formulations can be informative on what the formulation-sensitive parameters are, thereby informing us on where to apply T/R ratios in the model, additional risk will be incurred without pilot data on the final formulation. Third, the batch of reference and test

formulation used for planning should be the same as for the pivotal trial, especially if there is known batch-to-batch variability and if the GMRs for the endpoints in the pilot data deviate much from 1.0 (e.g., 0.9 or 1.1). This will reduce inducing additional variability that could increase the risk of the pivotal trial failing due to factors outside of the MIBE planning and approach.

Regardless of these mitigation factors, invariably limitations will remain in terms of what can practically be obtained for pilot data. These may include collecting pilot data in healthy subjects, while the pivotal trial may require patients. Additionally, while the pivotal trial may be a crossover trial, the pilot trial(s) may be of parallel design. This leads to an inability to assess within-subject variability or between-occasion variability, so the variability for a pivotal crossover trial may need to be assumed from the total variability obtained in the parallel pilot data.

While the more robust and representative the pilot data is of the planned pivotal trial, the more likely the assumptions will match the results from the pivotal trial, due to chance or some unknown factor, results from the pivotal trial can be quite disparate from what was assumed from the pilot data. Such scenarios were investigated here in terms of the variability that was used to plan the pivotal abbreviated BE and full BE trials being much different from what results in the pivotal abbreviated BE trial.

Large disparities in planned vs observed variabilities were shown to not increase the regulatory risk of approving a non-generic product with this MIBE approach, as full BE Type I error rate was maintained at or decreased from 5% (Figure 28). As with a conventional approach, power is much reduced when the observed variability is much higher than expected, indicating that this MIBE method is similarly sensitive to

underpowering, which highlights again that the application of MIBE does not bypass the need for robust pilot data. Likewise, the observed variability being much lower than expected results in the MIBE trial being overpowered, as with a conventional approach.

- *Our MIBE Approach Does Not Require Simulating Full BE Trials with Parameter Uncertainty*

When BE is assessed virtually with a simulation-based approach, confidence intervals around the point estimate are generated from the distribution of GMRs across the simulation repetitions. Thus, the clinical trial simulations technically should be performed with parameter uncertainty (X. Chen et al. 2024; C. Hu 2022; Kümmel et al. 2018). However, we demonstrate here that practically, simulating with parameter uncertainty is not necessary and Type I error rate is protected regardless due to the framework in deciding the abbreviated and full BE trial sizes.

Simulating with parameter uncertainty necessitates larger abbreviated BE trial sizes to achieve comparable power when restricting full BE trial sizes to the trial size to power a conventional study. Yet, as full BE Type I error rate increases at a much slower rate with increasing full BE trial size, when simulating with parameter uncertainty, smaller abbreviated trials may be possible if the full BE trial size is not restrained by the conventional design trial size. This should be explored in future work, as we have demonstrated a reduction in trial size of 33-50% in our work with simulating without parameter uncertainty.

9.5 Conclusion

We demonstrated here how to plan for MIBE in a systematic manner that lends credibility to the model-integrated approach. Additionally, we demonstrated the robustness of our simulation-based approach to assessing BE and the overall MIBE framework by evaluating the sensitivity of our MIBE framework to scenarios beyond the original MIBE plan.

9.6 References

- ASME. 2018. “V V - Assessing Credibility of Computational Modeling through Verification and Validation: Application to Medical Devices.” 2018. <https://www.asme.org/codes-standards/find-codes-standards/assessing-credibility-of-computational-modeling-through-verification-and-validation-application-to-medical-devices>.
- Bois, Frederic Y., and Céline Brochot. 2024. “A Bayesian Framework for Virtual Comparative Trials and Bioequivalence Assessments.” *Frontiers in Pharmacology* 15 (July). <https://doi.org/10.3389/fphar.2024.1404619>.
- Borselen, Marjolein D. van, Laurens Auke Æmiel Sluijterman, Rick Greupink, and Saskia N. de Wildt. 2024. “Towards More Robust Evaluation of the Predictive Performance of Physiologically Based Pharmacokinetic Models: Using Confidence Intervals to Support Use of Model-Informed Dosing in Clinical Care.” *Clinical Pharmacokinetics* 63 (3): 343–55. <https://doi.org/10.1007/s40262-023-01326-3>.
- Chen, Xiaomei, Henrik B. Nyberg, Mark Donnelly, Liang Zhao, Lanyan Fang, Mats O. Karlsson, and Andrew C. Hooker. 2024. “Development and Comparison of Model-integrated Evidence Approaches for Bioequivalence Studies with Pharmacokinetic End Points.” *CPT: Pharmacometrics & Systems Pharmacology*, August. <https://doi.org/10.1002/psp4.13216>.
- Dubois, Anne, Sandro Gsteiger, Etienne Pigeolet, and France Mentré. 2010. “Bioequivalence Tests Based on Individual Estimates Using Non-Compartmental or Model-Based Analyses: Evaluation of Estimates of Sample Means and Type I Error for Different Designs.” *Pharmaceutical Research* 27 (1): 92–104. <https://doi.org/10.1007/s11095-009-9980-5>.

- Fang, Lanyan, Myong Jin Kim, Zhichuan Li, Yaning Wang, Charles E. DiLiberti, Jessie Au, Andrew Hooker, Murray P. Ducharme, Robert Lionberger, and Liang Zhao. 2018. “Model-Informed Drug Development and Review for Generic Products: Summary of FDA Public Workshop.” *Clinical Pharmacology and Therapeutics* 104 (1): 27–30. <https://doi.org/10.1002/cpt.1065>.
- Francis, Jose, Rosie Mngqibisa, Helen McIlleron, Michelle A Kendall, Xingye Wu, Kelly E. Dooley, Cynthia Firnhaber, Catherine Godfrey, Susan E. Cohn, and Paolo Denti. 2021. “A Semimechanistic Pharmacokinetic Model for Depot Medroxyprogesterone Acetate and Drug–Drug Interactions With Antiretroviral and Antituberculosis Treatment.” *Clinical Pharmacology & Therapeutics* 110 (4): 1057–65. <https://doi.org/10.1002/cpt.2324>.
- Hu, Chuanpu. 2022. “Variability and Uncertainty: Interpretation and Usage of Pharmacometric Simulations and Intervals.” *Journal of Pharmacokinetics and Pharmacodynamics*, 487–91. <https://doi.org/10.1007/s10928-022-09817-9>.
- Jain, John, Caryn Dutton, Antonia Nicosia, Charlie Wajszczuk, Frederick R. Bode, and Daniel R. Mishell. 2004. “Pharmacokinetics, Ovulation Suppression and Return to Ovulation Following a Lower Dose Subcutaneous Formulation of Depo-Provera®.” *Contraception* 70 (1): 11–18. <https://doi.org/10.1016/j.contraception.2004.01.011>.
- Kuemmel, Colleen, Yuching Yang, Xinyuan Zhang, Jeffry Florian, Hao Zhu, Million Tegenge, Shiew Mei Huang, Yaning Wang, Tina Morrison, and Issam Zineh. 2020. “Consideration of a Credibility Assessment Framework in Model-Informed Drug Development: Potential Application to Physiologically-Based Pharmacokinetic Modeling and Simulation.” *CPT: Pharmacometrics and Systems Pharmacology* 9 (1): 21–28. <https://doi.org/10.1002/psp4.12479>.
- Kümmel, Anne, Peter L. Bonate, Jasper Dingemanse, and Andreas Krause. 2018. “Confidence and Prediction Intervals for Pharmacometric Models.” *CPT: Pharmacometrics and Systems Pharmacology* 7 (6): 360–73. <https://doi.org/10.1002/psp4.12286>.
- Labes, Detlew; Schutz, Helmut; Lang, Benjamin. 2024. “PowerTOST: Power and Sample Size for (Bio)Equivalence Studies.” March 18, 2024. <https://cran.r-project.org/web/packages/PowerTOST/index.html>.
- Rackauckas, Chris, Yingbo Ma, Andreas Noack, Vaibhav Dixit, Shubham Maddhashiya, Patrick Kofod Mogensen, José Bayoán Santiago Calderón, et al. 2020. “Accelerated Predictive Healthcare Analytics with Pumas, a High Performance Pharmaceutical Modeling and Simulation Platform.” *BioRxiv*. <https://doi.org/10.1101/2020.11.28.402297>.
- U.S. Food and Drug Administration. 2023. “Assessing the Credibility of Computational Modeling and Simulation in Medical Device Submissions - Guidance for Industry and Food and Drug Administration Staff.” <https://www.regulations.gov>.

- . 2022b. “Statistical Approaches to Establishing Bioequivalence - Guidance for Industry.” <https://www.fda.gov/drugs/guidance-compliance-regulatory-information/guidances-drugs>.
- . n.d.-a. “Depo-SubQ Provera 104 Clinical Pharmacology and Biopharmaceutics Review(s).” Accessed February 2, 2024.
- . n.d.-b. “Draft Guidance on Medroxyprogesterone Acetate.” Accessed February 2, 2024. <http://www.accessdata.fda.gov/scripts/cder/dissolution/>.

Chapter 10: Discussion

In our work here, we demonstrated the application of modeling and simulation to challenges in therapeutics and generic drug development. For the first project, an integrated approach utilizing *in vitro*, *in vivo*, and human data with PK modeling and simulation was performed to optimize rifampin dosing for orthopedic implant-associated infection of *S. aureus*. For the second project, a model-integrated bioequivalence (MIBE) framework with a simulation-based virtual BE assessment was proposed with Depo-SubQ Provera 104 as the example product.

For the first project, the PK of mice and humans were shown to be different with both microdosing and therapeutic dosing, which precluded the use of a single model with allometric scaling between species. For microdosing, clearance was ten times lower in mice, which was attributed to the higher protein binding in mice (97% vs 90%). Bone penetration of rifampin was found to be 10 and 15% in mice and humans, respectively, which is much lower than reported in literature from single time point experiments (20-50%) (Sirot et al. 1983; 1977; Cluzel et al. 1984). For therapeutic dosing, a mouse model was developed from literature, as the two models in literature failed to reproduce the expected PK profiles (Chunli Chen et al. 2016; Bartelink et al. 2017). A human model from Svensson et al was used for the human model (Svensson et al. 2018). Notably, the mouse model did not have any of the PK non-linearities (i.e., more than dose-proportional increase in bioavailability, autoinduction, and saturable clearance) present in the human model.

Simulations with the therapeutic dose models with standard- and high-dose regimens demonstrated that bone exposures of rifampin are much lower than previously

thought, with concentrations maintained at below the planktonic *S. aureus* breakpoint of 1 mg/L. This suggests that cure rates of 70-90% could potentially be improved with high-dose rifampin regimens of 35-40 mg/kg, as opposed to the standard-dose regimens of 10 mg/kg (Zimmerli and Sendi 2019).

For the second project, an MIBE framework that involves four stages was proposed to facilitate the application of MIBE by generic companies. The stages were as follows: 1) preparation for MIBE, 2) planning MIBE, 3) conducting pivotal abbreviated BE trial, and 4) performing MIBE analysis. We demonstrated the implementation of the planning stage within the framework of the credibility assessment adapted from the American Society of Mechanical Engineers' V&V 40 (ASME 2018; U.S. Food and Drug Administration 2023; Kuemmel et al. 2020).

With a simulation-based virtual BE assessment, we demonstrated that an abbreviated BE trial size of 50-67% smaller in terms of number of subjects could be achieved for Depo-SubQ Provera 104. A framework was established for choosing the abbreviated and full BE trial size pairings, which was based on maximizing full BE power while maintaining acceptable Type I error rate. The full BE trial size was restricted to the trial size to power the trial by conventional analysis.

As part of the model qualification and credibility assessment, we proposed the primary model qualification should be based on whether the model could reproduce the central tendency and variability in PK parameters (e.g., C_{max}, AUC) through a quantitative predictive check (QPC). Additionally, we proposed that the model parameters should be estimated reliably—that is with minimal bias and imprecision—yet, the MIBE approach may be resilient to some bias and imprecision as long as the

formulation-related parameters are estimated reliably. Sensitivity analyses demonstrated that not only is the MIBE approach resilient to bias and imprecision of parameter estimates due to sparse sampling, the approach is also resilient to large discrepancies in variability assumed while planning versus the observed variability in the pivotal abbreviated trial.

While it is commonly assumed that the simulation-based virtual BE approach must simulate with parameter uncertainty to protect against Type I error, we demonstrate that Type I error is preserved with our overall approach. With the full BE trial size cap of the trial size for a conventional approach, simulating with parameter uncertainty reduces the power and necessitate larger abbreviated BE trial sizes. However, full BE Type I error rate was noted to rise at a much slower rate with increasing full BE trial size, when simulating with parameter uncertainty, which may allow for comparable abbreviated BE trial sizes if the full BE trial size is not limited.

Overall, by leveraging model-informed approaches across both projects, we were able to demonstrate the diverse and unique capabilities of tackling distinct challenges with quantitative approaches.

References

- ASME. 2018. “V V - Assessing Credibility of Computational Modeling through Verification and Validation: Application to Medical Devices.” 2018. <https://www.asme.org/codes-standards/find-codes-standards/assessing-credibility-of-computational-modeling-through-verification-and-validation-application-to-medical-devices>.
- Bartelink, I. H., N. Zhang, R. J. Keizer, N. Strydom, P. J. Converse, K. E. Dooley, E. L. Nuermberger, and R. M. Savic. 2017. “New Paradigm for Translational Modeling to Predict Long-Term Tuberculosis Treatment Response.” *Clinical and Translational Science* 10 (5): 366–79. <https://doi.org/10.1111/cts.12472>.
- Chen, Chunli, Fatima Ortega, Laura Alameda, Santiago Ferrer, and Ulrika S.H. Simonsson. 2016. “Population Pharmacokinetics, Optimised Design and Sample Size Determination for Rifampicin, Isoniazid, Ethambutol and Pyrazinamide in the Mouse.” *European Journal of Pharmaceutical Sciences* 93:319–33. <https://doi.org/10.1016/j.ejps.2016.07.017>.
- Cluzel, R. A., R. Lopitiaux, J. Sirot, and S. Rampon. 1984. “Rifampicin in the Treatment of Osteoarticular Infections Due to Staphylococci.” *Journal of Antimicrobial Chemotherapy* 13 (suppl C): 23–29. https://doi.org/10.1093/jac/13.suppl_C.23.
- Kuempel, Colleen, Yuching Yang, Xinyuan Zhang, Jeffry Florian, Hao Zhu, Million Tegenge, Shiew Mei Huang, Yaning Wang, Tina Morrison, and Issam Zineh. 2020. “Consideration of a Credibility Assessment Framework in Model-Informed Drug Development: Potential Application to Physiologically-Based Pharmacokinetic Modeling and Simulation.” *CPT: Pharmacometrics and Systems Pharmacology* 9 (1): 21–28. <https://doi.org/10.1002/psp4.12479>.
- Sirot, J, R Lopitiaux, R Cluzel, J J Delisle, and B Sauvezie. 1977. “[Rifampicin Diffusion in Non-Infected Human Bone (Author’s Transl)].” *Annales de Microbiologie* 128 (2): 229–36.
- Sirot, J, L Prive, R Lopitiaux, and Y Glanddier. 1983. “[Diffusion of Rifampicin into Spongy and Compact Bone Tissue during Total Hip Prosthesis Operation].” *Pathologie-Biologie* 31 (5): 438–41.
- Svensson, Robin J., Rob E. Aarnoutse, Andreas H. Diacon, Rodney Dawson, Stephen H. Gillespie, Martin J. Boeree, and Ulrika S.H. Simonsson. 2018. “A Population Pharmacokinetic Model Incorporating Saturable Pharmacokinetics and Autoinduction for High Rifampicin Doses.” *Clinical Pharmacology and Therapeutics* 103 (4): 674–83. <https://doi.org/10.1002/cpt.778>.
- U.S. Food and Drug Administration. 2023. “Assessing the Credibility of Computational Modeling and Simulation in Medical Device Submissions - Guidance for Industry and Food and Drug Administration Staff.” <https://www.regulations.gov>.

Zimmerli, Werner, and Parham Sendi. 2019. "Role of Rifampin against Staphylococcal Biofilm Infections in Vitro, in Animal Models, and in Orthopedic-Device-Related Infections." *Antimicrobial Agents and Chemotherapy*. American Society for Microbiology. <https://doi.org/10.1128/AAC.01746-18>.

Appendix

Scripts

ABE_MPA_SD_pl_BE_main.jl

```
#####  
# title: Single-Dose Parallel Design Abbreviated BE Main Script  
#####  
  
@info "packages"  
using Distributed, CSV, Serialization, Random  
  
@info "load ABE functions"  
@everywhere include("ABE_MPA_SD_pl_BE_fxns.jl")  
  
@info "setup results location"  
RESULTS_DIR = mktempdir()  
ENV["RESULTS_FILE"] = RESULTS_DIR  
  
@info "Nreps, T/R ratio, Nsubj for ABE sims"  
Nreps_ABE = 1000  
#input_tr_ratio = [0.80, 0.85, 0.90, 0.95]  
input_tr_ratio = [0.80, 0.95]  
## for 25% BSV  
#BSV = 0.246  
#Nsubj_ABE = [24, 36, 48, 60, 72, 84, 96]  
## for 50% BSV  
BSV = 0.472  
Nsubj_ABE = [72, 108, 144, 168, 216, 264, 312]  
  
@info "trial obstimes"  
@everywhere obstimes =  
[0.001,2,4,5,6,7,8,10,12,14,16,20,24,29,36,43,50,57,64,71,78,85,90,104,132  
,150,180,210] # 28 samples  
#@everywhere obstimes =  
[0.001,2,4,5,6,7,8,10,12,14,16,24,36,50,71,85,104,132,150,180,210]  
# 21 samples  
#@everywhere obstimes =  
[0.001,2,4,5,6,7,8,10,12,14,36,85,150,210]  
# 14 samples  
  
@info "running main map"  
  
_rng = Random.default_rng()
```

```

Random.seed!(_rng, 1234)

ABE_results = @time pmap(Iterators.product(input_tr_ratio, Nsubj_ABE,
BSV)) do (tr, nsubj_ABE, bsv)
    @info "tr = $tr, nsubj = $nsubj_ABE"
    i_BE_LB_GMR_UB_CV_df, i_BE_passed_df, BE_passrate_df =
ABE_sims(_rng;
                                                    Nr
eps_ABE,
                                                    in
put_tr_ratio = tr,
                                                    Ns
ubj_ABE = nsubj_ABE,
                                                    BS
V = bsv
                                                    )

    return i_BE_LB_GMR_UB_CV_df, i_BE_passed_df, BE_passrate_df
end;

@info "post-process results"

i_BE_LB_GMR_UB_CV      = [i[1] for i in ABE_results]
i_BE_passed            = [i[2] for i in ABE_results]
BE_passrate           = [i[3] for i in ABE_results]

i_BE_LB_GMR_UB_CV_df  = reduce(vcat, i_BE_LB_GMR_UB_CV)
i_BE_passed_df        = reduce(vcat, i_BE_passed)
BE_passrate_df        = reduce(vcat, BE_passrate)

@info "save results"
CSV.write(joinpath(REULTS_DIR,
    "i_BE_LB_GMR_UB_CV_ABE_Nreps$(Nreps_ABE)_$(BSV)bsv_Nsubj$(Nsubj_ABE[1])_$(
Nsubj_ABE[end]).csv"), i_BE_LB_GMR_UB_CV_df)
CSV.write(joinpath(REULTS_DIR,
    "i_BE_passed_ABE_Nreps$(Nreps_ABE)_$(BSV)bsv_Nsubj$(Nsubj_ABE[1])_$(Nsubj_
ABE[end]).csv"), i_BE_passed_df)
CSV.write(joinpath(REULTS_DIR,
    "BE_passrate_ABE_Nreps$(Nreps_ABE)_$(BSV)bsv_Nsubj$(Nsubj_ABE[1])_$(Nsubj_
ABE[end]).csv"), BE_passrate_df)

```

ABE_MPA_SD_pl_BE_fxns.jl

```

#####
# title: Single-Dose Parallel Design Abbreviated BE Functions Script

```

#####

using Pumas, CSV, Random, Bioequivalence

@info "parallel ABE trial simulation model"

zero-order absorption, 1-cmt, combined error model

sim_model_abs0_1cmt_pl_ABE = @model begin

 @param begin

 # tv

 tvtr_ratio ∈ RealDomain(lower=0.0001)

 tvCL ∈ RealDomain(lower=0.0001)

 tvVc ∈ RealDomain(lower=0.0001)

 tvDuration ∈ RealDomain(lower=0.0001)

 # BSV

 ωCL_BSV ∈ RealDomain(lower=0.0001)

 ωVc_BSV ∈ RealDomain(lower=0.0001)

 ωDuration_BSV ∈ RealDomain(lower=0.0001)

 # RUV

 σ_add ∈ RealDomain(lower=0.0001)

 σ_prop ∈ RealDomain(lower=0.0001)

 end

 @random begin

 # BSV

 ηCL ~ Normal(0.0, ωCL_BSV)

 ηVc ~ Normal(0.0, ωVc_BSV)

 ηduration ~ Normal(0.0, ωDuration_BSV)

 end

 @covariates rep_ABE Nreps_ABE input_tr_ratio Nsubj_ABE BSV
sequence seq_n period occ formulation isT

 @pre begin

 CL = tvCL * exp(ηCL)

 Vc = tvVc * exp(ηVc)

 end

 @dosecontrol begin

 duration = (Central = tvDuration*exp(ηduration),)

 bioav = (Central = (isT == 1) ? tvtr_ratio :

one(tvtr_ratio),)

 end

```

@dynamics Central1

@derived begin
  dv ~ @. Normal((Central/Vc), sqrt( $\sigma_{add}^2 + ((Central/Vc) * \sigma_{prop})^2$ ))
end
end

@info "parameters for parallel ABE trial simulation"
params_ABE_sim = (tvCL = 1051, # L/day/70kg
                 tvVc = 82153, # L/70kg
                 tvDuration = 2.00, # days
                 #wCL_BSV = 0.2, # 80%
of initial
                 #wVc_BSV = 0.37, # 90%
of initial
                 wDuration_BSV = 1.09,
                  $\sigma_{add}$  = 0.0147, # ng/mL (fixed)
(Francis, et al. 2021)
                  $\sigma_{prop}$  = 0.177) # (fixed)
(Francis, et al. 2021)

function run_ABE_sims(rng::AbstractRNG; Nreps_ABE::Integer,
input_tr_ratio::Real, Nsubj_ABE::Integer, BSV::Real)
  ev_SD = DosageRegimen(104*10^3, time=0, cmt=1, rate=-2) # 104mg dose
to 104x10^3ug b/c ug/L = ng/mL

  pop_df = DataFrame(Population(map(j -> Subject(id=j, events=ev_SD),
1:Nsubj_ABE)))
  pop_df[!, :rep_ABE] .= missing
  pop_df[!, :Nreps_ABE] .= Nreps_ABE
  pop_df[!, :input_tr_ratio] .= input_tr_ratio
  pop_df[!, :Nsubj_ABE] .= Nsubj_ABE
  pop_df[!, :BSV] .= BSV
  pop_df[!, :sequence] .= ifelse.(parse.(Int64, pop_df.id) .<=
Nsubj_ABE/2, "R", "T")
  pop_df[!, :seq_n] .= ifelse.(pop_df.sequence .== "R", 1, 2)
  pop_df[!, :period] .= 1
  pop_df[!, :occ] = combine(groupby(pop_df, :id), :evid
.> cumsum => :occ).occ
  pop_df[!, :formulation] .= ifelse.(pop_df.seq_n .== 1, "R", "T")
  pop_df[!, :isT] .= ifelse.(pop_df.formulation .== "T", 1,
0)
  pop_df[!, :dv] .= missing

```

```

sims = map(1:Nreps_ABE) do i
  pop_df[!, :rep_ABE] .= i

  pop = read_pumas(pop_df,
    id = :id,
    time = :time,
    amt = :amt,
    cmt = :cmt,
    observations = [:dv],
    covariates = [:rep_ABE, :Nreps_ABE,
:input_tr_ratio, :Nsubj_ABE, :BSV, :sequence, :seq_n, :period, :occ,
:formulation, :isT],
    covariates_direction = :left,
    evid = :evid)

  rand_effs = [sample_randeffs(rng, sim_model_abs0_1cmt_pl_ABE,
(params_ABE_sim...,
tv
tr_ratio = input_tr_ratio,
ωC
L_BSV = BSV,
ωV
c_BSV = BSV))
for subject in pop]

  sim_df = DataFrame(simobs(sim_model_abs0_1cmt_pl_ABE, pop,
(params_ABE_sim...,
tvtr_r
atio = input_tr_ratio,
ωCL_BS
V = BSV,
ωVc_BS
V = BSV),
rand_effs,
obstimes = obstimes,
ensemblealg = EnsembleSerial(),
rng=rng
)
)
sim_df[!, :route] .= "ev"

return sim_df
end

sims_df = reduce(vcat, sims)

```

```

    return sims_df
end

function run_ABE_NCA(sims_df::DataFrame)
    # removes neg conc's to prevent neg conc warning printout from NCA
    # have to use coalesce b/c of missing values
    temp_df = sims_df[coalesce.(sims_df.dv .>= 0, true), :]

    NCApop = read_nca(temp_df,
        id           = :id,
        time         = :time,
        observations = :dv,
        amt          = :amt,
        group        = [:rep_ABE, :Nreps_ABE,
:input_tr_ratio, :Nsubj_ABE, :BSV, :sequence, :seq_n, :period, :occ,
:formulation, :isT],
        llq          = 0.02,
        concblq      = 0.,
        route        = :route
    )

    cmax           = NCA.cmax(NCApop)
    aucinf         = NCA.auc(NCApop)

    NCAresults_df = leftjoin(cmax, aucinf, on = [:id, :rep_ABE,
:Nreps_ABE, :input_tr_ratio, :Nsubj_ABE, :BSV, :sequence, :seq_n, :period,
:occ, :formulation, :isT])

    return NCAresults_df
end

function run_ABE_BE(nca_df::DataFrame)
    @info "run BE analysis"
    BE_outputs_df = @time combine(groupby(nca_df, [:rep_ABE, :Nreps_ABE,
:input_tr_ratio, :Nsubj_ABE, :BSV])) do df
        (cmax_output = pumas_be(df, endpoint = :cmax, reml = true),
         aucinf_output = pumas_be(df, endpoint = :auc, reml = true)
        )
    end

    @info "generate cmax/auc LB, GMR, UB, CV"
    i_BE_LB_GMR_UB_CV = []

    for i in 1:nrow(BE_outputs_df)

```

```

rep_ABE      = BE_outputs_df[i, :rep_ABE]
Nreps_ABE   = BE_outputs_df[i, :Nreps_ABE]
input_tr_ratio = BE_outputs_df[i, :input_tr_ratio]
Nsubj_ABE   = BE_outputs_df[i, :Nsubj_ABE]
BSV         = BE_outputs_df[i, :BSV]

cmax_LB     = BE_outputs_df[i, :cmax_output].result.LB[1]
cmax_GMR    = BE_outputs_df[i, :cmax_output].result.GMR[1]
cmax_UB     = BE_outputs_df[i, :cmax_output].result.UB[1]
cmax_CV     = BE_outputs_df[i, :cmax_output].result.CV[1]

aucinf_LB   = BE_outputs_df[i, :aucinf_output].result.LB[1]
aucinf_GMR  = BE_outputs_df[i, :aucinf_output].result.GMR[1]
aucinf_UB   = BE_outputs_df[i, :aucinf_output].result.UB[1]
aucinf_CV   = BE_outputs_df[i, :aucinf_output].result.CV[1]

push!(i_BE_LB_GMR_UB_CV, (rep_ABE, Nreps_ABE, input_tr_ratio,
Nsubj_ABE, BSV,
                                cmax_LB, cmax_GMR, cmax_UB, cmax_CV,
                                aucinf_LB, aucinf_GMR, aucinf_UB,
aucinf_CV))
end

i_BE_LB_GMR_UB_CV_df = DataFrame(i_BE_LB_GMR_UB_CV)
rename!(i_BE_LB_GMR_UB_CV_df, [:rep_ABE, :Nreps_ABE, :input_tr_ratio,
:Nsubj_ABE, :BSV,
                                :cmax_LB, :cmax_GMR, :cmax_UB, :cmax_CV,
                                :aucinf_LB, :aucinf_GMR, :aucinf_UB,
:aucinf_CV])

@info "determine whether passes BE"
i_BE_passed_df = combine(groupby(i_BE_LB_GMR_UB_CV_df, [:rep_ABE,
:Nreps_ABE, :input_tr_ratio, :Nsubj_ABE, :BSV])) do df
  (# copying over LB, GMR, UB, and CV to save values
  cmax_LB      = df.cmax_LB,
  cmax_GMR     = df.cmax_GMR,
  cmax_UB      = df.cmax_UB,
  cmax_CV      = df.cmax_CV,

  aucinf_LB    = df.aucinf_LB,
  aucinf_GMR   = df.aucinf_GMR,
  aucinf_UB    = df.aucinf_UB,
  aucinf_CV    = df.aucinf_CV,

  # whether passes BE

```

```

    cmax_pass      = (df.cmax_LB .> 0.8) .& (df.cmax_UB .< 1.25),
    aucinf_pass   = (df.aucinf_LB .> 0.8) .& (df.aucinf_UB .<
1.25),

    # whether passes BE for both cmax and aucinf
    overall_pass  = (df.cmax_LB .> 0.8) .& (df.cmax_UB .< 1.25) .&
1.25)
                    (df.aucinf_LB .> 0.8) .& (df.aucinf_UB .<
)
end

@info "calculate BE pass rate"
BE_passrate_df = combine(groupby(i_BE_passed_df, [:Nreps_ABE,
:input_tr_ratio, :Nsubj_ABE, :BSV])) do df
    (# copying over LB, GMR, UB, and CV to save values
    avg_cmax_LB      = mean(df.cmax_LB),
    avg_cmax_GMR    = mean(df.cmax_GMR),
    avg_cmax_UB     = mean(df.cmax_UB),
    avg_cmax_CV     = mean(df.cmax_CV),

    avg_aucinf_LB   = mean(df.aucinf_LB),
    avg_aucinf_GMR  = mean(df.aucinf_GMR),
    avg_aucinf_UB   = mean(df.aucinf_UB),
    avg_aucinf_CV   = mean(df.aucinf_CV),

    # pass rate
    cmax_passrate   = mean(df.cmax_pass) * 100,
    aucinf_passrate = mean(df.aucinf_pass) * 100,
    overall_passrate = mean(df.overall_pass) * 100
    )
end

return i_BE_LB_GMR_UB_CV_df, i_BE_passed_df, BE_passrate_df
end

function ABE_sims(rng::AbstractRNG; Nreps_ABE::Integer,
input_tr_ratio::Real, Nsubj_ABE::Integer, BSV::Real)
    sims_df = run_ABE_sims(r
ng;
                                                                    Nr
eps_ABE,
                                                                    in
put_tr_ratio,
                                                                    Ns
ubj_ABE,

```

```

                                                    BS
V
                                                    )
    nca_df = run_ABE_NC
A(sims_df)
    i_BE_LB_GMR_UB_CV_df, i_BE_passed_df,
BE_passrate_df = run_ABE_BE(nca_df)

    return i_BE_LB_GMR_UB_CV_df, i_BE_passed_df, BE_passrate_df
end

```

FBE_MPA_SD_pl_BE_main.jl

```

#####
# title: Single-Dose Parallel Design Full BE Main Script
#####

@info "packages"
using Distributed, CSV, Serialization, Random

@info "load FBE functions"
@everywhere include("FBE_MPA_SD_pl_BE_fxns.jl")

@info "setup results location"
RESULTS_DIR = mktempdir()
ENV["RESULTS_FILE"] = RESULTS_DIR

@info "Nreps, T/R ratio, Nsubj, BSV, uncertainty factor for ABE/FBE sims"
Nreps_ABE = 50
Nreps_FBE = 100
#input_tr_ratio = [0.80, 0.95]
input_tr_ratio = [0.85]
## for 25% BSV
#BSV = 0.246
#Nsubj_ABE = [24, 36, 48]      # 33, 50, 66.7% of 72 (conventional BE
80% power target)
#Nsubj_ABE = [36]
#Nsubj_FBE = [24, 36, 48, 72]
Nsubj_FBE = [72]
## for 50% BSV
BSV = 0.472
#Nsubj_ABE = [72, 108, 144]   # 33, 50, 66.7% of 216 (conventional BE
80% power target)
Nsubj_ABE = [108]
#Nsubj_FBE = [72, 108, 144, 216]

```

```

Nsubj_FBE = [216]
uncertainty_factor = 0.000001
#uncertainty_factor = 1

## for wrong about BSV scenario
#BSV = 0.246
#Nsubj_ABE = [144]
#Nsubj_FBE = [216]

#BSV = 0.472
#Nsubj_ABE = [36]
#Nsubj_FBE = [72]

@info "trial obstimes"
@everywhere obstimes =
[0.001,2,4,5,6,7,8,10,12,14,16,20,24,29,36,43,50,57,64,71,78,85,90,104,132
,150,180,210] # 28 samples (100%)
#@everywhere obstimes =
[0.001,2,4,5,6,7,8,10,12,14,16,24,36,50,71,85,104,132,150,180,210]
# 21 samples (75%)
#@everywhere obstimes =
[0.001,2,4,5,6,7,8,10,12,14,36,85,150,210]
# 14 samples (50%)
#@everywhere obstimes =
[0.001,2,6,12,85,150,210]
# 7 samples (25%)

@info "running main map"

_rng = Random.default_rng()
seedn = 4567
Random.seed!(_rng, seedn)

FBE_results = @time map(Iterators.product(input_tr_ratio, Nsubj_ABE, BSV))
do (tr, nsubj_ABE, bsv)
  @info "tr = $tr, nsubj = $nsubj_ABE, bsv = $bsv"

  coeftbls_ABE_df,
  RSEs_ABE_df,
  PDs_ABE_df,
  PEs_ABE_df,
  i_BE_LB_GMR_UB_df,
  i_BE_passed_df,
  BE_passrate_df,
  i_rep_ABE_LB_GMR_UB_pass_df,

```

```

BE_GMR90CI_passrate_df = FBE_sims(_rng;
                                Nreps_ABE,
                                Nreps_FBE,
                                input_tr_ratio = tr,
                                Nsubj_ABE = nsubj_ABE,
                                Nsubj_FBE,
                                BSV = bsv,
                                uncertainty_factor
                                )

return coeftbls_ABE_df, RSEs_ABE_df, PDs_ABE_df, PEs_ABE_df,
i_BE_LB_GMR_UB_df, i_BE_passed_df, BE_passrate_df,
i_rep_ABE_LB_GMR_UB_pass_df, BE_GMR90CI_passrate_df
end;

@info "post-process results"

coeftbls_ABE = [i[1] for i in FBE_results]
RSEs_ABE = [i[2] for i in FBE_results]
PDs_ABE = [i[3] for i in FBE_results]
PEs_ABE = [i[4] for i in FBE_results]
i_BE_LB_GMR_UB = [i[5] for i in FBE_results]
i_BE_passed = [i[6] for i in FBE_results]
BE_passrate = [i[7] for i in FBE_results]
i_rep_ABE_LB_GMR_UB_pass = [i[8] for i in FBE_results]
BE_GMR90CI_passrate = [i[9] for i in FBE_results]

coeftbls_ABE_df = reduce(vcat, coeftbls_ABE)
RSEs_ABE_df = reduce(vcat, RSEs_ABE)
PDs_ABE_df = reduce(vcat, PDs_ABE)
PEs_ABE_df = reduce(vcat, PEs_ABE)
i_BE_LB_GMR_UB_df = reduce(vcat, i_BE_LB_GMR_UB)
i_BE_passed_df = reduce(vcat, i_BE_passed)
BE_passrate_df = reduce(vcat, BE_passrate)
i_rep_ABE_LB_GMR_UB_pass_df = reduce(vcat, i_rep_ABE_LB_GMR_UB_pass)
BE_GMR90CI_passrate_df = reduce(vcat, BE_GMR90CI_passrate)

@info "save results"
## w/o uncertainty and single Nsubj_ABE scenario

CSV.write(joinpath(RESULTS_DIR,
"coeftbls_ABE_$(Nsubj_ABE[1])Nsubj_ABE_Nreps$(Nreps_ABE)_$(Nreps_FBE)_$(BSV
)bsv_$(seedn)rng.csv"), coeftbls_ABE_df)

```

```

CSV.write(joinpath(RESULTS_DIR,
"RSEs_ABE_$(Nsubj_ABE[1])NsubjABE_Nreps$(Nreps_ABE)_$(Nreps_FBE)_$(BSV)bsv_
_$(seedn)rng.csv"), RSEs_ABE_df)
CSV.write(joinpath(RESULTS_DIR,
"PDs_ABE_$(Nsubj_ABE[1])NsubjABE_Nreps$(Nreps_ABE)_$(Nreps_FBE)_$(BSV)bsv_
$(seedn)rng.csv"), PDs_ABE_df)
CSV.write(joinpath(RESULTS_DIR,
"PEs_ABE_$(Nsubj_ABE[1])NsubjABE_Nreps$(Nreps_ABE)_$(Nreps_FBE)_$(BSV)bsv_
$(seedn)rng.csv"), PEs_ABE_df)
CSV.write(joinpath(RESULTS_DIR,
"i_BE_LB_GMR_UB_$(Nsubj_ABE[1])NsubjABE_Nreps$(Nreps_ABE)_$(Nreps_FBE)_$(B
SV)bsv_$(seedn)rng.csv"), i_BE_LB_GMR_UB_df)
CSV.write(joinpath(RESULTS_DIR,
"i_BE_passed_$(Nsubj_ABE[1])NsubjABE_Nreps$(Nreps_ABE)_$(Nreps_FBE)_$(BSV)
bsv_$(seedn)rng.csv"), i_BE_passed_df)
CSV.write(joinpath(RESULTS_DIR,
"BE_passrate_$(Nsubj_ABE[1])NsubjABE_Nreps$(Nreps_ABE)_$(Nreps_FBE)_$(BSV)
bsv_$(seedn)rng.csv"), BE_passrate_df)
CSV.write(joinpath(RESULTS_DIR,
"i_rep_ABE_LB_GMR_UB_pass_$(Nsubj_ABE[1])NsubjABE_Nreps$(Nreps_ABE)_$(Nrep
s_FBE)_$(BSV)bsv_$(seedn)rng.csv"), i_rep_ABE_LB_GMR_UB_pass_df)
CSV.write(joinpath(RESULTS_DIR,
"BE_GMR90CI_passrate_$(Nsubj_ABE[1])NsubjABE_Nreps$(Nreps_ABE)_$(Nreps_FBE
)_$(BSV)bsv_$(seedn)rng.csv"), BE_GMR90CI_passrate_df)

```

w/ uncertainty and single Nsubj_ABE scenario

```

# CSV.write(joinpath(RESULTS_DIR,
"coeftbls_ABE_$(Nsubj_ABE[1])NsubjABE_Nreps$(Nreps_ABE)_$(Nreps_FBE)_$(BSV
)bsv_uncert_$(seedn)rng.csv"), coeftbls_ABE_df)
# CSV.write(joinpath(RESULTS_DIR,
"RSEs_ABE_$(Nsubj_ABE[1])NsubjABE_Nreps$(Nreps_ABE)_$(Nreps_FBE)_$(BSV)bsv
_uncert_$(seedn)rng.csv"), RSEs_ABE_df)
# CSV.write(joinpath(RESULTS_DIR,
"PDs_ABE_$(Nsubj_ABE[1])NsubjABE_Nreps$(Nreps_ABE)_$(Nreps_FBE)_$(BSV)bsv_
uncert_$(seedn)rng.csv"), PDs_ABE_df)
# CSV.write(joinpath(RESULTS_DIR,
"PEs_ABE_$(Nsubj_ABE[1])NsubjABE_Nreps$(Nreps_ABE)_$(Nreps_FBE)_$(BSV)bsv_
uncert_$(seedn)rng.csv"), PEs_ABE_df)
# CSV.write(joinpath(RESULTS_DIR,
"i_BE_LB_GMR_UB_$(Nsubj_ABE[1])NsubjABE_Nreps$(Nreps_ABE)_$(Nreps_FBE)_$(B
SV)bsv_uncert_$(seedn)rng.csv"), i_BE_LB_GMR_UB_df)
# CSV.write(joinpath(RESULTS_DIR,
"i_BE_passed_$(Nsubj_ABE[1])NsubjABE_Nreps$(Nreps_ABE)_$(Nreps_FBE)_$(BSV)
bsv_uncert_$(seedn)rng.csv"), i_BE_passed_df)

```

```

# CSV.write(joinpath(RESULTS_DIR,
"BE_passrate_$(Nsubj_ABE[1])NsubjABE_Nreps$(Nreps_ABE)_$(Nreps_FBE)_$(BSV)
bsv_uncert_$(seedn)rng.csv"), BE_passrate_df)
# CSV.write(joinpath(RESULTS_DIR,
"i_rep_ABE_LB_GMR_UB_pass_$(Nsubj_ABE[1])NsubjABE_Nreps$(Nreps_ABE)_$(Nreps_FBE)_$(BSV)bsv_uncert_$(seedn)rng.csv"), i_rep_ABE_LB_GMR_UB_pass_df)
# CSV.write(joinpath(RESULTS_DIR,
"BE_GMR90CI_passrate_$(Nsubj_ABE[1])NsubjABE_Nreps$(Nreps_ABE)_$(Nreps_FBE)_$(BSV)bsv_uncert_$(seedn)rng.csv"), BE_GMR90CI_passrate_df)

```

FBE_MPA_SD_pl_BE_fxns.jl

```

#####
# title: Single-Dose Parallel Design Full BE Functions Script
#####

```

```
using Pumas, CSV, Random, Bioequivalence
```

```
include("ABE_MPA_SD_pl_BE_fxns.jl")
```

```
@info "parallel ABE trial estimation model/FBE trial simulation model"
```

```
# zero-order absorption, 1-cmt model, prop residual error model
```

```
pl_ABE_est_FBE_sim_model_abs0_1cmt = @model begin
```

```
  @param begin
```

```
    # tv
```

```
    tvtr_ratio ∈ RealDomain(lower = 0.0001)
```

```
    tvCL ∈ RealDomain(lower = 0.0001)
```

```
    tvVc ∈ RealDomain(lower = 0.0001)
```

```
    tvDuration ∈ RealDomain(lower = 0.0001)
```

```
    # BSV
```

```
    ωCL_BSV ∈ RealDomain(lower = 0.0001)
```

```
    ωVc_BSV ∈ RealDomain(lower = 0.0001)
```

```
    #ωDuration_BSV ∈ RealDomain(lower = 0.0001)
```

```
    # RUV
```

```
    σ_add ∈ RealDomain(lower = 0.0001)
```

```
    σ_prop ∈ RealDomain(lower = 0.0001)
```

```
  end
```

```
  @random begin
```

```
    # BSV
```

```
    ηCL ~ Normal(0.0, ωCL_BSV)
```

```
    ηVc ~ Normal(0.0, ωVc_BSV)
```

```
    #ηDuration ~ Normal(0.0, ωDuration_BSV)
```

```

end

@covariates      rep_ABE Nreps_ABE rep_FBE Nreps_FBE input_tr_ratio
Nsubj_ABE Nsubj_FBE BSV cmax_LB_ABE cmax_GMR_ABE aucinf_LB_ABE
aucinf_GMR_ABE sequence seq_n period occ formulation isT

@pre begin
  tr_ratio      = tvtr_ratio
  CL            = tvCL * exp(ηCL)
  Vc           = tvVc * exp(ηVc)
end

@dosecontrol begin
  #duration      = (Central = tvDuration * exp(ηDuration),)
  duration      = (Central = tvDuration,)
  bioav         = (Central = (isT == 1) ? tvtr_ratio :
one(tvtr_ratio),)
end

@dynamics        Central1

@derived begin
  dv            ~ @. Normal((Central/Vc), sqrt(σ_add^2 +
((Central/Vc) * σ_prop)^2))
end

end

@info "parameters for parallel ABE trial simulation model estimation"
params_ABE_est = (tvtr_ratio      = 1.0,
                  tvCL           = 1051,      # L/day/70kg
                  tvVc           = 82153,    # L/70kg
                  tvDuration     = 2.00,    # days
                  #wCL_BSV       = 0.2,      # 80%
of initial
                  #wVc_BSV       = 0.37,    # 90%
of initial
                  #wDuration_BSV = 1.09,
                  σ_add          = 0.0147,   # ng/mL (fixed)
(Francis, et al. 2021)
                  σ_prop         = 0.177)    # (fixed)
(Francis, et al. 2021)

function run_ABE_estimations(sims_ABE_df::DataFrame,
i_BE_LB_GMR_UB_CV_ABE_df::DataFrame, Nreps_ABE::Integer)
  fits = map(1:Nreps_ABE) do i

```

```

# filter ABE_sims_df to rep_ABE == i to make Pumas pop
filt_sims_df = filter(:rep_ABE ==> x -> x == i, sims_ABE_df)
# create new columns w/ dummy values for use w/ FBE simulations
filt_sims_df[!, :rep_FBE] .= 0
filt_sims_df[!, :Nreps_FBE] .= 0
filt_sims_df[!, :Nsubj_FBE] .= 0
filt_sims_df[!, :cmax_LB_ABE] .= i_BE_LB_GMR_UB_CV_ABE_df[i,
:cmax_LB]
    filt_sims_df[!, :cmax_GMR_ABE] .= i_BE_LB_GMR_UB_CV_ABE_df[i,
:cmax_GMR]
    filt_sims_df[!, :aucinf_LB_ABE] .= i_BE_LB_GMR_UB_CV_ABE_df[i,
:aucinf_LB]
    filt_sims_df[!, :aucinf_GMR_ABE] .= i_BE_LB_GMR_UB_CV_ABE_df[i,
:aucinf_GMR]

@info "read_pumas of ABE trial simulations"
pop = read_pumas(filt_sims_df,
                 id           = :id,
                 time        = :time,
                 amt         = :amt,
                 cmt         = :cmt,
                 observations = [:dv],
                 route       = :route,
                 covariates  = [:rep_ABE, :Nreps_ABE,
:rep_FBE, :Nreps_FBE, :input_tr_ratio, :Nsubj_ABE, :Nsubj_FBE, :BSV,
                 :cmax_LB_ABE,
:cmax_GMR_ABE, :aucinf_LB_ABE, :aucinf_GMR_ABE,
                 :sequence, :seq_n,
:period, :occ, :formulation, :isT],
                 covariates_direction = :left,
                 evid        = :evid)

@info "estimation of parallel ABE trial simulations"
i_fit = try
    fit(pl_ABE_est_FBE_sim_model_abs0_1cmt,
        pop,
        (params_ABE_est...,
         ωCL_BSV = BSV,
         ωVc_BSV = BSV),
        Pumas.FOCE(),
        ensemblealg = EnsembleSerial(),
        optim_options = (show_trace=false,));
catch
    missing
end

```

```

        return i_fit
    end

    fits = collect(skipmissing(fits))

    # can't use try/catch for vcov b/c Pumas doesn't error when vcov
fails
    vcovs = map(fits) do i_fit
        i_vcov = ifelse(typeof(vcov(i_fit)) !=
Pumas.PumasFailedCovariance,
                        vcov(i_fit),
                        missing)

        return i_vcov
    end

    missing_indices = []

    for j in 1:length(vcovs)
        if ismissing(vcovs[j])
            push!(missing_indices, j)
        end
    end

    vcovs = collect(skipmissing(vcovs))

    # updates fit objects to remove fits w/ failed vcov calculation
deleteat!(fits, missing_indices)

    return fits, vcovs
end

function
run_ABE_est_diag(fits_ABE::AbstractVector{<:Pumas.FittedPumasModel},
                 vcovs_ABE::AbstractVector{<:Symmetric{Float64,
Matrix{Float64}}},
                 input_tr_ratio::Real,
                 Nsubj_ABE::Integer,
                 BSV::Real
                 )
    @info "generate SEs"

    # create empty df for SEs
    SEs_df = DataFrame(tvtr_ratio=[], tvCL=[],

```

```

        tvVc=[], tvDuration=[],
        ωCL_BSV=[], ωVc_BSV=[],
        σ_add=[], σ_prop=[]
    )

for i in 1:length(vcovs_ABE)
    i_SE = sqrt.(diag(vcovs_ABE[i]))

    push!(SEs_df, i_SE)
end

# add rep_ABE col
SEs_df[!, :rep_ABE] .= rownumber.(eachrow(SEs_df))

@info "generate coeftbls"

coeftbls_ABE = map(1:length(fits_ABE)) do i
    i_coeftbl = coeftable(fits_ABE[i])
    i_coeftbl[!, :input_tr_ratio] .= input_tr_ratio
    i_coeftbl[!, :Nsubj_ABE] .= Nsubj_ABE
    i_coeftbl[!, :BSV] .= BSV
    i_coeftbl[!, :rep_ABE] .= i

    return i_coeftbl
end

coeftbls_ABE_df = reduce(vcat, coeftbls_ABE)
# long-to-wide transformation
coeftbls_ABE_df = unstack(coeftbls_ABE_df, :parameter, :estimate)

@info "generate RSEs"

RSEs_df = copy(coeftbls_ABE_df)

RSEs_df[!, :RSE_tvtr_ratio] .= SEs_df.tvtr_ratio ./
coeftbls_ABE_df.tvtr_ratio .* 100
RSEs_df[!, :RSE_tvCL] .= SEs_df.tvCL ./ coeftbls_ABE_df.tvCL .* 100
RSEs_df[!, :RSE_tvVc] .= SEs_df.tvVc ./ coeftbls_ABE_df.tvVc .* 100
RSEs_df[!, :RSE_tvDuration] .= SEs_df.tvDuration ./
coeftbls_ABE_df.tvDuration .* 100
RSEs_df[!, :RSE_ωCL_BSV] .= SEs_df.ωCL_BSV ./ coeftbls_ABE_df.ωCL_BSV
.* 100
RSEs_df[!, :RSE_ωVc_BSV] .= SEs_df.ωVc_BSV ./ coeftbls_ABE_df.ωVc_BSV
.* 100
RSEs_df[!, :RSE_σ_add] .= SEs_df.σ_add ./ coeftbls_ABE_df.σ_add .* 100

```

```

RSEs_df[!, :RSE_σ_prop] .= SEs_df.σ_prop ./ coeftbls_ABE_df.σ_prop .*
100

@info "generate population level PEs"

# reference parameters from ABE simulations, including T/R ratio
temp_params = (tvtr_ratio = input_tr_ratio, params_ABE_sim..., ωCL_BSV
= BSV, ωVc_BSV = BSV)

# percent difference
PDs_df = combine(groupby(coeftbls_ABE_df, [:input_tr_ratio,
:Nsubj_ABE, :BSV, :rep_ABE])) do df
    (PD_tvtr_ratio      = (df.tvtr_ratio .- temp_params.tvtr_ratio)
./ temp_params.tvtr_ratio .* 100,
    PD_tvCL             = (df.tvCL .- temp_params.tvCL) ./
temp_params.tvCL .* 100,
    PD_tvVc             = (df.tvVc .- temp_params.tvVc) ./
temp_params.tvVc .* 100,
    PD_tvDuration       = (df.tvDuration .- temp_params.tvDuration)
./ temp_params.tvDuration .* 100,
    PD_ωCL              = (df.ωCL_BSV .- temp_params.ωCL_BSV) ./
temp_params.ωCL_BSV .* 100,
    PD_ωVc              = (df.ωVc_BSV .- temp_params.ωVc_BSV) ./
temp_params.ωVc_BSV .* 100,
    #PD_ωDuration       = (df.ωDuration_BSV .-
temp_params.ωDuration_BSV) ./ temp_params.ωDuration_BSV .* 100,
    PD_σ_add            = (df.σ_add .- temp_params.σ_add) ./
temp_params.σ_add .* 100,
    PD_σ_prop           = (df.σ_prop .- temp_params.σ_prop) ./
temp_params.σ_prop .* 100
    )
end

PEs_df = combine(groupby(coeftbls_ABE_df, [:input_tr_ratio,
:Nsubj_ABE, :BSV])) do df
    (# MDAPE
    MDAPE_tvtr_ratio    = median.(eachcol(abs.(df.tvtr_ratio .-
temp_params.tvtr_ratio) ./ temp_params.tvtr_ratio) .* 100),
    MDAPE_tvCL          = median.(eachcol(abs.(df.tvCL .-
temp_params.tvCL) ./ temp_params.tvCL) .* 100),
    MDAPE_tvVc          = median.(eachcol(abs.(df.tvVc .-
temp_params.tvVc) ./ temp_params.tvVc) .* 100),
    MDAPE_tvDuration    = median.(eachcol(abs.(df.tvDuration .-
temp_params.tvDuration) ./ temp_params.tvDuration) .* 100),

```

```

        MdAPE_wCL          = median.(eachcol(abs.(df.wCL_BSV .-
temp_params.wCL_BSV) ./ temp_params.wCL_BSV) .* 100),
        MdAPE_wVc         = median.(eachcol(abs.(df.wVc_BSV .-
temp_params.wVc_BSV) ./ temp_params.wVc_BSV) .* 100),
        #MdAPE_wDuration   = median.(eachcol(abs.(df.wDuration_BSV .-
temp_params.wDuration_BSV) ./ temp_params.wDuration_BSV) .* 100),
        MdAPE_σ_add       = median.(eachcol(abs.(df.σ_add .-
temp_params.σ_add) ./ temp_params.σ_add) .* 100),
        MdAPE_σ_prop      = median.(eachcol(abs.(df.σ_prop .-
temp_params.σ_prop) ./ temp_params.σ_prop) .* 100),

        # MdPE
        MdPE_tvtr_ratio   = median.(eachcol((df.tvtr_ratio .-
temp_params.tvtr_ratio) ./ temp_params.tvtr_ratio) .* 100),
        MdPE_tvCL        = median.(eachcol((df.tvCL .-
temp_params.tvCL) ./ temp_params.tvCL) .* 100),
        MdPE_tvVc        = median.(eachcol((df.tvVc .-
temp_params.tvVc) ./ temp_params.tvVc) .* 100),
        MdPE_tvDuration   = median.(eachcol((df.tvDuration .-
temp_params.tvDuration) ./ temp_params.tvDuration) .* 100),
        MdPE_wCL         = median.(eachcol((df.wCL_BSV .-
temp_params.wCL_BSV) ./ temp_params.wCL_BSV) .* 100),
        MdPE_wVc         = median.(eachcol((df.wVc_BSV .-
temp_params.wVc_BSV) ./ temp_params.wVc_BSV) .* 100),
        #MdPE_wDuration   = median.(eachcol((df.wDuration .-
temp_params.wDuration) ./ temp_params.wDuration) .* 100),
        MdPE_σ_add       = median.(eachcol((df.σ_add .-
temp_params.σ_add) ./ temp_params.σ_add) .* 100),
        MdPE_σ_prop      = median.(eachcol((df.σ_prop .-
temp_params.σ_prop) ./ temp_params.σ_prop) .* 100)
    )
end

return coeftbls_ABE_df, RSEs_df, PDs_df, PEs_df
end

```

```

function make_FBE_pop(rep_ABE::Integer,
                    fit_ABE::Pumas.FittedPumasModel,
                    Nreps_ABE::Integer,
                    Nreps_FBE::Integer,
                    input_tr_ratio::Real,
                    Nsubj_ABE::Integer,
                    Nsubj_FBE::Integer,
                    BSV::Real
    )

```

```

ev_SD = DosageRegimen(104*10^3, time=0, cmt=1, rate=-2) # 104mg dose
to 104x10^3ug b/c ug/L = ng/mL

```

```

pop_df = DataFrame(Population(map(j -> Subject(id=j, events=ev_SD,
time=obstimes), 1:Nsubj_FBE)))
pop_df[!, :rep_ABE]      .= rep_ABE
pop_df[!, :Nreps_ABE]   .= Nreps_ABE
pop_df[!, :rep_FBE]     .= 0 # dummy value
pop_df[!, :Nreps_FBE]   .= Nreps_FBE
pop_df[!, :input_tr_ratio] .= input_tr_ratio
pop_df[!, :Nsubj_ABE]   .= Nsubj_ABE
pop_df[!, :Nsubj_FBE]   .= Nsubj_FBE
pop_df[!, :BSV]         .= BSV
pop_df[!,
:cmax_LB_ABE]          .= fit_ABE.data[1].covariates(0.0).cmax_LB_ABE
pop_df[!,
:cmax_GMR_ABE]         .= fit_ABE.data[1].covariates(0.0).cmax_GMR_ABE
pop_df[!,
:aucinf_LB_ABE]        .= fit_ABE.data[1].covariates(0.0).aucinf_LB_ABE
pop_df[!,
:aucinf_GMR_ABE]       .= fit_ABE.data[1].covariates(0.0).aucinf_GMR_ABE
pop_df[!, :sequence]   .= ifelse.(parse.(Int64, pop_df.id) .<=
Nsubj_FBE/2, "R", "T")
pop_df[!, :seq_n]      .= ifelse.(pop_df.sequence .== "R", 1, 2)
pop_df[!, :period]     .= 1
pop_df[!, :occ]        = combine(groupby(pop_df, :id), :evid
.=> cumsum => :occ).occ
pop_df[!, :formulation] .= ifelse.(pop_df.seq_n .== 1, "R", "T")
pop_df[!, :isT]        .= ifelse.(pop_df.formulation .== "T", 1,
0)
pop_df[!, :dv]         .= missing
#=

```

```

## add in obstimes b/c needed for simobs when simulating w/
uncertainty and giving population

```

```

id_obstimes_df = DataFrame(Base.product(1:Nsubj_FBE, [0,
obstimes...]))
rename!(id_obstimes_df, ["id", "time"])
id_obstimes_df.id .= string.(id_obstimes_df.id)

pop_df = outerjoin(pop_df, id_obstimes_df, on=[:id, :time])
sort(pop_df, [:id, :time])

pop_df[!, :evid] .= ifelse.(pop_df.time .== 0, pop_df.evid, 0)
=#

```

```

pop = read_pumas(pop_df,
                 id           = :id,
                 time        = :time,
                 amt         = :amt,
                 cmt         = :cmt,
                 observations = [:dv],
                 covariates  = [:rep_ABE, :Nreps_ABE,
:rep_FBE, :Nreps_FBE, :input_tr_ratio, :Nsubj_ABE, :Nsubj_FBE, :BSV,
                 :cmax_LB_ABE,
:cmax_GMR_ABE, :aucinf_LB_ABE, :aucinf_GMR_ABE,
                 :sequence, :seq_n,
:period, :occ, :formulation, :isT],
                 covariates_direction = :left,
                 evid        = :evid)

```

```

return pop
end

```

```

function run_FBE_sims(rng::AbstractRNG;
                    fits_ABE::AbstractVector{<:Pumas.FittedPumasModel},
                    vcovs_ABE::AbstractVector{<:Symmetric{Float64,
Matrix{Float64}}},
                    Nreps_ABE::Integer,
                    Nreps_FBE::Integer,
                    input_tr_ratio::Real,
                    Nsubj_ABE::Integer,
                    Nsubj_FBE::Integer,
                    BSV::Real,
                    uncertainty_factor::Real
                    )
grand_sims_FBE_vec = []

```

```

for i in 1:length(fits_ABE)
    pop = make_FBE_pop(i, fits_ABE[i], Nreps_ABE, Nreps_FBE,
input_tr_ratio, Nsubj_ABE, Nsubj_FBE, BSV)

```

```

    sims_FBE = simobs(fits_ABE[i], pop,
vcovs_ABE[i]*uncertainty_factor; samples=Nreps_FBE, rng=rng)

```

```

    sims_FBE_vec = []

```

```

for j in 1:length(sims_FBE)
    i_sim_FBE_df = DataFrame(sims_FBE[j])
    i_sim_FBE_df[!, :rep_FBE] .= j
    i_sim_FBE_df[!, :route] .= "ev"

```

```

        push!(sims_FBE_vec, i_sim_FBE_df)
    end

    sims_FBE_df = reduce(vcat, sims_FBE_vec)

    push!(grand_sims_FBE_vec, sims_FBE_df)
end

grand_sims_FBE_df = reduce(vcat, grand_sims_FBE_vec)

return grand_sims_FBE_df
end

function run_FBE_NCA(sims_df::DataFrame)
    # removes neg conc's to prevent neg conc warning printout from NCA
    # have to use coalesce b/c of missing values
    temp_df = sims_df[coalesce.(sims_df.dv .>= 0, true), :]

    NCApop = read_nca(temp_df,
        id = :id,
        time = :time,
        observations = :dv,
        amt = :amt,
        group = [:rep_ABE, :Nreps_ABE, :rep_FBE,
:Nreps_FBE, :input_tr_ratio, :Nsubj_ABE, :Nsubj_FBE, :BSV,
:cmax_LB_ABE, :cmax_GMR_ABE,
:aucinf_LB_ABE, :aucinf_GMR_ABE,
:sequence, :seq_n, :period, :occ,
:formulation, :isT],
        llq = 0.02,
        concblq = 0.,
        route = :route
    )

    cmax = NCA.cmax(NCApop)
    aucinf = NCA.auc(NCApop)

    NCAresults_df = leftjoin(cmax, aucinf, on = [:id, :rep_ABE,
:Nreps_ABE, :rep_FBE, :Nreps_FBE, :input_tr_ratio, :Nsubj_ABE, :Nsubj_FBE,
:BSV, :cmax_LB_ABE, :cmax_GMR_ABE, :aucinf_LB_ABE, :aucinf_GMR_ABE,
:sequence, :seq_n, :period, :occ, :formulation, :isT])

    return NCAresults_df
end

```

```

function run_FBE_BE(nca_df::DataFrame)
  @info "run BE analysis"
  BE_outputs_df = @time combine(groupby(nca_df, [:rep_ABE, :Nreps_ABE,
:rep_FBE, :Nreps_FBE, :input_tr_ratio, :Nsubj_ABE, :Nsubj_FBE, :BSV,
:cmax_LB_ABE, :cmax_GMR_ABE, :aucinf_LB_ABE, :aucinf_GMR_ABE])) do df
    (cmax_output = pumas_be(df, endpoint = :cmax, reml = true),
    aucinf_output = pumas_be(df, endpoint = :auc, reml = true)
    )
  end

  @info "generate cmax/auc LB, GMR, UB"
  i_BE_LB_GMR_UB = []

  for i in 1:nrow(BE_outputs_df)
    rep_ABE = BE_outputs_df[i, :rep_ABE]
    Nreps_ABE = BE_outputs_df[i, :Nreps_ABE]
    rep_FBE = BE_outputs_df[i, :rep_FBE]
    Nreps_FBE = BE_outputs_df[i, :Nreps_FBE]
    input_tr_ratio = BE_outputs_df[i, :input_tr_ratio]
    Nsubj_ABE = BE_outputs_df[i, :Nsubj_ABE]
    Nsubj_FBE = BE_outputs_df[i, :Nsubj_FBE]
    BSV = BE_outputs_df[i, :BSV]
    cmax_LB_ABE = BE_outputs_df[i, :cmax_LB_ABE]
    cmax_GMR_ABE = BE_outputs_df[i, :cmax_GMR_ABE]
    aucinf_LB_ABE = BE_outputs_df[i, :aucinf_LB_ABE]
    aucinf_GMR_ABE = BE_outputs_df[i, :aucinf_GMR_ABE]

    cmax_LB = BE_outputs_df[i, :cmax_output].result.LB[1]
    cmax_GMR = BE_outputs_df[i, :cmax_output].result.GMR[1]
    cmax_UB = BE_outputs_df[i, :cmax_output].result.UB[1]

    aucinf_LB = BE_outputs_df[i, :aucinf_output].result.LB[1]
    aucinf_GMR = BE_outputs_df[i, :aucinf_output].result.GMR[1]
    aucinf_UB = BE_outputs_df[i, :aucinf_output].result.UB[1]

    push!(i_BE_LB_GMR_UB, (rep_ABE, Nreps_ABE, rep_FBE, Nreps_FBE,
input_tr_ratio, Nsubj_ABE, Nsubj_FBE, BSV, cmax_LB_ABE, cmax_GMR_ABE,
aucinf_LB_ABE, aucinf_GMR_ABE, cmax_LB, cmax_GMR, cmax_UB, aucinf_LB,
aucinf_GMR, aucinf_UB))
  end

  i_BE_LB_GMR_UB_df = DataFrame(i_BE_LB_GMR_UB)
  rename!(i_BE_LB_GMR_UB_df, [:rep_ABE, :Nreps_ABE, :rep_FBE,
:Nreps_FBE, :input_tr_ratio, :Nsubj_ABE, :Nsubj_FBE, :BSV, :cmax_LB_ABE,

```

```

:cmx_GMR_ABE, :aucinf_LB_ABE, :aucinf_GMR_ABE, :cmx_LB, :cmx_GMR,
:cmx_UB, :aucinf_LB, :aucinf_GMR, :aucinf_UB])

  @info "determine whether *any rep* passes BE"
  i_BE_passed_df = combine(groupby(i_BE_LB_GMR_UB_df, [:rep_ABE,
:Nreps_ABE, :rep_FBE, :Nreps_FBE, :input_tr_ratio, :Nsubj_ABE, :Nsubj_FBE,
:BSV, :cmx_LB_ABE, :cmx_GMR_ABE, :aucinf_LB_ABE, :aucinf_GMR_ABE])) do
df
  (# copying over LB, GMR, and UB to save values
  cmx_LB      = df.cmx_LB,
  cmx_GMR     = df.cmx_GMR,
  cmx_UB      = df.cmx_UB,

  aucinf_LB   = df.aucinf_LB,
  aucinf_GMR  = df.aucinf_GMR,
  aucinf_UB   = df.aucinf_UB,

  # whether passes BE
  cmx_pass    = (df.cmx_LB .> 0.8) .& (df.cmx_UB .< 1.25),
  aucinf_pass = (df.aucinf_LB .> 0.8) .& (df.aucinf_UB .<
1.25),

  # whether passes BE for both cmx and aucinf
  overall_pass = (df.cmx_LB .> 0.8) .& (df.cmx_UB .< 1.25) .&
                (df.aucinf_LB .> 0.8) .& (df.aucinf_UB .<
1.25)
  )
end

  @info "calculate BE *any rep* passrate"
  BE_passrate_df = combine(groupby(i_BE_passed_df, [:Nreps_ABE,
:Nreps_FBE, :input_tr_ratio, :Nsubj_ABE, :Nsubj_FBE, :BSV, :cmx_LB_ABE,
:cmx_GMR_ABE, :aucinf_LB_ABE, :aucinf_GMR_ABE])) do df
  (# copying over LB, GMR, and UB to save values
  avg_cmx_LB      = mean(df.cmx_LB),
  avg_cmx_GMR     = mean(df.cmx_GMR),
  avg_cmx_UB      = mean(df.cmx_UB),

  avg_aucinf_LB   = mean(df.aucinf_LB),
  avg_aucinf_GMR  = mean(df.aucinf_GMR),
  avg_aucinf_UB   = mean(df.aucinf_UB),

  # pass rate
  cmx_passrate    = mean(df.cmx_pass) * 100,
  aucinf_passrate = mean(df.aucinf_pass) * 100,

```

```

        overall_passrate = mean(df.overall_pass) * 100
    )
end

@info "determine individual BE GMR"
i_BE_GMR_df = combine(groupby(i_BE_LB_GMR_UB_df, [:rep_ABE,
:Nreps_ABE, :rep_FBE, :Nreps_FBE, :input_tr_ratio, :Nsubj_ABE, :Nsubj_FBE,
:BSV, :cmax_LB_ABE, :cmax_GMR_ABE, :aucinf_LB_ABE, :aucinf_GMR_ABE])) do df
    (cmax_GMR = df.cmax_GMR[1],
    aucinf_GMR = df.aucinf_GMR[1]
    )
end

@info "calculate 90% CI of FBE GMRs for each rep_ABE and determine
whether passed BE"
i_rep_ABE_LB_GMR_UB_pass_df = combine(groupby(i_BE_GMR_df, [:rep_ABE,
:Nreps_ABE, :Nreps_FBE, :input_tr_ratio, :Nsubj_ABE, :Nsubj_FBE, :BSV,
:cmax_LB_ABE, :cmax_GMR_ABE, :aucinf_LB_ABE, :aucinf_GMR_ABE])) do df
    (cmax_GMR_LB = quantile(df.cmax_GMR, 0.05),
    cmax_GMR_GMR = quantile(df.cmax_GMR, 0.5),
    cmax_GMR_UB = quantile(df.cmax_GMR, 0.95),
    aucinf_GMR_LB = quantile(df.aucinf_GMR, 0.05),
    aucinf_GMR_GMR = quantile(df.aucinf_GMR, 0.5),
    aucinf_GMR_UB = quantile(df.aucinf_GMR, 0.95),

    # whether passes BE
    cmax_pass = (quantile(df.cmax_GMR, 0.05) .> 0.8) .&
(quantile(df.cmax_GMR, 0.95) .< 1.25),
    aucinf_pass = (quantile(df.aucinf_GMR, 0.05) .> 0.8) .&
(quantile(df.aucinf_GMR, 0.95) .< 1.25),

    # whether passes both cmax and aucinf
    overall_pass = (quantile(df.cmax_GMR, 0.05) .> 0.8) .&
(quantile(df.cmax_GMR, 0.95) .< 1.25) .&
(quantile(df.aucinf_GMR, 0.05) .> 0.8) .&
(quantile(df.aucinf_GMR, 0.95) .< 1.25)
    )
end

@info "calculate BE pass rate based on 90% CI of FBE GMRs for each
rep_ABE"
BE_GMR90CI_passrate_df = combine(groupby(i_rep_ABE_LB_GMR_UB_pass_df,
[:Nreps_ABE, :Nreps_FBE, :input_tr_ratio, :Nsubj_ABE, :Nsubj_FBE, :BSV])) do df

```

```

    (# copying over LB, GMR, and UB to save values
    med_cmax_GMR_LB = median(df.cmax_GMR_LB),
    med_cmax_GMR_GMR = median(df.cmax_GMR_GMR),
    med_cmax_GMR_UB = median(df.cmax_GMR_UB),
    med_aucinf_GMR_LB = median(df.aucinf_GMR_LB),
    med_aucinf_GMR_GMR = median(df.aucinf_GMR_GMR),
    med_aucinf_GMR_UB = median(df.aucinf_GMR_UB),

    # pass rate
    cmax_passrate = mean(df.cmax_pass) * 100,
    aucinf_passrate = mean(df.aucinf_pass) * 100,
    overall_passrate = mean(df.overall_pass) * 100
  )
end

return i_BE_LB_GMR_UB_df, i_BE_passed_df, BE_passrate_df,
i_rep_ABE_LB_GMR_UB_pass_df, BE_GMR90CI_passrate_df
end

function FBE_sims(rng::AbstractRNG;
  Nreps_ABE::Integer,
  Nreps_FBE::Integer,
  input_tr_ratio::Real,
  Nsubj_ABE::Integer,
  Nsubj_FBE::AbstractVector{<:Integer},
  BSV::Real,
  uncertainty_factor::Real
)
  sims_ABE_df = run_ABE_sims(rng;
    Nreps_ABE,
    input_tr_ratio,
    Nsubj_ABE,
    BSV
  )

  nca_ABE_df = run_ABE_NCA(sims_ABE_df)
  i_BE_LB_GMR_UB_CV_ABE_df,
  i_BE_passed_ABE_df,
  BE_passrate_ABE_df = run_ABE_BE(nca_ABE_df)

  fits_ABE, vcovs_ABE = run_ABE_estimations(sims_ABE_df,
  i_BE_LB_GMR_UB_CV_ABE_df, Nreps_ABE)

  coeftbls_ABE_df,
  RSEs_ABE_df,

```

```

        PDs_ABE_df,
        PEs_ABE_df          = run_ABE_est_diag(fits_ABE, vcovs_ABE,
input_tr_ratio, Nsubj_ABE, BSV)

    res_FBE
    sims_FBE_df            = pmap(Nsubj_FBE) do nsubj_FBE
                                = run_FBE_sims(rng;
                                                fits_ABE,
                                                vcovs_ABE,
                                                Nreps_ABE,
                                                Nreps_FBE,
                                                input_tr_ratio,
                                                Nsubj_ABE,
                                                Nsubj_FBE =
nsubj_FBE,

                                                                BSV,
                                                                uncertainty_factor

                                                                )

    nca_df                  = run_FBE_NCA(sims_FBE_df)
    i_BE_LB_GMR_UB_df, i_BE_passed_df,
    BE_passrate_df,
    i_rep_ABE_LB_GMR_UB_pass_df,
    BE_GMR90CI_passrate_df = run_FBE_BE(nca_df)

    return i_BE_LB_GMR_UB_df, i_BE_passed_df, BE_passrate_df,
i_rep_ABE_LB_GMR_UB_pass_df, BE_GMR90CI_passrate_df
end

@info "post-process FBE results"
i_BE_LB_GMR_UB          = [i[1] for i in res_FBE]
i_BE_passed             = [i[2] for i in res_FBE]
BE_passrate             = [i[3] for i in res_FBE]
i_rep_ABE_LB_GMR_UB_pass = [i[4] for i in res_FBE]
BE_GMR90CI_passrate    = [i[5] for i in res_FBE]

i_BE_LB_GMR_UB_df      = reduce(vcat, i_BE_LB_GMR_UB)
i_BE_passed_df         = reduce(vcat, i_BE_passed)
BE_passrate_df         = reduce(vcat, BE_passrate)
i_rep_ABE_LB_GMR_UB_pass_df = reduce(vcat, i_rep_ABE_LB_GMR_UB_pass)
BE_GMR90CI_passrate_df = reduce(vcat, BE_GMR90CI_passrate)

return coeftbls_ABE_df, RSEs_ABE_df, PDs_ABE_df, PEs_ABE_df,
i_BE_LB_GMR_UB_df, i_BE_passed_df, BE_passrate_df,
i_rep_ABE_LB_GMR_UB_pass_df, BE_GMR90CI_passrate_df
end

```

batch_processing_combining_output_files.jl

```
using Pumas, CSV, Random, Bioequivalence

cd("./complex_generics")

pathname = "./results/Depo-SubQ Provera 104/Manuscript v5/FBE/"

@info "global scenarios"

Nreps_ABE = 50
Nreps_FBE = 100

#BSV = 0.246
#Nsubj_ABE = 24
#Nsubj_ABE = 36
#Nsubj_ABE = 48

BSV = 0.472
#Nsubj_ABE = 72
#Nsubj_ABE = 108
Nsubj_ABE = 144

@info "coeftbls_ABE"

seedn = 1234
coeftbls_ABE_df1 = CSV.read(joinpath(pathname,
"coeftbls_ABE_$(Nsubj_ABE)NsubjABE_Nreps$(Nreps_ABE)_$(Nreps_FBE)_$(BSV)bs
v_$(seedn)rng.csv"), DataFrame)
seedn = 2345
coeftbls_ABE_df2 = CSV.read(joinpath(pathname,
"coeftbls_ABE_$(Nsubj_ABE)NsubjABE_Nreps$(Nreps_ABE)_$(Nreps_FBE)_$(BSV)bs
v_$(seedn)rng.csv"), DataFrame)
seedn = 3456
coeftbls_ABE_df3 = CSV.read(joinpath(pathname,
"coeftbls_ABE_$(Nsubj_ABE)NsubjABE_Nreps$(Nreps_ABE)_$(Nreps_FBE)_$(BSV)bs
v_$(seedn)rng.csv"), DataFrame)
seedn = 4567
coeftbls_ABE_df4 = CSV.read(joinpath(pathname,
"coeftbls_ABE_$(Nsubj_ABE)NsubjABE_Nreps$(Nreps_ABE)_$(Nreps_FBE)_$(BSV)bs
v_$(seedn)rng.csv"), DataFrame)

coeftbls_ABE_df = vcat(coeftbls_ABE_df1, coeftbls_ABE_df2,
coeftbls_ABE_df3, coeftbls_ABE_df4)
```

```

transform!(groupby(coeftbls_ABE_df, [:input_tr_ratio, :Nsubj_ABE]),
:rep_ABE .=> (x -> 1:length(x)) => :rep_ABE)
sort!(coeftbls_ABE_df, [:input_tr_ratio, :Nsubj_ABE])

CSV.write(joinpath(pathname,
"coeftbls_ABE_$(Nsubj_ABE)NsubjABE_Nreps$(Nreps_ABE)_$(Nreps_FBE)_$(BSV)bs
v.csv"), coeftbls_ABE_df)

@info "RSEs_ABE"

seedn = 1234
RSEs_ABE_df1 = CSV.read(joinpath(pathname,
"RSEs_ABE_$(Nsubj_ABE)NsubjABE_Nreps$(Nreps_ABE)_$(Nreps_FBE)_$(BSV)bsv_$(
seedn)rng.csv"), DataFrame)
seedn = 2345
RSEs_ABE_df2 = CSV.read(joinpath(pathname,
"RSEs_ABE_$(Nsubj_ABE)NsubjABE_Nreps$(Nreps_ABE)_$(Nreps_FBE)_$(BSV)bsv_$(
seedn)rng.csv"), DataFrame)
seedn = 3456
RSEs_ABE_df3 = CSV.read(joinpath(pathname,
"RSEs_ABE_$(Nsubj_ABE)NsubjABE_Nreps$(Nreps_ABE)_$(Nreps_FBE)_$(BSV)bsv_$(
seedn)rng.csv"), DataFrame)
seedn = 4567
RSEs_ABE_df4 = CSV.read(joinpath(pathname,
"RSEs_ABE_$(Nsubj_ABE)NsubjABE_Nreps$(Nreps_ABE)_$(Nreps_FBE)_$(BSV)bsv_$(
seedn)rng.csv"), DataFrame)

RSEs_ABE_df = vcat(RSEs_ABE_df1, RSEs_ABE_df2, RSEs_ABE_df3, RSEs_ABE_df4)

transform!(groupby(RSEs_ABE_df, [:input_tr_ratio, :Nsubj_ABE]), :rep_ABE
.> (x -> 1:length(x)) => :rep_ABE)
sort!(RSEs_ABE_df, [:input_tr_ratio, :Nsubj_ABE])

CSV.write(joinpath(pathname,
"RSEs_ABE_$(Nsubj_ABE)NsubjABE_Nreps$(Nreps_ABE)_$(Nreps_FBE)_$(BSV)bsv.cs
v"), RSEs_ABE_df)

@info "PDs_ABE"

seedn = 1234
PDs_ABE_df1 = CSV.read(joinpath(pathname,
"PDs_ABE_$(Nsubj_ABE)NsubjABE_Nreps$(Nreps_ABE)_$(Nreps_FBE)_$(BSV)bsv_$(s
eedn)rng.csv"), DataFrame)
seedn = 2345

```

```

PDs_ABE_df2 = CSV.read(joinpath(pathname,
"PDs_ABE_$(Nsubj_ABE)NsubjABE_Nreps$(Nreps_ABE)_$(Nreps_FBE)_$(BSV)bsv_$(s
eedn)rng.csv"), DataFrame)
seedn = 3456
PDs_ABE_df3 = CSV.read(joinpath(pathname,
"PDs_ABE_$(Nsubj_ABE)NsubjABE_Nreps$(Nreps_ABE)_$(Nreps_FBE)_$(BSV)bsv_$(s
eedn)rng.csv"), DataFrame)
seedn = 4567
PDs_ABE_df4 = CSV.read(joinpath(pathname,
"PDs_ABE_$(Nsubj_ABE)NsubjABE_Nreps$(Nreps_ABE)_$(Nreps_FBE)_$(BSV)bsv_$(s
eedn)rng.csv"), DataFrame)

PDs_ABE_df = vcat(PDs_ABE_df1, PDs_ABE_df2, PDs_ABE_df3, PDs_ABE_df4)

transform!(groupby(PDs_ABE_df, [:input_tr_ratio, :Nsubj_ABE]), :rep_ABE
.=> (x -> 1:length(x)) => :rep_ABE)
sort!(PDs_ABE_df, [:input_tr_ratio, :Nsubj_ABE])

CSV.write(joinpath(pathname,
"PDs_ABE_$(Nsubj_ABE)NsubjABE_Nreps$(Nreps_ABE)_$(Nreps_FBE)_$(BSV)bsv.csv
"), PDs_ABE_df)

@info "PEs_ABE"

seedn = 1234
PEs_ABE_df1 = CSV.read(joinpath(pathname,
"PEs_ABE_$(Nsubj_ABE)NsubjABE_Nreps$(Nreps_ABE)_$(Nreps_FBE)_$(BSV)bsv_$(s
eedn)rng.csv"), DataFrame)
seedn = 2345
PEs_ABE_df2 = CSV.read(joinpath(pathname,
"PEs_ABE_$(Nsubj_ABE)NsubjABE_Nreps$(Nreps_ABE)_$(Nreps_FBE)_$(BSV)bsv_$(s
eedn)rng.csv"), DataFrame)
seedn = 3456
PEs_ABE_df3 = CSV.read(joinpath(pathname,
"PEs_ABE_$(Nsubj_ABE)NsubjABE_Nreps$(Nreps_ABE)_$(Nreps_FBE)_$(BSV)bsv_$(s
eedn)rng.csv"), DataFrame)
seedn = 4567
PEs_ABE_df4 = CSV.read(joinpath(pathname,
"PEs_ABE_$(Nsubj_ABE)NsubjABE_Nreps$(Nreps_ABE)_$(Nreps_FBE)_$(BSV)bsv_$(s
eedn)rng.csv"), DataFrame)

PEs_ABE_df = vcat(PEs_ABE_df1, PEs_ABE_df2, PEs_ABE_df3, PEs_ABE_df4)

PEs_ABE_df = combine(groupby(PEs_ABE_df, [:input_tr_ratio, :Nsubj_ABE]))
do df

```

```

    (# MdAPE
MdAPE_tvtr_ratio      = mean(df.MdAPE_tvtr_ratio),
MdAPE_tvCL            = mean(df.MdAPE_tvCL),
MdAPE_tvVc           = mean(df.MdAPE_tvVc),
MdAPE_tvDuration     = mean(df.MdAPE_tvDuration),
MdAPE_wCL            = mean(df.MdAPE_wCL),
MdAPE_wVc            = mean(df.MdAPE_wVc),
MdAPE_σ_prop         = mean(df.MdAPE_σ_prop),

    # MdPE
MdPE_tvtr_ratio      = mean(df.MdPE_tvtr_ratio),
MdPE_tvCL            = mean(df.MdPE_tvCL),
MdPE_tvVc           = mean(df.MdPE_tvVc),
MdPE_tvDuration     = mean(df.MdPE_tvDuration),
MdPE_wCL            = mean(df.MdPE_wCL),
MdPE_wVc            = mean(df.MdPE_wVc),
MdPE_σ_prop         = mean(df.MdPE_σ_prop),
  )
end

CSV.write(joinpath(pathname,
"PEs_ABE_$(Nsubj_ABE)NsubjABE_Nreps$(Nreps_ABE)_$(Nreps_FBE)_$(BSV)bsv.csv
"), PEs_ABE_df)

@info "i_BE_LB_GMR_UB"

seedn = 1234
i_BE_LB_GMR_UB_df1 = CSV.read(joinpath(pathname,
"i_BE_LB_GMR_UB_$(Nsubj_ABE)NsubjABE_Nreps$(Nreps_ABE)_$(Nreps_FBE)_$(BSV)
bsv_$(seedn)rng.csv"), DataFrame)
seedn = 2345
i_BE_LB_GMR_UB_df2 = CSV.read(joinpath(pathname,
"i_BE_LB_GMR_UB_$(Nsubj_ABE)NsubjABE_Nreps$(Nreps_ABE)_$(Nreps_FBE)_$(BSV)
bsv_$(seedn)rng.csv"), DataFrame)
seedn = 3456
i_BE_LB_GMR_UB_df3 = CSV.read(joinpath(pathname,
"i_BE_LB_GMR_UB_$(Nsubj_ABE)NsubjABE_Nreps$(Nreps_ABE)_$(Nreps_FBE)_$(BSV)
bsv_$(seedn)rng.csv"), DataFrame)
seedn = 4567
i_BE_LB_GMR_UB_df4 = CSV.read(joinpath(pathname,
"i_BE_LB_GMR_UB_$(Nsubj_ABE)NsubjABE_Nreps$(Nreps_ABE)_$(Nreps_FBE)_$(BSV)
bsv_$(seedn)rng.csv"), DataFrame)

i_BE_LB_GMR_UB_df = vcat(i_BE_LB_GMR_UB_df1, i_BE_LB_GMR_UB_df2,
i_BE_LB_GMR_UB_df3, i_BE_LB_GMR_UB_df4)

```

```

transform!(groupby(i_BE_LB_GMR_UB_df, [:input_tr_ratio, :Nsubj_ABE,
:Nsubj_FBE, :rep_FBE]), :rep_ABE .=> (x -> 1:length(x)) => :rep_ABE)
sort!(i_BE_LB_GMR_UB_df, [:input_tr_ratio, :Nsubj_ABE, :Nsubj_FBE,
:rep_ABE, :rep_FBE])

CSV.write(joinpath(pathname,
"i_BE_LB_GMR_UB_$(Nsubj_ABE)NsubjABE_Nreps$(Nreps_ABE)_$(Nreps_FBE)_$(BSV)
bsv.csv"), i_BE_LB_GMR_UB_df)

@info "i_BE_passed"

seedn = 1234
i_BE_passed_df1 = CSV.read(joinpath(pathname,
"i_BE_passed_$(Nsubj_ABE)NsubjABE_Nreps$(Nreps_ABE)_$(Nreps_FBE)_$(BSV)bsv
_$(seedn)rng.csv"), DataFrame)
seedn = 2345
i_BE_passed_df2 = CSV.read(joinpath(pathname,
"i_BE_passed_$(Nsubj_ABE)NsubjABE_Nreps$(Nreps_ABE)_$(Nreps_FBE)_$(BSV)bsv
_$(seedn)rng.csv"), DataFrame)
seedn = 3456
i_BE_passed_df3 = CSV.read(joinpath(pathname,
"i_BE_passed_$(Nsubj_ABE)NsubjABE_Nreps$(Nreps_ABE)_$(Nreps_FBE)_$(BSV)bsv
_$(seedn)rng.csv"), DataFrame)
seedn = 4567
i_BE_passed_df4 = CSV.read(joinpath(pathname,
"i_BE_passed_$(Nsubj_ABE)NsubjABE_Nreps$(Nreps_ABE)_$(Nreps_FBE)_$(BSV)bsv
_$(seedn)rng.csv"), DataFrame)

i_BE_passed_df = vcat(i_BE_passed_df1, i_BE_passed_df2, i_BE_passed_df3,
i_BE_passed_df4)

transform!(groupby(i_BE_passed_df, [:input_tr_ratio, :Nsubj_ABE,
:Nsubj_FBE, :rep_FBE]), :rep_ABE .=> (x -> 1:length(x)) => :rep_ABE)
sort!(i_BE_passed_df, [:input_tr_ratio, :Nsubj_ABE, :Nsubj_FBE, :rep_ABE,
:rep_FBE])

CSV.write(joinpath(pathname,
"i_BE_passed_$(Nsubj_ABE)NsubjABE_Nreps$(Nreps_ABE)_$(Nreps_FBE)_$(BSV)bsv
.csv"), i_BE_LB_GMR_UB_df)

@info "any rep BE passrate"

## calculate BE *any rep* passrate

```

```

BE_passrate_df = combine(groupby(i_BE_passed_df, [:Nreps_ABE, :Nreps_FBE,
:input_tr_ratio, :Nsubj_ABE, :Nsubj_FBE])) do df
  (# copying over LB, GMR, and UB to save values
  avg_cmax_LB      = mean(df.cmax_LB),
  avg_cmax_GMR    = mean(df.cmax_GMR),
  avg_cmax_UB     = mean(df.cmax_UB),

  avg_aucinf_LB   = mean(df.aucinf_LB),
  avg_aucinf_GMR  = mean(df.aucinf_GMR),
  avg_aucinf_UB   = mean(df.aucinf_UB),

  # pass rate
  cmax_passrate   = mean(df.cmax_pass) * 100,
  aucinf_passrate = mean(df.aucinf_pass) * 100,
  overall_passrate = mean(df.overall_pass) * 100
  )
end

CSV.write(joinpath(pathname,
"BE_passrate_$(Nsubj_ABE)NsubjABE_Nreps$(Nreps_ABE)_$(Nreps_FBE)_$(BSV)bsv
.csv"), BE_passrate_df)

@info "i_rep_ABE_LB_GMR_UB_pass"

## determine individual BE GMR
i_BE_GMR_df = combine(groupby(i_BE_LB_GMR_UB_df, [:rep_ABE, :Nreps_ABE,
:rep_FBE, :Nreps_FBE, :input_tr_ratio, :Nsubj_ABE, :Nsubj_FBE])) do df
  (cmax_GMR = df.cmax_GMR[1],
  aucinf_GMR = df.aucinf_GMR[1]
  )
end

## calculate 90% CI of FBE GMRs for each rep_ABE and determine whether
passed BE
i_rep_ABE_LB_GMR_UB_pass_df = combine(groupby(i_BE_GMR_df, [:rep_ABE,
:Nreps_ABE, :Nreps_FBE, :input_tr_ratio, :Nsubj_ABE, :Nsubj_FBE])) do df
  (cmax_GMR_LB      = quantile(df.cmax_GMR, 0.05),
  cmax_GMR_GMR     = quantile(df.cmax_GMR, 0.5),
  cmax_GMR_UB      = quantile(df.cmax_GMR, 0.95),
  aucinf_GMR_LB    = quantile(df.aucinf_GMR, 0.05),
  aucinf_GMR_GMR   = quantile(df.aucinf_GMR, 0.5),
  aucinf_GMR_UB    = quantile(df.aucinf_GMR, 0.95),

  # whether passes BE

```

```

    cmax_pass      = (quantile(df.cmax_GMR, 0.05) .> 0.8) .&
(quantile(df.cmax_GMR, 0.95) .< 1.25),
    aucinf_pass    = (quantile(df.aucinf_GMR, 0.05) .> 0.8) .&
(quantile(df.aucinf_GMR, 0.95) .< 1.25),

    # whether passes both cmax and aucinf
    overall_pass   = (quantile(df.cmax_GMR, 0.05) .> 0.8) .&
(quantile(df.cmax_GMR, 0.95) .< 1.25) .&
                                (quantile(df.aucinf_GMR, 0.05) .> 0.8) .&
(quantile(df.aucinf_GMR, 0.95) .< 1.25)
  )
end

CSV.write(joinpath(pathname,
"i_rep_ABE_LB_GMR_UB_pass_$(Nsubj_ABE)NsubjABE_Nreps$(Nreps_ABE)_$(Nreps_F
BE)_$(BSV)bsv.csv"), i_rep_ABE_LB_GMR_UB_pass_df)

@info "BE_GMR90CI_passrate"

## calculate BE pass rate based on 90% CI of FBE GMRs for each rep_ABE
BE_GMR90CI_passrate_df = combine(groupby(i_rep_ABE_LB_GMR_UB_pass_df,
[:Nreps_ABE, :Nreps_FBE, :input_tr_ratio, :Nsubj_ABE, :Nsubj_FBE])) do df
  (# copying over LB, GMR, and UB to save values
  med_cmax_GMR_LB      = median(df.cmax_GMR_LB),
  med_cmax_GMR_GMR     = median(df.cmax_GMR_GMR),
  med_cmax_GMR_UB      = median(df.cmax_GMR_UB),
  med_aucinf_GMR_LB    = median(df.aucinf_GMR_LB),
  med_aucinf_GMR_GMR   = median(df.aucinf_GMR_GMR),
  med_aucinf_GMR_UB    = median(df.aucinf_GMR_UB),

  # pass rate
  cmax_passrate        = mean(df.cmax_pass) * 100,
  aucinf_passrate      = mean(df.aucinf_pass) * 100,
  overall_passrate     = mean(df.overall_pass) * 100
  )
end

CSV.write(joinpath(pathname,
"BE_GMR90CI_passrate_$(Nsubj_ABE)NsubjABE_Nreps$(Nreps_ABE)_$(Nreps_FBE)_$(
BSV)bsv.csv"), BE_GMR90CI_passrate_df)

#####
#####
#####
#####

```

```

@info "vcat Nsubj_ABE files"

## coeftbls_ABE

#Nsubj_ABE = 24
Nsubj_ABE = 72
coeftbls_ABE_df1 = CSV.read(joinpath(pathname,
"coeftbls_ABE_$(Nsubj_ABE)NsubjABE_Nreps$(Nreps_ABE)_$(Nreps_FBE)_$(BSV)bsv.csv"), DataFrame)
#Nsubj_ABE = 36
Nsubj_ABE = 108
coeftbls_ABE_df2 = CSV.read(joinpath(pathname,
"coeftbls_ABE_$(Nsubj_ABE)NsubjABE_Nreps$(Nreps_ABE)_$(Nreps_FBE)_$(BSV)bsv.csv"), DataFrame)
#Nsubj_ABE = 48
Nsubj_ABE = 144
coeftbls_ABE_df3 = CSV.read(joinpath(pathname,
"coeftbls_ABE_$(Nsubj_ABE)NsubjABE_Nreps$(Nreps_ABE)_$(Nreps_FBE)_$(BSV)bsv.csv"), DataFrame)

coeftbls_ABE_df = vcat(coeftbls_ABE_df1, coeftbls_ABE_df2,
coeftbls_ABE_df3)

CSV.write(joinpath(pathname,
"coeftbls_ABE_Nreps$(Nreps_ABE)_$(Nreps_FBE)_$(BSV)bsv.csv"),
coeftbls_ABE_df)

## RSEs_ABE

#Nsubj_ABE = 24
Nsubj_ABE = 72
RSEs_ABE_df1 = CSV.read(joinpath(pathname,
"RSEs_ABE_$(Nsubj_ABE)NsubjABE_Nreps$(Nreps_ABE)_$(Nreps_FBE)_$(BSV)bsv.csv"), DataFrame)
#Nsubj_ABE = 36
Nsubj_ABE = 108
RSEs_ABE_df2 = CSV.read(joinpath(pathname,
"RSEs_ABE_$(Nsubj_ABE)NsubjABE_Nreps$(Nreps_ABE)_$(Nreps_FBE)_$(BSV)bsv.csv"), DataFrame)
#Nsubj_ABE = 48
Nsubj_ABE = 144
RSEs_ABE_df3 = CSV.read(joinpath(pathname,
"RSEs_ABE_$(Nsubj_ABE)NsubjABE_Nreps$(Nreps_ABE)_$(Nreps_FBE)_$(BSV)bsv.csv"), DataFrame)

```

```

RSEs_ABE_df = vcat(RSEs_ABE_df1, RSEs_ABE_df2, RSEs_ABE_df3)

CSV.write(joinpath(pathname,
"RSEs_ABE_Nreps$(Nreps_ABE)_$(Nreps_FBE)_$(BSV)bsv.csv"), RSEs_ABE_df)

## PDs_ABE

#Nsubj_ABE = 24
Nsubj_ABE = 72
PDs_ABE_df1 = CSV.read(joinpath(pathname,
"PDs_ABE_$(Nsubj_ABE)NsubjABE_Nreps$(Nreps_ABE)_$(Nreps_FBE)_$(BSV)bsv.csv
"), DataFrame)
#Nsubj_ABE = 36
Nsubj_ABE = 108
PDs_ABE_df2 = CSV.read(joinpath(pathname,
"PDs_ABE_$(Nsubj_ABE)NsubjABE_Nreps$(Nreps_ABE)_$(Nreps_FBE)_$(BSV)bsv.csv
"), DataFrame)
#Nsubj_ABE = 48
Nsubj_ABE = 144
PDs_ABE_df3 = CSV.read(joinpath(pathname,
"PDs_ABE_$(Nsubj_ABE)NsubjABE_Nreps$(Nreps_ABE)_$(Nreps_FBE)_$(BSV)bsv.csv
"), DataFrame)

PDs_ABE_df = vcat(PDs_ABE_df1, PDs_ABE_df2, PDs_ABE_df3)

CSV.write(joinpath(pathname,
"PDs_ABE_Nreps$(Nreps_ABE)_$(Nreps_FBE)_$(BSV)bsv.csv"), PDs_ABE_df)

## PEs_ABE

#Nsubj_ABE = 24
Nsubj_ABE = 72
PEs_ABE_df1 = CSV.read(joinpath(pathname,
"PEs_ABE_$(Nsubj_ABE)NsubjABE_Nreps$(Nreps_ABE)_$(Nreps_FBE)_$(BSV)bsv.csv
"), DataFrame)
#Nsubj_ABE = 36
Nsubj_ABE = 108
PEs_ABE_df2 = CSV.read(joinpath(pathname,
"PEs_ABE_$(Nsubj_ABE)NsubjABE_Nreps$(Nreps_ABE)_$(Nreps_FBE)_$(BSV)bsv.csv
"), DataFrame)
#Nsubj_ABE = 48
Nsubj_ABE = 144

```

```

PEs_ABE_df3 = CSV.read(joinpath(pathname,
"PEs_ABE_$(Nsubj_ABE)NsubjABE_Nreps$(Nreps_ABE)_$(Nreps_FBE)_$(BSV)bsv.csv
"), DataFrame)

PEs_ABE_df = vcat(PEs_ABE_df1, PEs_ABE_df2, PEs_ABE_df3)

CSV.write(joinpath(pathname,
"PEs_ABE_Nreps$(Nreps_ABE)_$(Nreps_FBE)_$(BSV)bsv.csv"), PEs_ABE_df)

## i_BE_LB_GMR_UB

#Nsubj_ABE = 24
Nsubj_ABE = 72
i_BE_LB_GMR_UB_df1 = CSV.read(joinpath(pathname,
"i_BE_LB_GMR_UB_$(Nsubj_ABE)NsubjABE_Nreps$(Nreps_ABE)_$(Nreps_FBE)_$(BSV)
bsv.csv"), DataFrame)
#Nsubj_ABE = 36
Nsubj_ABE = 108
i_BE_LB_GMR_UB_df2 = CSV.read(joinpath(pathname,
"i_BE_LB_GMR_UB_$(Nsubj_ABE)NsubjABE_Nreps$(Nreps_ABE)_$(Nreps_FBE)_$(BSV)
bsv.csv"), DataFrame)
#Nsubj_ABE = 48
Nsubj_ABE = 144
i_BE_LB_GMR_UB_df3 = CSV.read(joinpath(pathname,
"i_BE_LB_GMR_UB_$(Nsubj_ABE)NsubjABE_Nreps$(Nreps_ABE)_$(Nreps_FBE)_$(BSV)
bsv.csv"), DataFrame)

i_BE_LB_GMR_UB_df = vcat(i_BE_LB_GMR_UB_df1, i_BE_LB_GMR_UB_df2,
i_BE_LB_GMR_UB_df3)

CSV.write(joinpath(pathname,
"i_BE_LB_GMR_UB_Nreps$(Nreps_ABE)_$(Nreps_FBE)_$(BSV)bsv.csv"),
i_BE_LB_GMR_UB_df)

## i_BE_passed

#Nsubj_ABE = 24
Nsubj_ABE = 72
i_BE_passed_df1 = CSV.read(joinpath(pathname,
"i_BE_passed_$(Nsubj_ABE)NsubjABE_Nreps$(Nreps_ABE)_$(Nreps_FBE)_$(BSV)bsv
.csv"), DataFrame)
#Nsubj_ABE = 36
Nsubj_ABE = 108

```

```

i_BE_passed_df2 = CSV.read(joinpath(pathname,
  "i_BE_passed_$(Nsubj_ABE)NsubjABE_Nreps$(Nreps_ABE)_$(Nreps_FBE)_$(BSV)bsv
.csv"), DataFrame)
#Nsubj_ABE = 48
Nsubj_ABE = 144
i_BE_passed_df3 = CSV.read(joinpath(pathname,
  "i_BE_passed_$(Nsubj_ABE)NsubjABE_Nreps$(Nreps_ABE)_$(Nreps_FBE)_$(BSV)bsv
.csv"), DataFrame)

i_BE_passed_df = vcat(i_BE_passed_df1, i_BE_passed_df2, i_BE_passed_df3)

CSV.write(joinpath(pathname,
  "i_BE_passed_Nreps$(Nreps_ABE)_$(Nreps_FBE)_$(BSV)bsv.csv"),
  i_BE_passed_df)

## BE_passrate

#Nsubj_ABE = 24
Nsubj_ABE = 72
BE_passrate_df1 = CSV.read(joinpath(pathname,
  "BE_passrate_$(Nsubj_ABE)NsubjABE_Nreps$(Nreps_ABE)_$(Nreps_FBE)_$(BSV)bsv
.csv"), DataFrame)
#Nsubj_ABE = 36
Nsubj_ABE = 108
BE_passrate_df2 = CSV.read(joinpath(pathname,
  "BE_passrate_$(Nsubj_ABE)NsubjABE_Nreps$(Nreps_ABE)_$(Nreps_FBE)_$(BSV)bsv
.csv"), DataFrame)
#Nsubj_ABE = 48
Nsubj_ABE = 144
BE_passrate_df3 = CSV.read(joinpath(pathname,
  "BE_passrate_$(Nsubj_ABE)NsubjABE_Nreps$(Nreps_ABE)_$(Nreps_FBE)_$(BSV)bsv
.csv"), DataFrame)

BE_passrate_df = vcat(BE_passrate_df1, BE_passrate_df2, BE_passrate_df3)

CSV.write(joinpath(pathname,
  "BE_passrate_Nreps$(Nreps_ABE)_$(Nreps_FBE)_$(BSV)bsv.csv"),
  BE_passrate_df)

## i_rep_ABE_LB_GMR_UB_pass

#Nsubj_ABE = 24
Nsubj_ABE = 72

```

```

i_rep_ABE_LB_GMR_UB_pass_df1 = CSV.read(joinpath(pathname,
"i_rep_ABE_LB_GMR_UB_pass_$(Nsubj_ABE)NsubjABE_Nreps$(Nreps_ABE)_$(Nreps_F
BE)_$(BSV)bsv.csv"), DataFrame)
#Nsubj_ABE = 36
Nsubj_ABE = 108
i_rep_ABE_LB_GMR_UB_pass_df2 = CSV.read(joinpath(pathname,
"i_rep_ABE_LB_GMR_UB_pass_$(Nsubj_ABE)NsubjABE_Nreps$(Nreps_ABE)_$(Nreps_F
BE)_$(BSV)bsv.csv"), DataFrame)
#Nsubj_ABE = 48
Nsubj_ABE = 144
i_rep_ABE_LB_GMR_UB_pass_df3 = CSV.read(joinpath(pathname,
"i_rep_ABE_LB_GMR_UB_pass_$(Nsubj_ABE)NsubjABE_Nreps$(Nreps_ABE)_$(Nreps_F
BE)_$(BSV)bsv.csv"), DataFrame)

i_rep_ABE_LB_GMR_UB_pass_df = vcat(i_rep_ABE_LB_GMR_UB_pass_df1,
i_rep_ABE_LB_GMR_UB_pass_df2, i_rep_ABE_LB_GMR_UB_pass_df3)

CSV.write(joinpath(pathname,
"i_rep_ABE_LB_GMR_UB_pass_Nreps$(Nreps_ABE)_$(Nreps_FBE)_$(BSV)bsv.csv"),
i_rep_ABE_LB_GMR_UB_pass_df)

## BE_GMR90CI_passrate

#Nsubj_ABE = 24
Nsubj_ABE = 72
BE_GMR90CI_passrate_df1 = CSV.read(joinpath(pathname,
"BE_GMR90CI_passrate_$(Nsubj_ABE)NsubjABE_Nreps$(Nreps_ABE)_$(Nreps_FBE)_$(
BSV)bsv.csv"), DataFrame)
#Nsubj_ABE = 36
Nsubj_ABE = 108
BE_GMR90CI_passrate_df2 = CSV.read(joinpath(pathname,
"BE_GMR90CI_passrate_$(Nsubj_ABE)NsubjABE_Nreps$(Nreps_ABE)_$(Nreps_FBE)_$(
BSV)bsv.csv"), DataFrame)
#Nsubj_ABE = 48
Nsubj_ABE = 144
BE_GMR90CI_passrate_df3 = CSV.read(joinpath(pathname,
"BE_GMR90CI_passrate_$(Nsubj_ABE)NsubjABE_Nreps$(Nreps_ABE)_$(Nreps_FBE)_$(
BSV)bsv.csv"), DataFrame)

BE_GMR90CI_passrate_df = vcat(BE_GMR90CI_passrate_df1,
BE_GMR90CI_passrate_df2, BE_GMR90CI_passrate_df3)

CSV.write(joinpath(pathname,
"BE_GMR90CI_passrate_Nreps$(Nreps_ABE)_$(Nreps_FBE)_$(BSV)bsv.csv"),
BE_GMR90CI_passrate_df)

```

References

- Aarnoutse, R. E., G. S. Kibiki, K. Reither, H. H. Semvua, F. Haraka, C. M. Mtabho, S. G. Mpagama, et al. 2017. "Pharmacokinetics, Tolerability, and Bacteriological Response of Rifampin Administered at 600, 900, and 1,200 Milligrams Daily in Patients with Pulmonary Tuberculosis." *Antimicrobial Agents and Chemotherapy* 61 (11): 1–13. <https://doi.org/10.1128/AAC.01054-17>.
- Abdelgawad, Noha, Maxwell Chirehwa, Charlotte Schutz, David Barr, Amy Ward, Saskia Janssen, Rosie Burton, et al. 2024. "Pharmacokinetics of Antitubercular Drugs in Patients Hospitalized with HIV-Associated Tuberculosis: A Population Modeling Analysis." *Wellcome Open Research* 7 (March):72. <https://doi.org/10.12688/wellcomeopenres.17660.3>.
- Acocella, G. 1978. "Clinical Pharmacokinetics of Rifampicin." *Clinical Pharmacokinetics* 3 (2): 108–27. <https://doi.org/10.2165/00003088-197803020-00002>.
- Administration, U.S. Food and Drug. n.d. "Model-Integrated Evidence (MIE) Industry Meeting Pilot Between FDA and Generic Drug Applicants." Accessed February 2, 2024. <https://www.fda.gov/drugs/abbreviated-new-drug-application-anda/model-integrated-evidence-mie-industry-meeting-pilot-between-fda-and-generic-drug-applicants>.
- Ahmadzia, Homa K., Naomi L.C. Luban, Shuhui Li, Dong Guo, Adam Miszta, Jogarao V.S. Gobburu, Jeffrey S. Berger, Andra H. James, Alisa S. Wolberg, and John van den Anker. 2021. "Optimal Use of Intravenous Tranexamic Acid for Hemorrhage Prevention in Pregnant Women." *American Journal of Obstetrics and Gynecology* 225 (1): 85.e1-85.e11. <https://doi.org/10.1016/j.ajog.2020.11.035>.
- Alghamdi, Wael A, Mohammad H. Al-Shaer, and Charles A. Peloquin. 2018. "Protein Binding of First-Line Antituberculosis Drugs." *Antimicrobial Agents and Chemotherapy* 62 (7): 1–7. <https://doi.org/10.1128/AAC.00641-18>.
- Almeida, Deepak, Paul J. Converse, Zahoor Ahmad, Kelly E. Dooley, Eric L. Nuermberger, and Jacques H. Grosset. 2011. "Activities of Rifampin, Rifapentine and Clarithromycin Alone and in Combination against Mycobacterium Ulcerans Disease in Mice." *PLoS Neglected Tropical Diseases* 5 (1). <https://doi.org/10.1371/journal.pntd.0000933>.
- ASME. 2018. "V V - Assessing Credibility of Computational Modeling through Verification and Validation: Application to Medical Devices." 2018. <https://www.asme.org/codes-standards/find-codes-standards/assessing-credibility-of-computational-modeling-through-verification-and-validation-application-to-medical-devices>.

- Auwers, P Van der, J Klastersky, J P Thys, F Meunier-Carpentier, and J C Legrand. 1985. “Double-Blind, Placebo-Controlled Study of Oxacillin Combined with Rifampin in the Treatment of Staphylococcal Infections.” *Antimicrobial Agents and Chemotherapy* 28 (4): 467–72. <https://doi.org/10.1128/AAC.28.4.467>.
- Auwers, P. Van Der, F. Meunier-Carpentier, and J. Klastersky. 1983. “Clinical Study of Combination Therapy with Oxacillin and Rifampin for Staphylococcal Infections.” *Clinical Infectious Diseases* 5 (Supplement_3): S515–21. https://doi.org/10.1093/clinids/5.Supplement_3.S515.
- Baddour, Larry M., Walter R. Wilson, Arnold S. Bayer, Vance G. Fowler, Imad M. Tleyjeh, Michael J. Rybak, Bruno Barsic, et al. 2015. “Infective Endocarditis in Adults: Diagnosis, Antimicrobial Therapy, and Management of Complications: A Scientific Statement for Healthcare Professionals from the American Heart Association.” *Circulation*. Lippincott Williams and Wilkins. <https://doi.org/10.1161/CIR.0000000000000296>.
- Bartelink, I. H., N. Zhang, R. J. Keizer, N. Strydom, P. J. Converse, K. E. Dooley, E. L. Nuermberger, and R. M. Savic. 2017. “New Paradigm for Translational Modeling to Predict Long-Term Tuberculosis Treatment Response.” *Clinical and Translational Science* 10 (5): 366–79. <https://doi.org/10.1111/cts.12472>.
- Bennett, John E.; Dolin, Raphael; Blaser, Martin J. 2019. *Mandell, Douglas, and Bennett’s Principles and Practice of Infectious Diseases*. 9th ed. Elsevier.
- Bernard, Louis, Cédric Arvieux, Benoit Brunschweiler, Sophie Touchais, Séverine Ansart, Jean-Pierre Bru, Eric Oziol, et al. 2021. “Antibiotic Therapy for 6 or 12 Weeks for Prosthetic Joint Infection.” *New England Journal of Medicine* 384 (21): 1991–2001. <https://doi.org/10.1056/NEJMoa2020198>.
- Berenthal, Nicholas M., Alexandra I. Stavrakis, Fabrizio Billi, John S. Cho, Thomas J. Kremen, Scott I. Simon, Ambrose L. Cheung, et al. 2010. “A Mouse Model of Post-Arthroplasty Staphylococcus Aureus Joint Infection to Evaluate in Vivo the Efficacy of Antimicrobial Implant Coatings.” *PLoS ONE* 5 (9): 1–11. <https://doi.org/10.1371/journal.pone.0012580>.
- Bjugård Nyberg, Henrik, Xiaomei Chen, Mark Donnelly, Lanyan Fang, Liang Zhao, Mats O. Karlsson, and Andrew C. Hooker. 2024. “Evaluation of Model-integrated Evidence Approaches for Pharmacokinetic Bioequivalence Studies Using Model Averaging Methods.” *CPT: Pharmacometrics & Systems Pharmacology*, August. <https://doi.org/10.1002/psp4.13217>.
- Boeree, Martin J., Andreas H. Diacon, Rodney Dawson, Kim Narunsky, Jeannine Du Bois, Amour Venter, Patrick P.J. Phillips, et al. 2015. “A Dose-Ranging Trial to Optimize the Dose of Rifampin in the Treatment of Tuberculosis.” *American Journal of Respiratory and Critical Care Medicine* 191 (9): 1058–65. <https://doi.org/10.1164/rccm.201407-1264OC>.

- Boeree, Martin J., Norbert Heinrich, Rob Aarnoutse, Andreas H. Diacon, Rodney Dawson, Sunita Rehal, Gibson S. Kibiki, et al. 2017. "High-Dose Rifampicin, Moxifloxacin, and SQ109 for Treating Tuberculosis: A Multi-Arm, Multi-Stage Randomised Controlled Trial." *The Lancet Infectious Diseases* 17 (1): 39–49. [https://doi.org/10.1016/S1473-3099\(16\)30274-2](https://doi.org/10.1016/S1473-3099(16)30274-2).
- Bois, Frederic Y., and Céline Brochot. 2024. "A Bayesian Framework for Virtual Comparative Trials and Bioequivalence Assessments." *Frontiers in Pharmacology* 15 (July). <https://doi.org/10.3389/fphar.2024.1404619>.
- Boman, G, and V. A. Ringberger. 1974. "Binding of Rifampicin by Human Plasma Proteins." *European Journal of Clinical Pharmacology* 7 (5): 369–73. <https://doi.org/10.1007/BF00558209>.
- Bonate, Peter L. 2000. "Clinical Trial Simulation in Drug Development." *Pharmaceutical Research*. Vol. 17. <https://doi.org/10.1023/a:1007548719885>.
- Borselen, Marjolein D. van, Laurens Auke Æmiel Sluijterman, Rick Greupink, and Saskia N. de Wildt. 2024. "Towards More Robust Evaluation of the Predictive Performance of Physiologically Based Pharmacokinetic Models: Using Confidence Intervals to Support Use of Model-Informed Dosing in Clinical Care." *Clinical Pharmacokinetics* 63 (3): 343–55. <https://doi.org/10.1007/s40262-023-01326-3>.
- Brake, L. H.M. Te, R. Ruslami, H. Later-Nijland, F. Mooren, M. Teulen, L. Apriani, J. B. Koenderink, et al. 2015. "Exposure to Total and Protein-Unbound Rifampin Is Not Affected by Malnutrition in Indonesian Tuberculosis Patients." *Antimicrobial Agents and Chemotherapy* 59 (6): 3233–39. <https://doi.org/10.1128/AAC.03485-14>.
- Brake, Lindsey H.M. te, Veronique de Jager, Kim Narunsky, Naadira Vanker, Elin M. Svensson, Patrick P.J. Phillips, Stephen H. Gillespie, et al. 2021. "Increased Bactericidal Activity but Dose-Limiting Intolerability at 50 Mg·kg⁻¹ Rifampicin." *European Respiratory Journal* 58 (1). <https://doi.org/10.1183/13993003.00955-2020>.
- Brissos, Sofia, Miguel Ruiz Veguilla, David Taylor, and Vicent Balanzá-Martinez. 2014. "The Role of Long-Acting Injectable Antipsychotics in Schizophrenia: A Critical Appraisal." *Therapeutic Advances in Psychopharmacology* 4 (5): 198–219. <https://doi.org/10.1177/2045125314540297>.
- Bruno, Rene, Jin Y. Jin, Kimberly Maxfield, Lauren Milligan, Chao Liu, Yaning Wang, Amy E. McKee, and Issam Zineh. 2019. "Proceedings of a Workshop: US Food and Drug Administration-International Society of Pharmacometrics Model-Informed Drug Development in Oncology." In *Clinical Pharmacology and Therapeutics*, 106:81–83. Nature Publishing Group. <https://doi.org/10.1002/cpt.1421>.
- Bruzzese, Tiberio, Claudio Rimaroli, Angelo Bonabello, Giovanni Mozzi, Samyuktha Ajay, and Noshir D. Cooverj. 2000. "Pharmacokinetics and Tissue Distribution of

Rifametane, a New 3- Azinomethyl-Rifamycin Derivative, in Several Animal Species.” *Arzneimittel-Forschung/Drug Research* 50 (1): 60–71. <https://doi.org/10.1055/s-0031-1300165>.

- Bunn, Haden T., Jogarao V.S. Gobburu, and Lindsey M. Floryance. 2023. “Bayesian Model-Guided Antimicrobial Therapy in Pediatrics.” *Frontiers in Pharmacology*. Frontiers Media SA. <https://doi.org/10.3389/fphar.2023.1118771>.
- Cassat, James E., Jessica L. Moore, Kevin J. Wilson, Zach Stark, Boone M. Prentice, Raf Van de Plas, William J. Perry, et al. 2018. “Integrated Molecular Imaging Reveals Tissue Heterogeneity Driving Host-Pathogen Interactions.” *Science Translational Medicine* 10 (432). <https://doi.org/10.1126/scitranslmed.aan6361>.
- Chastre, Jean, Michel Wolff, Jean-Yves Fagon, Sylvie Chevret, Franck Thomas, Delphine Wermert, Eva Clementi, et al. 2003. “Comparison of 8 vs 15 Days of Antibiotic Therapy for Ventilator-Associated Pneumonia in Adults.” *JAMA* 290 (19): 2588. <https://doi.org/10.1001/jama.290.19.2588>.
- Chen, Chao, Susana Gardete, Robert Sander Jansen, Annanya Shetty, Thomas Dick, Kyu Y Rhee, and Véronique Dartois. 2018. “Verapamil Targets Membrane Energetics in Mycobacterium Tuberculosis.” *Antimicrobial Agents and Chemotherapy* 62 (5): 11–13. <https://doi.org/10.1128/AAC.02107-17>.
- Chen, Chunli, Fatima Ortega, Laura Alameda, Santiago Ferrer, and Ulrika S.H. Simonsson. 2016. “Population Pharmacokinetics, Optimised Design and Sample Size Determination for Rifampicin, Isoniazid, Ethambutol and Pyrazinamide in the Mouse.” *European Journal of Pharmaceutical Sciences* 93:319–33. <https://doi.org/10.1016/j.ejps.2016.07.017>.
- Chen, Xiaomei, Henrik B. Nyberg, Mark Donnelly, Liang Zhao, Lanyan Fang, Mats O. Karlsson, and Andrew C. Hooker. 2024. “Development and Comparison of Model-integrated Evidence Approaches for Bioequivalence Studies with Pharmacokinetic End Points.” *CPT: Pharmacometrics & Systems Pharmacology*, August. <https://doi.org/10.1002/psp4.13216>.
- Chigutsa, Emmanuel, Jotam G. Pasipanodya, Marianne E. Visser, Paul D. van Helden, Peter J. Smith, Frederick A. Sirgel, Tawanda Gumbo, and Helen McIlleron. 2015. “Impact of Nonlinear Interactions of Pharmacokinetics and MICs on Sputum Bacillary Kill Rates as a Marker of Sterilizing Effect in Tuberculosis.” *Antimicrobial Agents and Chemotherapy* 59 (1): 38–45. <https://doi.org/10.1128/AAC.03931-14>.
- Cluzel, R. A., R. Lopitiaux, J. Sirot, and S. Rampon. 1984. “Rifampicin in the Treatment of Osteoarticular Infections Due to Staphylococci.” *Journal of Antimicrobial Chemotherapy* 13 (suppl C): 23–29. https://doi.org/10.1093/jac/13.suppl_C.23.

- Costerton, J. W., Philip S. Stewart, and E. P. Greenberg. 1999. "Bacterial Biofilms: A Common Cause of Persistent Infections." *Science* 284 (5418): 1318–22. <https://doi.org/10.1126/science.284.5418.1318>.
- Creinin, Mitchell D., Rolf Jansen, Robert M. Starr, Joga Gobburu, Mathangi Gopalakrishnan, and Andrea Olariu. 2016. "Levonorgestrel Release Rates over 5 Years with the Liletta® 52-Mg Intrauterine System." *Contraception* 94 (4): 353–56. <https://doi.org/10.1016/j.contraception.2016.04.010>.
- Cremers, Serge CLM, Marelise EMW Eekhoff, Jan Den Hartigh, Neveen AT Hamdy, Pieter Vermeij, and Socrates E Papapoulos. 2003. "Relationships Between Pharmacokinetics and Rate of Bone Turnover After Intravenous Bisphosphonate (Olpadronate) in Patients With Paget's Disease of Bone." *Journal of Bone and Mineral Research* 18 (5): 868–75. <https://doi.org/10.1359/jbmr.2003.18.5.868>.
- Davit, Barbara M., Mei Ling Chen, Dale P. Conner, Sam H. Haidar, Stephanie Kim, Christina H. Lee, Robert A. Lionberger, et al. 2012. "Implementation of a Reference-Scaled Average Bioequivalence Approach for Highly Variable Generic Drug Products by the Us Food and Drug Administration." *AAPS Journal* 14 (4): 915–24. <https://doi.org/10.1208/s12248-012-9406-x>.
- DeMarco, Vincent P., Alvaro A. Ordonez, Mariah Klunk, Brendan Prideaux, Hui Wang, Zhang Zhuo, Peter J. Tonge, et al. 2015. "Determination of ¹¹C-Rifampin Pharmacokinetics within Mycobacterium Tuberculosis-Infected Mice by Using Dynamic Positron Emission Tomography Bioimaging." *Antimicrobial Agents and Chemotherapy* 59 (9): 5768–74. <https://doi.org/10.1128/AAC.01146-15>.
- Diacon, A. H., R. F. Patientia, A. Venter, P. D. van Helden, P. J. Smith, H. McIlleron, J. S. Maritz, and P. R. Donald. 2007. "Early Bactericidal Activity of High-Dose Rifampin in Patients with Pulmonary Tuberculosis Evidenced by Positive Sputum Smears." *Antimicrobial Agents and Chemotherapy* 51 (8): 2994–96. <https://doi.org/10.1128/AAC.01474-06>.
- Dubois, Anne, Sandro Gsteiger, Etienne Pigeolet, and France Mentré. 2010. "Bioequivalence Tests Based on Individual Estimates Using Non-Compartmental or Model-Based Analyses: Evaluation of Estimates of Sample Means and Type I Error for Different Designs." *Pharmaceutical Research* 27 (1): 92–104. <https://doi.org/10.1007/s11095-009-9980-5>.
- Dubois, Anne, Marc Lavielle, Sandro Gsteiger, Etienne Pigeolet, and France Mentré. 2011. "Model-Based Analyses of Bioequivalence Crossover Trials Using the Stochastic Approximation Expectation Maximisation Algorithm." *Statistics in Medicine* 30 (21): 2582–2600. <https://doi.org/10.1002/sim.4286>.
- Euba, G., O. Murillo, N. Fernández-Sabé, J. Mascaró, J. Cabo, A. Pérez, F. Tubau, R. Verdaguer, F. Gudiol, and J. Ariza. 2009. "Long-Term Follow-Up Trial of Oral Rifampin-Cotrimoxazole Combination versus Intravenous Cloxacillin in Treatment

of Chronic Staphylococcal Osteomyelitis.” *Antimicrobial Agents and Chemotherapy* 53 (6): 2672–76. <https://doi.org/10.1128/AAC.01504-08>.

Ewijk-Beneken Kolmer, Eleonora W.J. van, Marga J.A. Teulen, Erik C.A. van den Hombergh, Nielka E. van Erp, Lindsey H.M. te Brake, and Rob E. Aarnoutse. 2017. “Determination of Protein-Unbound, Active Rifampicin in Serum by Ultrafiltration and Ultra Performance Liquid Chromatography with UV Detection. A Method Suitable for Standard and High Doses of Rifampicin.” *Journal of Chromatography B: Analytical Technologies in the Biomedical and Life Sciences* 1063 (April 2017): 42–49. <https://doi.org/10.1016/j.jchromb.2017.08.004>.

Fang, Lanyan, Myong Jin Kim, Zhichuan Li, Yanning Wang, Charles E. DiLiberti, Jessie Au, Andrew Hooker, Murray P. Ducharme, Robert Lionberger, and Liang Zhao. 2018. “Model-Informed Drug Development and Review for Generic Products: Summary of FDA Public Workshop.” *Clinical Pharmacology and Therapeutics* 104 (1): 27–30. <https://doi.org/10.1002/cpt.1065>.

Fang, Lanyan, Ramana Uppoor, Mingjiang Xu, Satish Sharan, Hao Zhu, Nilufer Tampal, Bing Li, Lei Zhang, Robert Lionberger, and Liang Zhao. 2021. “Use of Partial Area Under the Curve in Bioavailability or Bioequivalence Assessments: A Regulatory Perspective.” *Clinical Pharmacology and Therapeutics* 0 (0): 1–8. <https://doi.org/10.1002/cpt.2174>.

Fischbacher, Arnaud, and Olivier Borens. 2019. “Prosthetic-Joint Infections: Mortality Over The Last 10 Years.” *Journal of Bone and Joint Infection* 4 (4): 198–202. <https://doi.org/10.7150/jbji.35428>.

Francis, Jose, Rosie Mngqibisa, Helen McIlleron, Michelle A Kendall, Xingye Wu, Kelly E. Dooley, Cynthia Firnhaber, Catherine Godfrey, Susan E. Cohn, and Paolo Denti. 2021. “A Semimechanistic Pharmacokinetic Model for Depot Medroxyprogesterone Acetate and Drug–Drug Interactions With Antiretroviral and Antituberculosis Treatment.” *Clinical Pharmacology & Therapeutics* 110 (4): 1057–65. <https://doi.org/10.1002/cpt.2324>.

Gong, Yuqing, Peijue Zhang, Miyoung Yoon, Hao Zhu, Ameya Kohojkar, Andrew C. Hooker, Murray P. Ducharme, et al. 2023. “Establishing the Suitability of Model-Integrated Evidence to Demonstrate Bioequivalence for Long-Acting Injectable and Implantable Drug Products: Summary of Workshop.” *CPT: Pharmacometrics and Systems Pharmacology*. American Society for Clinical Pharmacology and Therapeutics. <https://doi.org/10.1002/psp4.12931>.

Gordon, Oren, Donald E Lee, Bessie Liu, Brooke Langevin, Alvaro A Ordonez, Dustin A Dikeman, Babar Shafiq, et al. 2021. “Dynamic PET-Facilitated Modeling and High-Dose Rifampin Regimens for Staphylococcus Aureus Orthopedic Implant–Associated Infections.” *Science Translational Medicine* 13 (622). <https://doi.org/10.1126/scitranslmed.abl6851>.

- Holford, N., S. C. Ma, and B. A. Ploeger. 2010. "Clinical Trial Simulation: A Review." *Clinical Pharmacology and Therapeutics*. <https://doi.org/10.1038/clpt.2010.114>.
- Hosagrahara, Vinayak, Jitendar Reddy, Samit Ganguly, Vijender Panduga, Vijaykamal Ahuja, Manish Parab, and Jayashree Giridhar. 2013. "Effect of Repeated Dosing on Rifampin Exposure in BALB/c Mice." *European Journal of Pharmaceutical Sciences* 49 (1): 33–38. <https://doi.org/10.1016/j.ejps.2013.01.017>.
- Hu, Chuanpu. 2022. "Variability and Uncertainty: Interpretation and Usage of Pharmacometric Simulations and Intervals." *Journal of Pharmacokinetics and Pharmacodynamics*, 487–91. <https://doi.org/10.1007/s10928-022-09817-9>.
- Hu, Chuanpu, Katy H.P. Moore, Yong H. Kim, and Mark E. Sale. 2004. "Statistical Issues in a Modeling Approach to Assessing Bioequivalence or PK Similarity with Presence of Sparsely Sampled Subjects." *Journal of Pharmacokinetics and Pharmacodynamics* 31 (4): 321–39. <https://doi.org/10.1023/B:JOPA.0000042739.44458.e0>.
- Hu, Yanmin, Alexander Liu, Fatima Ortega-Muro, Laura Alameda-Martin, Denis Mitchison, and Anthony Coates. 2015. "High-Dose Rifampicin Kills Persisters, Shortens Treatment Duration, and Reduces Relapse Rate in Vitro and in Vivo." *Frontiers in Microbiology* 6 (JUN): 1–10. <https://doi.org/10.3389/fmicb.2015.00641>.
- Hunter, Robert L. 2018. "The Pathogenesis of Tuberculosis: The Early Infiltrate of Post-Primary (Adult Pulmonary) Tuberculosis: A Distinct Disease Entity." *Frontiers in Immunology* 9 (September). <https://doi.org/10.3389/fimmu.2018.02108>.
- Iversen, P, O S Nielsen, K M Jensen, and P O Madsen. 1983. "Comparison of Concentrations of Rifampin and a New Rifamycin Derivative, DL 473, in Canine Bone." *Antimicrobial Agents and Chemotherapy* 23 (2): 338–40. <https://doi.org/10.1128/AAC.23.2.338>.
- Jain, John, Caryn Dutton, Antonia Nicosia, Charlie Wajszczuk, Frederick R. Bode, and Daniel R. Mishell. 2004. "Pharmacokinetics, Ovulation Suppression and Return to Ovulation Following a Lower Dose Subcutaneous Formulation of Depo-Provera®." *Contraception* 70 (1): 11–18. <https://doi.org/10.1016/j.contraception.2004.01.011>.
- Jayaram, Ramesh, Sheshagiri Gaonkar, Parvinder Kaur, B. L. Suresh, B. N. Mahesh, R. Jayashree, Vrinda Nandi, et al. 2003. "Pharmacokinetics-Pharmacodynamics of Rifampin in an Aerosol Infection Model of Tuberculosis." *Antimicrobial Agents and Chemotherapy* 47 (7): 2118–24. <https://doi.org/10.1128/aac.47.7.2118-2124.2003>.
- Jones, H. M., and K. Rowland-Yeo. 2013. "Basic Concepts in Physiologically Based Pharmacokinetic Modeling in Drug Discovery and Development." *CPT: Pharmacometrics and Systems Pharmacology* 2 (8): 1–12. <https://doi.org/10.1038/psp.2013.41>.

- Karlsen, Øystein Espeland, Pål Borgen, Bjørn Bragnes, Wender Figved, Bjarne Grøgaard, Jonas Rydinge, Lars Sandberg, et al. 2020. “Rifampin Combination Therapy in Staphylococcal Prosthetic Joint Infections: A Randomized Controlled Trial.” *Journal of Orthopaedic Surgery and Research* 15 (1): 365. <https://doi.org/10.1186/s13018-020-01877-2>.
- Kuempel, Colleen, Yuching Yang, Xinyuan Zhang, Jeffrey Florian, Hao Zhu, Million Tegenge, Shiew Mei Huang, Yaning Wang, Tina Morrison, and Issam Zineh. 2020. “Consideration of a Credibility Assessment Framework in Model-Informed Drug Development: Potential Application to Physiologically-Based Pharmacokinetic Modeling and Simulation.” *CPT: Pharmacometrics and Systems Pharmacology* 9 (1): 21–28. <https://doi.org/10.1002/psp4.12479>.
- Kümmel, Anne, Peter L. Bonate, Jasper Dingemans, and Andreas Krause. 2018. “Confidence and Prediction Intervals for Pharmacometric Models.” *CPT: Pharmacometrics and Systems Pharmacology* 7 (6): 360–73. <https://doi.org/10.1002/psp4.12286>.
- Kurtz, Steven M., Edmund Lau, Heather Watson, Jordana K. Schmier, and Javad Parvizi. 2012. “Economic Burden of Periprosthetic Joint Infection in the United States.” *Journal of Arthroplasty* 27 (8 SUPPL.). <https://doi.org/10.1016/j.arth.2012.02.022>.
- Labes, Detlew; Schutz, Helmut; Lang, Benjamin. 2024. “PowerTOST: Power and Sample Size for (Bio)Equivalence Studies.” March 18, 2024. <https://cran.r-project.org/web/packages/PowerTOST/index.html>.
- Laffont, Celine M., Roberto Gomeni, Bo Zheng, Christian Heidebreder, Paul J. Fudala, and Azmi F. Nasser. 2015. “Population Pharmacokinetic Modeling and Simulation to Guide Dose Selection for RBP-7000, a New Sustained-Release Formulation of Risperidone.” *Journal of Clinical Pharmacology* 55 (1): 93–103. <https://doi.org/10.1002/jcph.366>.
- Lappin, Graham, Robert Noveck, and Tal Burt. 2013. “Microdosing and Drug Development: Past, Present and Future.” *Expert Opinion on Drug Metabolism & Toxicology* 9 (7): 817–34. <https://doi.org/10.1517/17425255.2013.786042>.
- LeCluyse, Edward L. 2001. “Pregnane X Receptor: Molecular Basis for Species Differences in CYP3A Induction by Xenobiotics.” *Chemico-Biological Interactions* 134 (3): 283–89. [https://doi.org/10.1016/S0009-2797\(01\)00163-6](https://doi.org/10.1016/S0009-2797(01)00163-6).
- Lee, Jieon, Kairui Feng, Mingjiang Xu, Xiajing Gong, Wanjie Sun, Jessica Kim, Zhen Zhang, Meng Wang, Lanyan Fang, and Liang Zhao. 2020. “Applications of Adaptive Designs in Generic Drug Development.” *Clinical Pharmacology and Therapeutics*. <https://doi.org/10.1002/cpt.2050>.
- Lee, Jieon, Yuqing Gong, Sid Bhoopathy, Charles E. DiLiberti, Andrew C. Hooker, Amin Rostami-Hodjegan, Stephan Schmidt, et al. 2020. “Public Workshop Summary

Report on Fiscal Year 2021 Generic Drug Regulatory Science Initiatives: Data Analysis and Model-Based Bioequivalence.” *Clinical Pharmacology and Therapeutics* 0 (0): 1–6. <https://doi.org/10.1002/cpt.2120>.

- Li, Ho-Kwong, Ines Rombach, Rhea Zambellas, A. Sarah Walker, Martin A. McNally, Bridget L. Atkins, Benjamin A. Lipsky, et al. 2019. “Oral versus Intravenous Antibiotics for Bone and Joint Infection.” *New England Journal of Medicine* 380 (5): 425–36. <https://doi.org/10.1056/NEJMoa1710926>.
- Litjens, Carlijn H.C., Rob E. Aarnoutse, Eleonora W.J. Van Ewijk-Beneken Kolmer, Elin M. Svensson, Angela Colbers, David M. Burger, Martin J. Boeree, et al. 2019. “Protein Binding of Rifampicin Is Not Saturated When Using High-Dose Rifampicin.” *Journal of Antimicrobial Chemotherapy* 74 (4): 986–90. <https://doi.org/10.1093/jac/dky527>.
- Liu, Catherine, Arnold Bayer, Sara E Cosgrove, Robert S Daum, Scott K Fridkin, Rachel J Gorwitz, Sheldon L Kaplan, et al. 2011. “Clinical Practice Guidelines by the Infectious Diseases Society of America for the Treatment of Methicillin- Resistant Staphylococcus Aureus Infections in Adults and Children” 52. <https://doi.org/10.1093/cid/ciq146>.
- Liu, Yingjun, Henry Pertinez, Fatima Ortega-Muro, Laura Alameda-Martin, Thomas Harrison, Geraint Davies, Anthony Coates, and Yanmin Hu. 2018. “Optimal Doses of Rifampicin in the Standard Drug Regimen to Shorten Tuberculosis Treatment Duration and Reduce Relapse by Eradicating Persistent Bacteria.” *Journal of Antimicrobial Chemotherapy* 73 (3): 724–31. <https://doi.org/10.1093/jac/dkx467>.
- Loingeville, Florence, Julie Bertrand, Thu Thuy Nguyen, Satish Sharan, Kairui Feng, Wanjie Sun, Jing Han, et al. 2020. “New Model–Based Bioequivalence Statistical Approaches for Pharmacokinetic Studies with Sparse Sampling.” *AAPS Journal* 22 (6): 1–8. <https://doi.org/10.1208/s12248-020-00507-3>.
- Madabushi, Rajanikanth, Paul Seo, Liang Zhao, Million Tegenge, and Hao Zhu. 2022. “Review: Role of Model-Informed Drug Development Approaches in the Lifecycle of Drug Development and Regulatory Decision-Making.” *Pharmaceutical Research*. Springer. <https://doi.org/10.1007/s11095-022-03288-w>.
- Maiga, Mamoudou, Bintou Ahmadou Ahidjo, Mariama C. Maiga, Laurene Cheung, Shaaretha Pelly, Shichun Lun, Flabou Bougoudogo, and William R. Bishai. 2015. “Efficacy of Adjunctive Tofacitinib Therapy in Mouse Models of Tuberculosis.” *EBioMedicine* 2 (8): 868–73. <https://doi.org/10.1016/j.ebiom.2015.07.014>.
- Merritt, Judith H., Daniel E. Kadouri, and George A. O’Toole. 2006. “Growing and Analyzing Static Biofilms.” *Current Protocols in Microbiology* 00 (1). <https://doi.org/10.1002/9780471729259.mc01b01s00>.

- Mould, D. R., and R. N. Upton. 2012. "Basic Concepts in Population Modeling, Simulation, and Model-Based Drug Development." *CPT: Pharmacometrics and Systems Pharmacology* 1 (1): 1–14. <https://doi.org/10.1038/psp.2012.4>.
- . 2013. "Basic Concepts in Population Modeling, Simulation, and Model-Based Drug Development - Part 2: Introduction to Pharmacokinetic Modeling Methods." *CPT: Pharmacometrics and Systems Pharmacology* 2 (4). <https://doi.org/10.1038/psp.2013.14>.
- Nguyen, S., A. Pasquet, L. Legout, E. Beltrand, L. Dubreuil, H. Migaud, Y. Yazdanpanah, and E. Senneville. 2009. "Efficacy and Tolerance of Rifampicin–Linezolid Compared with Rifampicin–Cotrimoxazole Combinations in Prolonged Oral Therapy for Bone and Joint Infections." *Clinical Microbiology and Infection* 15 (12): 1163–69. <https://doi.org/10.1111/j.1469-0691.2009.02761.x>.
- Norden, Carl W., Richard Bryant, Darwin Palmer, John Z. Montgomerie, and Joseph Wheat. 1986. "Chronic Osteomyelitis Caused by Staphylococcus Aureus: Controlled Clinical Trial of Nafcillin Therapy and Nafcillin-Rifampin Therapy." *Southern Medical Journal* 79 (8): 947–51. <https://doi.org/10.1097/00007611-198608000-00008>.
- Norden, Carl W., Joshua Fierer, and Richard E. Bryant. 1983. "Chronic Staphylococcal Osteomyelitis: Treatment with Regimens Containing Rifampin." *Clinical Infectious Diseases* 5 (Supplement_3): S495–501. https://doi.org/10.1093/clinids/5.Supplement_3.S495.
- O'Brien, Matthew N., Wenlei Jiang, Yan Wang, and David M. Loffredo. 2021. "Challenges and Opportunities in the Development of Complex Generic Long-Acting Injectable Drug Products." *Journal of Controlled Release* 336 (June): 144–58. <https://doi.org/10.1016/j.jconrel.2021.06.017>.
- Oda, Kazutaka, Hideyuki Saito, and Hirofumi Jono. 2023. "Bayesian Prediction-Based Individualized Dosing of Anti-Methicillin-Resistant Staphylococcus Aureus Treatment: Recent Advancements and Prospects in Therapeutic Drug Monitoring." *Pharmacology and Therapeutics*. Elsevier Inc. <https://doi.org/10.1016/j.pharmthera.2023.108433>.
- Ordonez, Alvaro A., Hechuan Wang, Gesham Magombedze, Camilo A. Ruiz-Bedoya, Shashikant Srivastava, Allen Chen, Elizabeth W. Tucker, et al. 2020. "Dynamic Imaging in Patients with Tuberculosis Reveals Heterogeneous Drug Exposures in Pulmonary Lesions." *Nature Medicine* 26 (4): 529–34. <https://doi.org/10.1038/s41591-020-0770-2>.
- Osmon, Douglas R, Elie F Berbari, Anthony R Berendt, Daniel Lew, Werner Zimmerli, James M Steckelberg, Nalini Rao, Arlen Hanssen, and Walter R Wilson. 2013. "Diagnosis and Management of Prosthetic Joint Infection: Clinical Practice

Guidelines by the Infectious Diseases Society of America.” *Clinical Infectious Diseases* 56 (1): e1–25. <https://doi.org/10.1093/cid/cis803>.

- Pal, Arindom, Fang Wu, Ross Walenga, Eleftheria Tsakalozou, Khondoker Alam, Yuqing Gong, Liang Zhao, and Lanyan Fang. 2024. “Leveraging Modeling and Simulation to Enhance the Efficiency of Bioequivalence Approaches for Generic Drugs: Highlights from the 2023 Generic Drug Science and Research Initiatives Public Workshop.” *The AAPS Journal* 26 (3): 45. <https://doi.org/10.1208/s12248-024-00916-8>.
- Pasipanodya, J. G., H. McIlleron, A. Burger, P. A. Wash, P. Smith, and T. Gumbo. 2013. “Serum Drug Concentrations Predictive of Pulmonary Tuberculosis Outcomes.” *Journal of Infectious Diseases* 208 (9): 1464–73. <https://doi.org/10.1093/infdis/jit352>.
- Pasipanodya, Jotam G, Wynand Smythe, Corinne S Merle, Piero L Olliaro, Devyani Deshpande, Gesham Magombedze, Helen McIlleron, and Tawanda Gumbo. 2018. “Artificial Intelligence–Derived 3-Way Concentration-Dependent Antagonism of Gatifloxacin, Pyrazinamide, and Rifampicin During Treatment of Pulmonary Tuberculosis.” *Clinical Infectious Diseases* 67 (suppl_3): S284–92. <https://doi.org/10.1093/cid/ciy610>.
- Peloquin, C. A., G. E. Velásquez, L. Lecca, R. I. Calderón, J. Coit, M. Milstein, E. Osso, et al. 2017. “Pharmacokinetic Evidence from the HIRIF Trial To Support Increased Doses of Rifampin for Tuberculosis.” *Antimicrobial Agents and Chemotherapy* 61 (8): 1–6. <https://doi.org/10.1128/AAC.00038-17>.
- Plaut, Roger D., Christopher P. Mocca, Ranjani Prabhakara, Tod J. Merkel, and Scott Stibitz. 2013. “Stably Luminescent Staphylococcus Aureus Clinical Strains for Use in Bioluminescent Imaging.” *PLoS ONE* 8 (3). <https://doi.org/10.1371/journal.pone.0059232>.
- Pozo, Jose L. Del, and Robin Patel. 2009. “Infection Associated with Prosthetic Joints.” *New England Journal of Medicine* 361 (8): 787–94. <https://doi.org/10.1056/NEJMcp0905029>.
- Pribaz, Jonathan R., Nicholas M. Bernthal, Fabrizio Billi, John S. Cho, Romela Irene Ramos, Y. Guo, Ambrose L. Cheung, Kevin P. Francis, and Lloyd S. Miller. 2012. “Mouse Model of Chronic Post-Arthroplasty Infection: Noninvasive in Vivo Bioluminescence Imaging to Monitor Bacterial Burden for Long-Term Study.” *Journal of Orthopaedic Research : Official Publication of the Orthopaedic Research Society* 30 (3): 335–40. <https://doi.org/10.1002/jor.21519>.
- Rackauckas, Chris, Yingbo Ma, Andreas Noack, Vaibhav Dixit, Shubham Maddhashiya, Patrick Kofod Mogensen, José Bayoán Santiago Calderón, et al. 2020. “Accelerated Predictive Healthcare Analytics with Pumas, a High Performance Pharmaceutical

Modeling and Simulation Platform.” *BioRxiv*.
<https://doi.org/10.1101/2020.11.28.402297>.

- Rao, Hari V., Robert P. Beliles, Gary M. Whitford, and Charles H. Turner. 1995. “A Physiologically Based Pharmacokinetic Model for Fluoride Uptake by Bone.” *Regulatory Toxicology and Pharmacology*. <https://doi.org/10.1006/rtph.1995.1065>.
- Rasigade, Jean Philippe, and François Vandenesch. 2014. “Staphylococcus Aureus: A Pathogen with Still Unresolved Issues.” *Infection, Genetics and Evolution* 21 (January):510–14. <https://doi.org/10.1016/j.meegid.2013.08.018>.
- Richter, Katharina, Freija Van Den Driessche, and Tom Coenye. 2017. “Innovative Approaches to Treat Staphylococcus Aureus Biofilm-Related Infections,” no. March, 61–70. <https://doi.org/10.1042/EBC20160056>.
- Rosenthal, Ian M., Rokeya Tasneen, Charles A. Peloquin, Ming Zhang, Deepak Almeida, Khisimuzi E. Mdluli, Petros C. Karakousis, Jacques H. Grosset, and Eric L. NuerMBERGER. 2012. “Dose-Ranging Comparison of Rifampin and Rifapentine in Two Pathologically Distinct Murine Models of Tuberculosis.” *Antimicrobial Agents and Chemotherapy* 56 (8): 4331–40. <https://doi.org/10.1128/AAC.00912-12>.
- Roth, B. 1984. “Penetration of Parenterally Administered Rifampicin into Bone Tissue.” *Chemotherapy* 30 (6): 358–65. <https://doi.org/10.1159/000238294>.
- Ruslami, Rovina, Hanneke M.J. Nijland, Bacht Alisjahbana, Ida Parwati, Reinout Van Crevel, and Rob E. Aarnoutse. 2007. “Pharmacokinetics and Tolerability of a Higher Rifampin Dose versus the Standard Dose in Pulmonary Tuberculosis Patients.” *Antimicrobial Agents and Chemotherapy* 51 (7): 2546–51. <https://doi.org/10.1128/AAC.01550-06>.
- Salem, Ahmed M., Tao Niu, Chao Li, Brady S. Moffett, Vijay Ivaturi, and Mathangi Gopalakrishnan. 2022. “Reassessing the Pediatric Dosing Recommendations for Unfractionated Heparin Using Real-World Data: A Pharmacokinetic–Pharmacodynamic Modeling Approach.” *Journal of Clinical Pharmacology* 62 (6): 733–46. <https://doi.org/10.1002/jcph.2007>.
- Schuirmann, Donald J. 1987. “A Comparison of the Two One-Sided Tests Procedure and the Power Approach for Assessing the Equivalence of Average Bioavailability.” *Journal of Pharmacokinetics and Biopharmaceutics* 15 (6): 657–80. <https://doi.org/10.1007/BF01068419>.
- Sharan, Satish, Lanyan Fang, Viera Lukacova, Xiaomei Chen, Andrew C. Hooker, and Mats O. Karlsson. 2021. “Model-Informed Drug Development for Long-Acting Injectable Products: Summary of American College of Clinical Pharmacology Symposium.” *Clinical Pharmacology in Drug Development* 10 (3): 220–28. <https://doi.org/10.1002/cpdd.928>.

- Sirof, J, R Lopitiaux, R Cluzel, J J Delisle, and B Sauvezie. 1977. “[Rifampicin Diffusion in Non-Infected Human Bone (Author’s Transl)].” *Annales de Microbiologie* 128 (2): 229–36.
- Sirof, J, L Prive, R Lopitiaux, and Y Glanddier. 1983. “[Diffusion of Rifampicin into Spongy and Compact Bone Tissue during Total Hip Prosthesis Operation].” *Pathologie-Biologie* 31 (5): 438–41.
- Steenwinkel, Jurriaan E.M. De, Rob E. Aarnoutse, Gerjo J. De Knegt, Marian T. Ten Kate, Marga Teulen, Henri A. Verbrugh, Martin J. Boeree, Dick Van Soolingen, and Irma A.J.M. Bakker-Woudenberg. 2013. “Optimization of the Rifampin Dosage to Improve the Therapeutic Efficacy in Tuberculosis Treatment Using a Murine Model.” *American Journal of Respiratory and Critical Care Medicine* 187 (10): 1127–34. <https://doi.org/10.1164/rccm.201207-1210OC>.
- Stevens, Georgia L., Gail Dawson, and Jacqueline Zummo. 2016. “Clinical Benefits and Impact of Early Use of Long-Acting Injectable Antipsychotics for Schizophrenia.” *Early Intervention in Psychiatry* 10 (5): 365–77. <https://doi.org/10.1111/eip.12278>.
- Stott, K. E., H. Pertinez, M. G.G. Sturkenboom, M. J. Boeree, R. Aarnoutse, G. Ramachandran, A. Requena-Méndez, et al. 2018. “Pharmacokinetics of Rifampicin in Adult TB Patients and Healthy Volunteers: A Systematic Review and Meta-Analysis.” *Journal of Antimicrobial Chemotherapy* 73 (9): 2305–13. <https://doi.org/10.1093/jac/dky152>.
- Susanto, Budi O., Elin M. Svensson, Lindsey te Brake, Rob E. Aarnoutse, Martin J. Boeree, and Ulrika S.H. Simonsson. 2023. “Model-Based Analysis of Bactericidal Activity and a New Dosing Strategy for Optimised-Dose Rifampicin.” *International Journal of Antimicrobial Agents* 61 (6). <https://doi.org/10.1016/j.ijantimicag.2023.106813>.
- Svensson, Robin J., Rob E. Aarnoutse, Andreas H. Diacon, Rodney Dawson, Stephen H. Gillespie, Martin J. Boeree, and Ulrika S.H. Simonsson. 2018. “A Population Pharmacokinetic Model Incorporating Saturable Pharmacokinetics and Autoinduction for High Rifampicin Doses.” *Clinical Pharmacology and Therapeutics* 103 (4): 674–83. <https://doi.org/10.1002/cpt.778>.
- Swaminathan, Soumya, Jotam G. Pasipanodya, Geetha Ramachandran, A. K. Hemanth Kumar, Shashikant Srivastava, Devyani Deshpande, Eric Nuermberger, and Tawanda Gumbo. 2016. “Drug Concentration Thresholds Predictive of Therapy Failure and Death in Children With Tuberculosis: Bread Crumb Trails in Random Forests.” *Clinical Infectious Diseases* 63 (suppl 3): S63–74. <https://doi.org/10.1093/cid/ciw471>.
- Tamma, Pranita D., Edina Avdic, David X. Li, Kathryn Dzintars, and Sara E. Cosgrove. 2017. “Association of Adverse Events With Antibiotic Use in Hospitalized Patients.”

JAMA Internal Medicine 177 (9): 1308.
<https://doi.org/10.1001/jamainternmed.2017.1938>.

- Tang, Hung Jen, Chi Chung Chen, Kuo Chen Cheng, Kuan Ying Wu, Yi Chung Lin, Chun Cheng Zhang, Tzu Chieh Weng, et al. 2013. “In Vitro Efficacies and Resistance Profiles of Rifampin-Based Combination Regimens for Biofilm-Embedded Methicillin-Resistant Staphylococcus Aureus.” *Antimicrobial Agents and Chemotherapy* 57 (11): 5717–20. <https://doi.org/10.1128/AAC.01236-13>.
- Terranova, Nadia, Didier Renard, Mohamed H. Shahin, Sujatha Menon, Youfang Cao, Cornelis E.C.A. Hop, Sean Hayes, et al. 2024. “Artificial Intelligence for Quantitative Modeling in Drug Discovery and Development: An Innovation and Quality Consortium Perspective on Use Cases and Best Practices.” *Clinical Pharmacology and Therapeutics* 115 (4): 658–72. <https://doi.org/10.1002/cpt.3053>.
- Thabit, Abrar K., Dania F. Fatani, Maryam S. Bamakhrama, Ola A. Barnawi, Lana O. Basudan, and Shahad F. Alhejaili. 2019. “Antibiotic Penetration into Bone and Joints: An Updated Review.” *International Journal of Infectious Diseases* 81 (April):128–36. <https://doi.org/10.1016/j.ijid.2019.02.005>.
- Thompson, John M., Vikram Saini, Alyssa G. Ashbaugh, Robert J. Miller, Alvaro A. Ordonez, Roger V. Ortines, Yu Wang, Robert S. Sterling, Sanjay K. Jain, and Lloyd S. Miller. 2017. “Oral-Only Linezolid-Rifampin Is Highly Effective Compared with Other Antibiotics for Periprosthetic Joint Infection: Study of a Mouse Model.” *Journal of Bone and Joint Surgery - American Volume*. Lippincott Williams and Wilkins. <https://doi.org/10.2106/JBJS.16.01002>.
- Tong, Steven Y.C., Joshua S. Davis, Emily Eichenberger, Thomas L. Holland, and Vance G. Fowler. 2015. “Staphylococcus Aureus Infections: Epidemiology, Pathophysiology, Clinical Manifestations, and Management.” *Clinical Microbiology Reviews* 28 (3): 603–61. <https://doi.org/10.1128/CMR.00134-14>.
- Tsakalozou, Eleftheria, Khondoker Alam, Andrew Babiskin, and Liang Zhao. 2022. “Physiologically-Based Pharmacokinetic Modeling to Support Determination of Bioequivalence for Dermatological Drug Products: Scientific and Regulatory Considerations.” *Clinical Pharmacology and Therapeutics*. John Wiley and Sons Inc. <https://doi.org/10.1002/cpt.2356>.
- Tsakalozou, Eleftheria, Andrew Babiskin, and Liang Zhao. 2021. “Physiologically-Based Pharmacokinetic Modeling to Support Bioequivalence and Approval of Generic Products: A Case for Diclofenac Sodium Topical Gel, 1%.” *CPT: Pharmacometrics and Systems Pharmacology*. American Society for Clinical Pharmacology and Therapeutics. <https://doi.org/10.1002/psp4.12600>.
- Tsakalozou, Eleftheria, Lanyan Fang, Youwei Bi, Michiel van den Heuvel, Tausif Ahmed, Yu Chung Tsang, Robert Lionberger, Amin Rostami-Hodjegan, and Liang Zhao. 2024. “Experience Learned and Perspectives on Using Model-Integrated Evidence

in the Regulatory Context for Generic Drug Products—a Meeting Report.” *The AAPS Journal* 26 (1): 14. <https://doi.org/10.1208/s12248-023-00884-5>.

Tucker, Elizabeth W., Beatriz Guglieri-Lopez, Alvaro A. Ordonez, Brittaney Ritchie, Mariah H. Klunk, Richa Sharma, Yong S. Chang, et al. 2018. “Noninvasive 11C-Rifampin Positron Emission Tomography Reveals Drug Biodistribution in Tuberculous Meningitis.” *Science Translational Medicine* 10 (470). <https://doi.org/10.1126/scitranslmed.aau0965>.

Tunkel, Allan R, Rodrigo Hasbun, Adarsh Bhimraj, Karin Byers, Sheldon L Kaplan, W Michael Scheld, Diederik van de Beek, Thomas P Bleck, Hugh J.L. Garton, and Joseph R Zunt. 2017. “2017 Infectious Diseases Society of America’s Clinical Practice Guidelines for Healthcare-Associated Ventriculitis and Meningitis*.” *Clinical Infectious Diseases* 64 (6): e34–65. <https://doi.org/10.1093/cid/ciw861>.

U.S. Food and Drug Administration. 2003. “Exposure-Response Relationships -- Study Design, Data Analysis, and Regulatory Applications.” May 2003.

———. 2022a. “Population Pharmacokinetics - Guidance for Industry.” February 2022.

———. 2022b. “Statistical Approaches to Establishing Bioequivalence - Guidance for Industry.” <https://www.fda.gov/drugs/guidance-compliance-regulatory-information/guidances-drugs>.

———. 2022c. “Successes and Opportunities in Modeling & Simulation for FDA.” <https://www.fda.gov/science-research/about-science-research-fda/modeling-simulation-fda>.

———. 2023. “Assessing the Credibility of Computational Modeling and Simulation in Medical Device Submissions - Guidance for Industry and Food and Drug Administration Staff.” <https://www.regulations.gov>.

———. 2024. “CDER Establishes New Quantitative Medicine Center of Excellence.” March 25, 2024. <https://www.fda.gov/drugs/drug-safety-and-availability/cder-establishes-new-quantitative-medicine-center-excellence>.

———. n.d.-a. “Depo-SubQ Provera 104 Clinical Pharmacology and Biopharmaceutics Review(s).” Accessed February 2, 2024.

———. n.d.-b. “Draft Guidance on Medroxyprogesterone Acetate.” Accessed February 2, 2024. <http://www.accessdata.fda.gov/scripts/cder/dissolution/>.

———. n.d.-c. “Model-Integrated Evidence (MIE) Industry Meeting Pilot Between FDA and Generic Drug Applicants.” Accessed September 17, 2024. <https://www.fda.gov/drugs/abbreviated-new-drug-application-anda/model-integrated-evidence-mie-industry-meeting-pilot-between-fda-and-generic-drug-applicants>.

- Wagner, Claudia C., and Oliver Langer. 2011. "Approaches Using Molecular Imaging Technology — Use of PET in Clinical Microdose Studies." *Advanced Drug Delivery Reviews* 63 (7): 539–46. <https://doi.org/10.1016/j.addr.2010.09.011>.
- Wolf, Brian R., Xin Lu, Yue Li, John J. Callaghan, and Peter Cram. 2012. "Adverse Outcomes in Hip Arthroplasty: Long-Term Trends." *Journal of Bone and Joint Surgery* 94 (14): e103(1). <https://doi.org/10.2106/JBJS.K.00011>.
- Yoon, Miyoung, Andrew Babiskin, Meng Hu, Fang Wu, Sam G. Raney, Lanyan Fang, and Liang Zhao. 2023. "Increasing Impact of Quantitative Methods and Modeling in Establishment of Bioequivalence and Characterization of Drug Delivery." *CPT: Pharmacometrics and Systems Pharmacology*. American Society for Clinical Pharmacology and Therapeutics. <https://doi.org/10.1002/psp4.12930>.
- Zhao, Liang, Myong Jin Kim, Lei Zhang, and Robert Lionberger. 2019. "Generating Model Integrated Evidence for Generic Drug Development and Assessment." *Clinical Pharmacology and Therapeutics* 105 (2): 338–49. <https://doi.org/10.1002/cpt.1282>.
- Zimmerli, Werner. 1998. "Role of Rifampin for Treatment of Orthopedic Implant–Related Staphylococcal Infections: A Randomized Controlled Trial." *JAMA* 279 (19): 1537. <https://doi.org/10.1001/jama.279.19.1537>.
- Zimmerli, Werner, and Parham Sendi. 2019. "Role of Rifampin against Staphylococcal Biofilm Infections in Vitro, in Animal Models, and in Orthopedic-Device-Related Infections." *Antimicrobial Agents and Chemotherapy*. American Society for Microbiology. <https://doi.org/10.1128/AAC.01746-18>.
- Zmistowski, Benjamin, Joseph A. Karam, Joel B. Durinka, David S. Casper, and Javad Parvizi. 2013. "Periprosthetic Joint Infection Increases the Risk of One-Year Mortality." *The Journal of Bone & Joint Surgery* 95 (24): 2177–84. <https://doi.org/10.2106/JBJS.L.00789>.